CHEMICAL REVIEWS

Review

Electrogenerated Chemiluminescence and Its Biorelated Applications

Wujian Miao

Chem. Rev., **2008**, 108 (7), 2506-2553 • DOI: 10.1021/cr068083a • Publication Date (Web): 28 May 2008

Electrogenerated Chemiluminescence and Its Biorelated Applications

Wujian Miao†

Department of Chemistry and Biochemistry, The University of Southern Mississippi, Hattiesburg, Mississippi 39406

Received November 19, 2007

Contents

1. Introduction

Electrogenerated chemiluminescence (also called electrochemiluminescence and abbreviated ECL) is the process whereby species generated at electrodes undergo high-energy electron-transfer reactions to form excited states that emit light.[1] The first detailed ECL studies were described by Hercules and Bard et al. in the mid-1960s,[2–4] although reports concerning light emission during electrolysis date back to the 1920s by Harvey.[5,6] After about 40 years study, ECL has now become a very powerful analytical technique and been widely used in the areas of, for example, immunoassay, food and water testing, and biowarfare agent detection.[7] ECL has also been successfully exploited as a detector of flow injection analysis (FIA), high-performance liquid chromatography (HPLC), capillary electrophoresis, and micro total analysis (μTAS).[8] Figure 1 illustrates a time line of various events in the development of ECL.

A literature survey using SciFinder Scholar reveals that more than 2000 journal articles, book chapters, and patents on various topics of ECL have been published. The overall number of publications, as shown in Figure 2, has increased exponentially over the past 20 years, of which 40–50% were biorelated. Similar amounts of ECL papers could be also found from the Thomson ISI Web of Science[27] as well as

† Telephone (601) 266 4716; fax (601) 266 6075; e-mail wujian.miao@usm.edu.

Wujian Miao received his undergraduate diploma in chemistry from Nantong University (Nantong, China) in 1982, his M.Sc. degree in analytical chemistry from Zhongshan University (Guangzhou, China, with Jinyuan Mo) in 1991, and his Ph.D. degree in electrochemistry from Monash University (Melbourne, Australia, with Alan M. Bond) in 2000. He then served as a Research Scientist in CSIRO (Melbourne, Australia), followed by a postdoctoral fellowship at the University of Texas at Austin with Allen J. Bard in 2001. Since 2004 he has served as an assistant professor of chemistry at the University of Southern Mississippi.

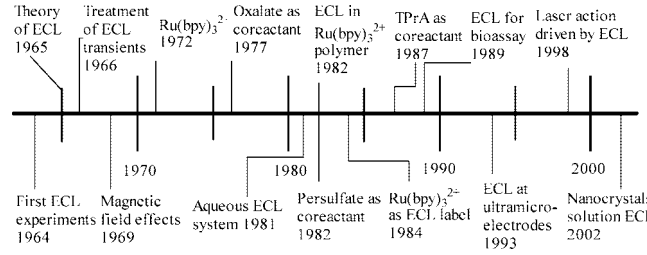

Figure 1. Time line of ECL: 1964–1965, first experiments;[2–4] 1965, theory;[9] 1966, transients;[10,11] 1969, magnetic field effects;[12] 1972, $Ru(bpy)_3^{2+}$;[13] 1977, oxalate;[14] 1981, aqueous;[15] 1982, $Ru(bpy)_3^{2+}$ polymer[16] and persulfate;[17] 1984, $Ru(bpy)_3^{2+}$ label;[18] 1987, tri-*n*-propylamine (TPrA);[19,20] 1989, bioassay;[21,22] 1993, ultramicroelectrodes;[23] 1998, laser action;[24] 2002, semiconductive nanocrystals[25] (modified on the basis of ref 26).

10.1021/cr068083a CCC: $71.00
Published on Web 05/28/2008

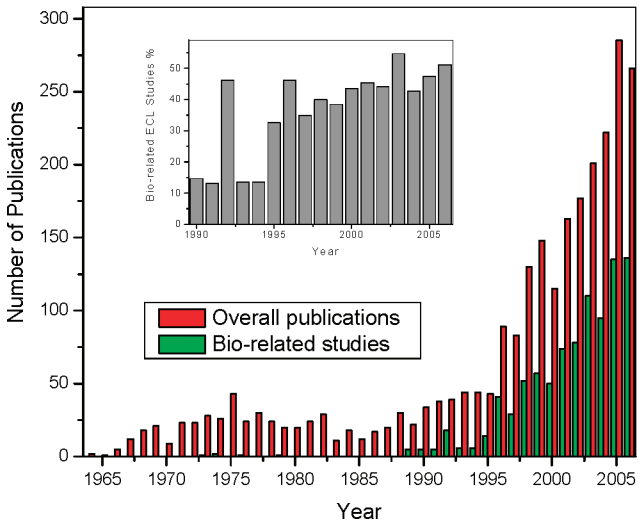

Figure 2. Number of ECL publications as a function of year published on the research topic of ECL according to SciFinder Scholar. (Inset) Percentage of biorelated ECL studies from 1989 to 2006.

Scheme 1. Ion Annihilation ECL

$$R - e \rightarrow R^{\bullet +} \text{ (oxidation at electrode)} \quad (1)$$

$$R + e \rightarrow R^{\bullet -} \text{ (reduction at electrode)} \quad (2)$$

$$R^{\bullet +} + R^{\bullet -} \rightarrow R + R^{*} \text{ (excited state formation)} \quad (3)$$

$$R^{*} \rightarrow R + h\nu \text{ (light emission)} \quad (4)$$

the Scopus database.[28] A considerable number of reviews on a wide variety of ECL subjects also are available in the literature,[8,29–64] in addition to a very recently published comprehensive ECL monograph.[7] In this first monograph, an overview and brief history of ECL, both experimental and theoretical aspects of ECL, and a review of the behavior of coreactants, organic molecules, and metal chelates, along with applications of ECL in immunoassay, flow injection, chromatography, capillary electrophoresis, and light production and display devices are thoroughly discussed. As a result, this paper will intend to cover briefly the fundamentals of ECL, its unique features with respect to other luminescence, and mechanisms of several types of ECL systems, followed by a review of new developments in the ECL field such as ECL instrumentation and ECL luminophores, and finally ECL applications with emphasis on the detection and determination of biorelated species will be presented. Particular attention will be given to publications that appeared between 2003 and early 2007. Readers are referred to several excellent references[7,51,58,60] and relevant Websites[65,66] for further and deep discussions on certain specific topics.

2. Types of Luminescence and Unique Features of ECL

Luminescence is the generation of light without heat. As pointed out in recent reviews,[26,51,67] light can be emitted via a number of luminescent processes, which include photoluminescence (PL), chemiluminescence (CL), and ECL. Table 1 lists typical types of luminescence and their origins. ECL is a form of CL, in which both ECL and CL involve the production of light by species that can undergo highly energetic electron-transfer reactions; however, luminescence in CL is initiated by the mixing of necessary reagents and often controlled by the careful manipulation of fluid flow. In contrast, luminescence in ECL is initiated and controlled by changing an electrode potential. Figure 3 schematically describes the general principles of PL, CL, and ECL.

As an analytical technique, ECL possesses several advantages over CL. First, in ECL the electrochemical reaction allows the time and position of the light-emitting reaction to be controlled. By controlling the time, light emission can be delayed until events such as immune or enzyme-catalyzed reactions have taken place. Control over position can be used to confine light emission to a region that is precisely located with respect to the detector, improving sensitivity by increasing the ratio of signal to noise. A good example of this is the combination of ECL with magnetic bead technology, which allows bound label to be distinguished from unbound label without a separation step (see following sections).[66,120] Control over position could also be used to determine the results of more than one analytical reaction in the same sample by interrogating each electrode in an array, either in sequence or simultaneously using a position sensitive detector.[65] Second, ECL can be more selective than CL, because the generation of excited states in ECL can be selectively controlled by varying the electrode potentials. Third, ECL is usually a nondestructive technique, because, in many cases, ECL emitters can be regenerated after the ECL emission.

Because ECL is a method of producing light at an electrode, in a sense, ECL represents a marriage between electrochemical and spectroscopic methods. ECL has many distinct advantages over other spectroscopy-based detection systems.[7,121] For example, compared with fluorescence methods, ECL does not involve a light source; hence, the attendant problems of scattered light and luminescent impurities are absent. Moreover, the specificity of the ECL reaction associated with the ECL label and the coreactant species decreases problems with side reactions, such as self-quenching.

3. Fundamentals of ECL

3.1. Ion Annihilation ECL

Although modern ECL applications are almost exclusively based on coreactant ECL (see next sections), the early ECL studies originated with ion annihilation ECL. Ion annihilation ECL involves the formation of an excited state as a result of an exergonic electron transfer between electrochemically generated species, often radical ions, at the surface of an electrode. As shown in Scheme 1, after the emitter (R) is electrochemically oxidized (eq 1) and reduced (eq 2), the newly formed radical cation ($R^{\bullet +}$) and anion ($R^{\bullet -}$) are annihilated to form the excited state species (R*) (eq 3) that emits light (eq 4).

Annihilation reactions (eq 3) also can occur in "mixed systems" where the radical cation and radical anion are from different molecules.[122] Depending on the energy available in an ion annihilation (eq 3), the produced R* could be either the lowest excited singlet state species ($^1R^*$) or the triplet state species ($^3R^*$). The enthalpy, which is directly related to the energy available in eq 3, can be calculated from the redox potentials for eqs 1 and 2 as defined in eq 5

$$-\Delta H_{ann} = E_p(R/R^{\bullet +}) - E_p(R/R^{\bullet -}) - 0.16 \quad (5)$$

where $-\Delta H_{ann}$ (in eV) is the enthalpy for ion annihilation, E_p is the peak potential for electrochemical oxidation or

Table 1. Different Types of Luminescence[a]

luminescence type	caused by	refs
photoluminescence (PL)	photoexcitation of compounds	68–70
chemiluminescence (CL)	chemical excitation of compounds	68–89
bioluminescence (BL)	luminous organisms	90
electrochemiluminescence (ECL)	electrogenerated chemical excitation	7, 29–62
electroluminescence (EL)	radiative recombination of electrons and holes in a material (usually a semiconductor) after an electrical current passes through the material or a strong electric field is applied	26, 91
radiochemiluminescence	radiation-induced chemical excitation	92–96
lyoluminescence	excitation induced by dissolution of an irradiated or other energy-donating solid	97, 98
sonoluminescence (SL)	excitation of compounds by ultrasonication, either by energy transfer from the intrinsic SL centers of water or by chemical excitation by hydroxyl radicals and atomic hydrogen	99–118

[a] Modified from refs 51 and 67. See ref 119 for a complete list of luminescence.

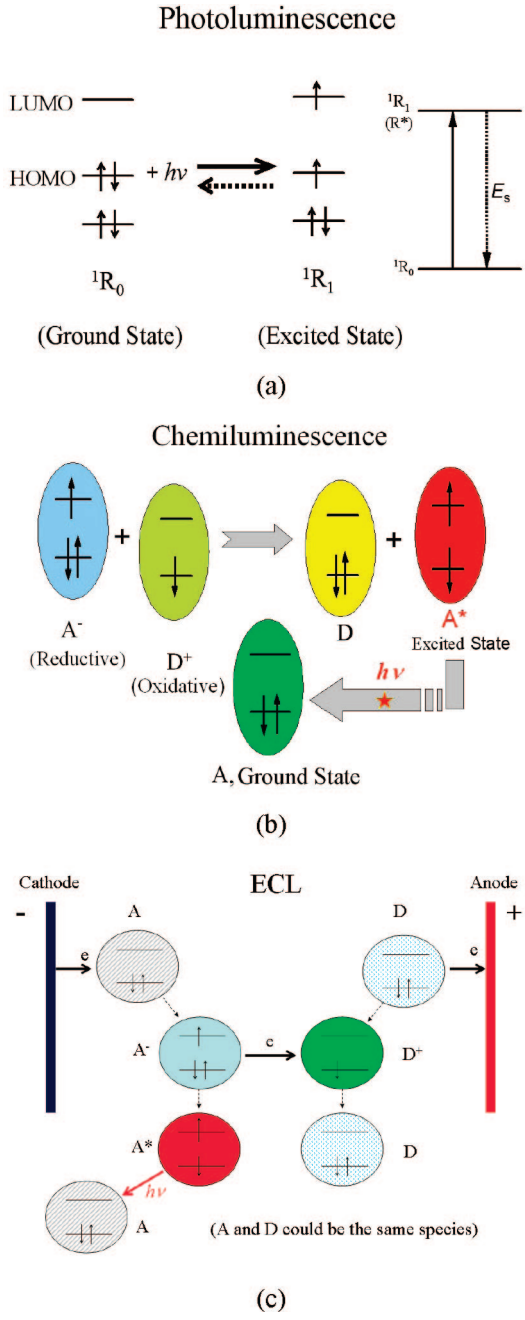

Figure 3. Schematic diagrams showing the general principles of (a) photoluminescence, (b) chemiluminescence, and (c) electrogenerated chemiluminescence. Reprinted with permission from ref 51. Copyright 2007 Elsevier.

reduction (in V), and 0.16 is the entropy approximation term ($T\Delta S$) at 25 °C (0.10 eV) with an addition of 0.057 eV resulting from the difference between the reversible potential and the peak potential of the redox reactions (eqs 1 and 2).[51] If the enthalpy ($-\Delta H_{ann}$) estimated from eq 5 is larger than the energy (E_s) required to produce the lowest excited singlet state from the ground state, it is possible to directly generate $^1R^*$ from eq 3, and this system is called the energy-sufficient system; the reaction is said to follow the S-route. A typical example of the energy-sufficient system is the $DPA^{\bullet+}/DPA^{\bullet-}$ (DPA = 9,10-diphenylanthracene) system.[123,124]

$$\text{S-route: } R^{\bullet+} + R^{\bullet-} \rightarrow R + {}^1R^* \quad \text{(excited singlet formation)} \quad (3a)$$

In contrast, if $-\Delta H_{ann}$ is smaller than E_s but larger than the triplet state energy (E_t), $^3R^*$ is initially formed, and then $^1R^*$ can be formed by the triplet−triplet annihilation (TTA) as shown in eq 6. This is called the energy-deficient system, and the reaction is said to follow the T-route. $TMPD^{\bullet+}/DPA^{\bullet-}$ and $TMPD^{\bullet+}$/AN (TMPD = *N*,*N*,*N*′,*N*′-tetramethyl-*p*-phenylenediamine and AN = anthracene) systems[12,124] are two examples of such energy-deficient systems. In a solution phase the efficiency of direct emission from $^3R^*$ is believed to be low due to the long radiactive lifetime of $^3R^*$ and its quenching by radical ions or other species, such as molecular oxygen.

$$\text{T-route: } R^{\bullet+} + R^{\bullet-} \rightarrow R + {}^3R^* \quad \text{(excited triplet formation)} \quad (3b)$$

$$^3R^* + {}^3R^* \rightarrow R + {}^1R^* \text{ (triplet−triplet annihilation)} \quad (6)$$

If $-\Delta H_{ann}$ is nearly marginal to E_s, the T-route can contribute to the formation of $^1R^*$ in addition to the S-route; hence, the system is often called the ST-route. A typical example is the rubrene anion−cation annihilation,[125–127] which has been finally confirmed by means of combined magnetic field/temperature[128] and solvent/temperature[129] investigations.

In addition to forming singlet and triplet excited states, ion annihilation reactions can lead to the direct formation of excimers (excited dimmers) and exciplexes (excited complexes). In most cases, the participating molecules must be able to align so that there is significant π-orbital overlap; thus, this occurs mostly among planar polycyclic aromatic hydrocarbons (PAHs) such as pyrene and perylene.[130,131] Other reactions such as TTA process can also lead to the

Scheme 2

$$R^{\bullet+} + R^{\bullet-} \rightarrow R_2^* \text{ (excimer formation)} \quad (7)$$

$$R^{\bullet+} + R'^{\bullet-} \rightarrow (RR')^* \text{ (exciplex formation)} \quad (8)$$

$$^3R^* + {}^3R^* \rightarrow {}^1R_2^* \text{ (TTA excimer formation)} \quad (9)$$

formation of excimers and/or exciplexes.[132] The reactions associated with the formation of excimers and exciplexes are said to follow the E-route. The relevant reactions are summarized in Scheme 2.

Excimer or exciplex emission is generally characterized by broad featureless emission red-shifted from the singlet emission of the molecule. Also, the emission wavelength and intensity change with solvent polarity. Exciplexes can be distinguished from excimers because the emission wavelength varies with the local dielectric, having greater energy in environments of low permittivity. Emission from the monomer and the excimer are very often observed in the same spectrum.[130,132,133] Although excimers and exciplexes can be often formed via photoexcitation as observed in fluorescence spectroscopy,[134] they are most likely to form in ECL due to the close proximity of the radical ions in the contact radical ion pair.[35,135–140] Moreover, as demonstrated in recent studies,[136,141] the radical ion annihilation pathway of ECL can generate emissive states different from those formed following photoexcitation, and the chemical environment (e.g., medium permittivity, ionic concentration, concentration of reagents) can be adjusted or chosen so as to tune the reaction rates and equilibria; these effects are manifested in the emission energy and the overall ECL efficiency.

For visible range emissions (~400–700 nm), E_s covers from 3.1 to 1.8 eV, according to eq 10. That is, to produce annihilation ECL, the potential window of an electrochemical system must be wide enough (from ~3.3 to 2 V, eq 5) so that sufficiently stable radical anions and cations can be generated. As a result, nonaqueous media, such as acetonitrile with tetra-*n*-butylammonium perchlorate (TBAP) as the supporting electrolyte, are extensively used in the study of ion annihilation ECL. Other commonly used solvent-supporting electrolyte systems for annihilation ECL studies can be found from refs 51 and 142. As will be discussed below, the first aqueous ECL system, which was coreactant ECL based, was not reported until 1981 by Rubinstein and Bard (see Figure 1)[15]

$$E_s = h\nu = hc/\lambda \quad (10)$$

where h is the Plank constant with a value of 6.63×10^{-34} J·s (4.13×10^{-15} eV), ν is the frequency (Hz), c is the speed of light (3.00×10^8 m/s), and λ is the wavelength of the emission.

Certain conditions need to be met for the efficient generation of ion annihilation ECL, which include[26] (1) stable radical ions of the precursor molecules in the electrolyte of interest, which can be evaluated via the cyclic voltammetric (CV) response; (2) good PL efficiency of a product of the electron transfer reaction, which often can be evaluated from the fluorescent experiment; and (3) sufficient energy in the electron transfer reaction to produce the excited state as described above.

3.2. Coreactant ECL

3.2.1. Overview

At present, all commercially available ECL analytical instruments are based on coreactant ECL technology. Therefore, understanding the ECL mechanisms of the relevant systems is important. Unlike ion annihilation ECL, in which electrolytic generation of both the oxidized and reduced ECL precursors is required, coreactant ECL is frequently generated with one directional potential scanning at an electrode in a solution containing luminophore species ("emitter") in the presence of a deliberately added reagent (coreactant). Depending on the polarity of the applied potential, both the luminophore and the coreactant species can be first oxidized or reduced at the electrode to form radicals, and intermediates formed from the coreactant then decompose to produce a powerful reducing or oxidizing species that reacts with the oxidized or reduced luminophore to produce the excited states that emit light. Because highly reducing intermediate species are generated after an electrochemical oxidation of a coreactant or highly oxidizing ones are produced after an electrochemical reduction, the corresponding ECL reactions are often referred to as "oxidative-reduction" ECL and "reductive-oxidation" ECL, respectively.[15,17] Thus, a coreactant is a species that, upon electrochemical oxidation or reduction, immediately undergoes chemical decomposition to form a strong reducing or oxidizing intermediate that can react with an oxidized or reduced ECL luminophore to generate excited states.

Use of a coreactant is useful especially when one of $R^{\bullet+}$ or $R^{\bullet-}$ is not stable enough for ECL reaction or when the ECL solvent has a narrow potential window so that $R^{\bullet+}$ or $R^{\bullet-}$ cannot be formed. Additionally, the use of a coreactant can make ECL possible even for some fluorescent compounds that have only a reversible electrochemical reduction or oxidation. When the annihilation reaction between oxidized and reduced species is not efficient, the use of a coreactant may produce more intense ECL. Finally, the oxygen quenching effect, which is often encountered in ion annihilation ECL, may be eliminated in oxidative-reduction type ECL, so that ECL analysis can be carried out in the air.

Note that, as indicated in eq 4 above and discussed in the following sections, in ion annihilation ECL, all starting species (R) can be regenerated after light emission, whereas in a coreactant ECL system, such as $Ru(bpy)_3^{2+}$ [$Ru(bpy)_3^{2+}$ = tris(2,2′-bipyridine) ruthenium (II)]/TPrA (TPrA = tri-*n*-propylamine), at the electrode surface, only luminophore species can be regenerated, whereas the coreactant is consumed via electrochemical−chemical reactions.

Table 2 lists typical coreactant ECL systems for which the ECL mechanisms have been well studied. In situ generated coreactant intermediates, as indicated by their standard redox potentials, are either strong reducing agents (in oxidative-reduction ECL) or strong oxidizing agents (in reductive-oxidation ECL).

To be a good ECL coreactant, a number of criteria need to be met,[143] which include solubility, stability, electrochemical properties, kinetics, quenching effect, ECL background, etc. Of these, the most important factor is the electrochemical properties of the coreactant. The coreactant should be easily oxidized or reduced with the luminophore species at or near the electrode and undergo a rapid chemical reaction to form an intermediate that has sufficient reducing

Table 2. Typical Coreactant ECL Systems

type of coreactant ECL	luminophore	coreactant	main coreactant intermediate	E^0 of intermediate (V, vs NHE)	refs	remarks
oxidative-reduction	$Ru(bpy)_3^{2+}$	oxalate ($C_2O_4^{2-}$)	$CO_2^{\bullet-}$	$CO_2/CO_2^{\bullet-}$ −1.9 V[144]	14, 15	*a*
	$Ru(bpy)_3^{2+}$	pyruvate/Ce(III)	$CH_3CO^{\bullet}$		15	*b*
	$Ru(bpy)_3^{2+}$	tri-*n*-propylamine (TPrA)	$TPrA^{\bullet+}$, $TPrA^{\bullet}$	$TPrA^{\bullet+}$/TPrA +1.1 V,[145] P_1/$TPrA^{\bullet}$ −1.5 V[146]	145	*c*
	$Ru(bpy)_3^{2+}$	hydrazine (N_2H_4)	N_2H_2, $N_2H_3^{\bullet}$	N_2H_2/N_2 < −2.3 V[147,148]	148–151	*d*
reductive-oxidation	$Ru(bpy)_3^{2+}$	persulfate ($S_2O_8^{2-}$)	$SO_4^{\bullet-}$	$SO_4^{\bullet-}$/ SO_4^{2-} ≥+2.9 V[152]	17, 153	*e*
	aromatic hydrocarbons	benzoyl peroxide	$PhCO_2^{\bullet}$	$PhCO_2^{\bullet}/PhCO_2^{-}$ +1.7 V[154]	133, 155, 156	*f*
	$Ru(bpy)_3^{2+}$	hydrogen peroxide (H_2O_2)	$OH^{\bullet}$	$OH^{\bullet}/OH^{-}$1.77–1.91 V[157–159]	160	*g*

[a] First reported "oxidative-reduction" type coreactant ECL. [b] Reduction nature of $CH_3CO^{\bullet}$ similar to $CO_2^{\bullet-}$. [c] Widely used in modern ECL instrumental analysis. [d] Complicated system. [e] First reported "reductive-oxidation" type coreactant ECL. [f] Hydrogen peroxide may be also used. [g] Study was done in pH 7.5 phosphate buffer solution, where electrochemically reduced $Ru(bpy)_3^{+}$ may be largely absorbed and precipitated on the electrode. >1 mM H_2O_2 with 0.10 mM $Ru(bpy)_3^{2+}$ quenched ECL significantly. No ECL was observed for "cathodic electrochemiluminescence"[161] in the presence of dissolved O_2 when the Pt counter electrode was isolated.

Table 3. General Mechanisms of Coreactant ECL Systems[a]

reaction process	oxidative-reduction ECL	reductive-oxidation ECL
redox reactions at electrode	$R - e \rightarrow R^{\bullet+}$ $C - e \rightarrow C^{\bullet+}$	$R + e \rightarrow R^{\bullet-}$ $C + e \rightarrow C^{\bullet-}$
homogeneous chemical reactions	$R^{\bullet+} + C \rightarrow R + C^{\bullet+}$ $C^{\bullet+} \rightarrow C^{\neq}_{Red}$ $C^{\neq}_{Red} + R \rightarrow R^{\bullet-} + P$	$R^{\bullet-} + C \rightarrow R + C^{\bullet-}$ $C^{\bullet-} \rightarrow C^{\neq}_{Ox}$ $C^{\neq}_{Ox} + R \rightarrow R^{\cdot+} + P$
excited state species formation	$R^{\bullet+} + R^{\bullet-} \rightarrow R + R^*$ or $R^{\bullet+} + C^{\neq}_{Red} \rightarrow R^* + P$	$R^{\bullet+} + R^{\bullet-} \rightarrow R + R^*$ or $R^{\bullet-} + C^{\neq}_{Ox} \rightarrow R^* + P$
light emission	$R^* \rightarrow R + h\nu$	$R^* \rightarrow R + h\nu$

[a] R, luminophore; C, coreactant; $C^{\neq}$, coreactant intermediate with subscript "Red" for reducing agent and "Ox" for oxidizing agent; P, product associated with $C^{\neq}$ reactions.

or oxidizing energy to react with the oxidized or reduced luminophore to form the excited state.

3.2.2. Typical Coreactant ECL Systems and Their Mechanisms

As summarized in Table 3, four processes generally are involved in all coreactant ECL systems toward the light emission, namely, (a) redox reactions at electrode, (b) homogeneous chemical reactions, (c) excited state species formation, and (d) light emission. Depending on the nature of the working electrode and the redox potential of the coreactant, both heterogeneous and homogeneous redox reactions of coreactant are possible. The formation of excited state species also has two general routes: the classical ion annihilation and the reaction involving coreactant intermediate.

Although there are a wide variety of molecules that exhibit ECL, the overwhelming majority of publications concerned with coreactant ECL and its analytical applications are based on chemistry involving $Ru(bpy)_3^{2+}$, or its derivatives, as the emitting species,[7] because of their excellent chemical, electrochemical, and photochemical properties even in aqueous media and in the presence of oxygen.[162] As a result, much of this section concerns $Ru(bpy)_3^{2+}$/coreactant ECL systems.

3.2.2.1. Oxalate ($C_2O_4^{2-}$) System. This was the first account of a coreactant ECL system reported in the literature by Bard's group in 1977,[14] and is a classical example of "oxidative-reduction" ECL. Scheme 3 presents the ECL mechanism of this system.[15]

In an aqueous solution, upon the anodic potential scanning at a Pt or carbon electrode, $Ru(bpy)_3^{2+}$ is first oxidized at the electrode to the $Ru(bpy)_3^{3+}$ cation. The cation is then capable of oxidizing the oxalate ($C_2O_4^{2-}$) in the diffusion layer close to the electrode surface to form an oxalate radical anion ($C_2O_4^{\bullet-}$). This breaks down to form a highly reducing radical anion ($CO_2^{\bullet-}$, $E^0 = -1.9$ V vs NHE[144]) and carbon dioxide. The reducing intermediate then either reduces the $Ru(bpy)_3^{3+}$ complex back to the parent complex in an excited state or reduces $Ru(bpy)_3^{2+}$ to form $Ru(bpy)_3^{+}$ that reacts with $Ru(bpy)_3^{3+}$ to generate the excited state $Ru(bpy)_3^{2+*}$, which emits light with $\lambda_{max} \sim 620$ nm. In acetonitrile (MeCN), however, oxalate has been shown to be easier to oxidize than the $Ru(bpy)_3^{2+}$ complex.[14] Thus, both reactants are oxidized at the electrode during light generation, as described in Table 3. The contribution of the direct oxidation of oxalate to the overall ECL behavior also depends on the surface property of the electrode, the concentration of oxalate, and the electrode potential applied.[163–165]

Production of ECL is very sensitive to the solution pH. In aqueous solutions, the ECL intensity of the $Ru(bpy)_3^{2+}$/

Scheme 3[a]

$$Ru(bpy)_3^{2+} - e \rightarrow Ru(bpy)_3^{3+} \quad (11)$$

$$Ru(bpy)_3^{3+} + C_2O_4^{2-} \rightarrow Ru(bpy)_3^{2+} + C_2O_4^{\bullet-} \quad (12)$$

$$C_2O_4^{\bullet-} \rightarrow CO_2^{\bullet-} + CO_2 \quad (13)$$

$$Ru(bpy)_3^{3+} + CO_2^{\bullet-} \rightarrow Ru(bpy)_3^{2+*} + CO_2 \quad (14)$$

$$Ru(bpy)_3^{2+} + CO_2^{\bullet-} \rightarrow Ru(bpy)_3^{+} + CO_2 \quad (15)$$

$$Ru(bpy)_3^{3+} + Ru(bpy)_3^{+} \rightarrow Ru(bpy)_3^{2+*} + Ru(bpy)_3^{2+} \quad (16)$$

$$Ru(bpy)_3^{2+*} \rightarrow Ru(bpy)_3^{2+} + h\nu \quad (17)$$

[a] Adapted with permission from ref 143. Copyright 2004 Marcel Dekker.

Scheme 4[a]

$$S_2O_8^{2-} + e \rightarrow S_2O_8^{\bullet 3-} \quad (18)$$

$$Ru(bpy)_3^{2+} + e \rightarrow Ru(bpy)_3^{+} \quad (19)$$

$$Ru(bpy)_3^{+} + S_2O_8^{2-} \rightarrow Ru(bpy)_3^{2+} + S_2O_8^{\bullet 3-} \quad (20)$$

$$S_2O_8^{\bullet 3-} \rightarrow SO_4^{2-} + SO_4^{\bullet -} \quad (21)$$

$$Ru(bpy)_3^{+} + SO_4^{\bullet -} \rightarrow Ru(bpy)_3^{2+*} + SO_4^{2-} \quad (22)$$

$$Ru(bpy)_3^{2+} + SO_4^{\bullet -} \rightarrow Ru(bpy)_3^{3+} + SO_4^{2-} \quad (23)$$

$$Ru(bpy)_3^{3+} + Ru(bpy)_3^{+} \rightarrow Ru(bpy)_3^{2+*} + Ru(bpy)_3^{2+} \quad (24)$$

[a] Adapted with permission from ref 143. Copyright 2004 Marcel Dekker.

oxalate system has been reported to have a maximum at pH ~6 in unbuffered solutions at Pt,[15] and also to be essentially constant from pH 4 to 8 in phosphate buffer solutions at GC[18,166] and from pH 5 to 8 in phosphate buffer solutions at ultra-microelectrodes.[165]

3.2.2.2. Peroxydisulfate (Persulfate, $S_2O_8^{2-}$) System. This was the first example of a so-called "reductive-oxidation" coreactant ECL system reported in the literature.[17,153] Because $Ru(bpy)_3^{+}$ is unstable in aqueous solutions and $(NH_4)_2S_2O_8$ has a low solubility in MeCN solutions, the MeCN−H_2O mixed solutions were chosen to produce intense ECL emission.[17] Scheme 4 summarizes the possible pathways for the production of $Ru(bpy)_3^{2+}$* when $S_2O_8^{2-}$ is used as the coreactant, in which the strongly oxidizing intermediate $SO_4^{\bullet -}$, generated during the reduction of $S_2O_8^{2-}$, has a redox potential of $E^0 \geq 3.15$ V vs SCE.[152] The ECL intensity of the $Ru(bpy)_3^{2+}/S_2O_8^{2-}$ system was found to be a function of $S_2O_8^{2-}$ concentration, and for 1 mM $Ru(bpy)_3^{2+}$ solution the maximum ECL intensity was obtained at 15–20 mM $S_2O_8^{2-}$.[17] This result is ascribed to the fact that the persulfate ion is a coreactant of $Ru(bpy)_3^{2+}$ as well as an effective quencher of the excited state $Ru(bpy)_3^{2+}$*.[167]

3.2.2.3. Amine-Related Systems.[51,143]

3.2.2.3.1. Tri-n-propylamine (TPrA) System. The majority of ECL applications reported so far involve $Ru(bpy)_3^{2+}$ or its derivatives as an emitter (or label) and TPrA as a coreactant, because the $Ru(bpy)_3^{2+}$/TPrA system exhibits the highest ECL efficiency and this system forms the basis of commercial systems for immunoassay and DNA analysis.[51,121,168] The ECL mechanism of this reaction is very complicated and has been investigated by many workers.[19,20,145,169–172] The mechanism presently presented in the literature and in some of the ECL instrument manufacturer's Websites including the technical application notes is often simplified. Generally, the ECL emission of this system as a function of applied potential consists of two waves (Figure 4). The first occurs with the direct oxidation of TPrA at the electrode, and this wave is often merged into the foot of the second wave when relatively high concentrations of $Ru(bpy)_3^{2+}$ (~millimolar) are used. The second wave appears where $Ru(bpy)_3^{2+}$ is oxidized.[145,172] Both waves are associated with the emission from $Ru(bpy)_3^{2+}$*.[172] The relative ECL intensity from the first wave is significant, particularly in dilute $Ru(bpy)_3^{2+}$ solutions (less than approximately micromolar) containing ~0.1 M TPrA. Thus, the bulk of the ECL signal obtained in this system with low concentrations of analytes, as in immunoassays and DNA probes with $Ru(bpy)_3^{2+}$ as an ECL label, probably originates from the first ECL wave. Scheme 5 summarizes the mechanism of the first ECL wave, where the cation radical species $TPrA^{\bullet +}$ formed during TPrA oxidation is a sufficiently stable intermediate with a half-life of ~0.2 ms that it can oxidize $Ru(bpy)_3^{+}$ [formed from

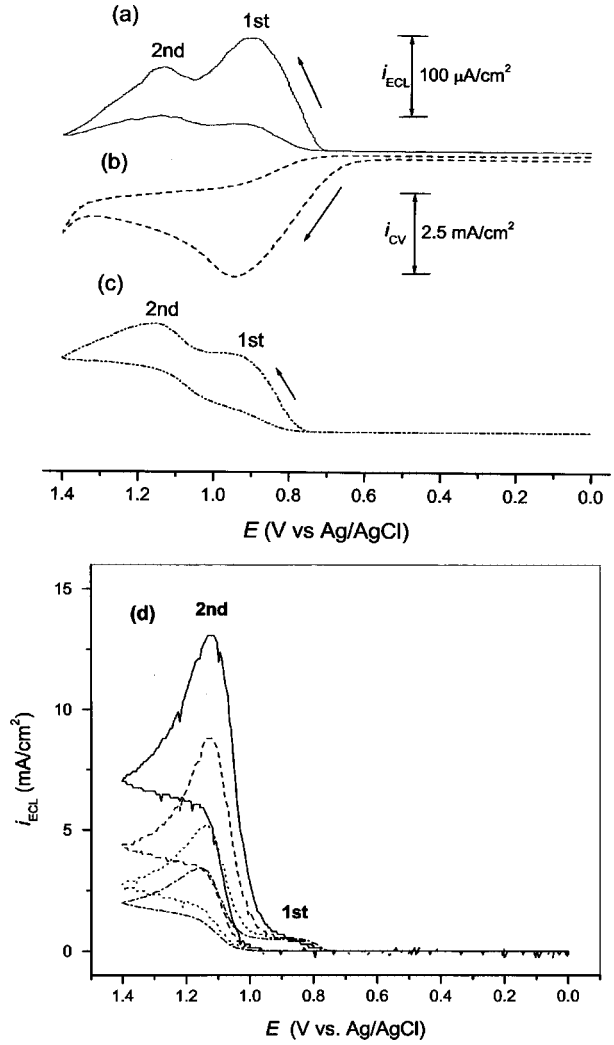

Figure 4. (a) ECL and (b) cyclic voltammogram of 1.0 nM $Ru(bpy)_3^{2+}$ in the presence of 0.10 M TPrA with 0.10 M Tris/0.10 M $LiClO_4$ buffer (pH 8) at a 3 mm diameter glassy carbon electrode at a scan rate of 50 mV/s. (c) As in (a) but with 1.0 μM $Ru(bpy)_3^{2+}$. The ECL intensity scale is given for (c) and was multiplied by 100 for (a). (d) First and second ECL responses in 0.10 M TPrA (0.20 M PBS, pH 8.5) with different $Ru(bpy)_3^{2+}$ concentrations: 1 mM (solid line), 0.50 mM (dashed line), 0.10 mM (dotted line), and 0.05 mM (dashed-dotted line), at a 3 mm diameter glassy carbon electrode at a scan rate of 100 mV/s. Reprinted with permission from ref 145. Copyright 2002 American Chemical Society.

Scheme 5[a]

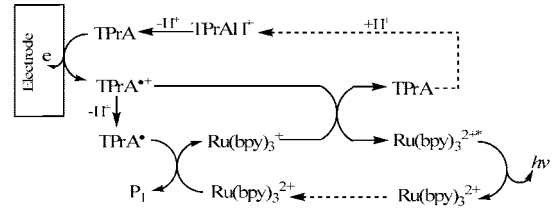

[where $TPrA^{\bullet +} = (CH_3CH_2CH_2)_3N^{\bullet +}$, $TPrAH^{+} = Pr_3NH^{+}$, $TPrA^{\bullet} = Pr_2NC^{\bullet}HCH_2CH_3$
$P_1 = Pr_2N^{+}{=}CHCH_2CH_3$]

[a] Reprinted with permission from ref 145. Copyright 2002 American Chemical Society.

Scheme 6[a]

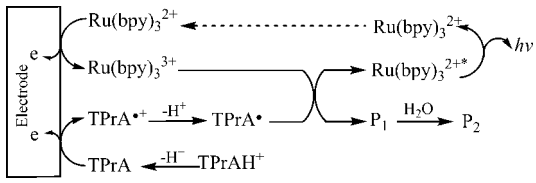

[a] Reprinted with permission from ref 145. Copyright 2002 American Chemical Society.

Scheme 7[a]

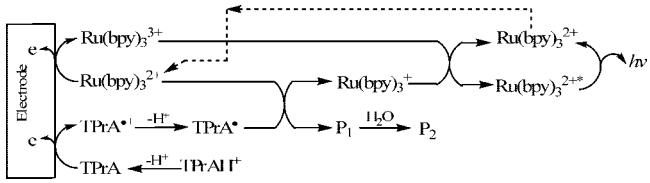

[a] Reprinted with permission from ref 145. Copyright 2002 American Chemical Society.

Scheme 8[a]

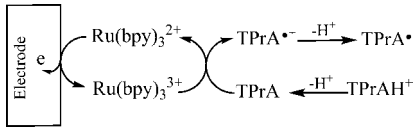

[a] Reprinted with permission from ref 145. Copyright 2002 American Chemical Society.

the reduction of $Ru(bpy)_3^{2+}$ by $TPrA^{\bullet}$ free radical] to give $Ru(bpy)_3^{2+}*$.[145]

The mechanism of the second ECL wave follows the classic "oxidative-reduction" coreactant mechanism (see section 3.2.1), where oxidation of TPrA generates a strongly reducing species $TPrA^{\bullet}$ ($E_{P1/TPrA^{\bullet}} \approx -1.7$ V vs SCE[146]). This oxidation can be via a "catalytic route", where electrogenerated $Ru(bpy)_3^{3+}$ reacts with TPrA, as well as by direct reaction of TPrA at the electrode described by both Schemes 6 and 7.[145]

The "catalytic route" involving homogeneous oxidation of TPrA with $Ru(bpy)_3^{3+}$ is shown in Scheme 8.[145] The contribution of this process to the overall ECL intensity depends upon the $Ru(bpy)_3^{2+}$ concentration and is small when relatively low concentrations of $Ru(bpy)_3^{2+}$ are used.[169]

Therefore, the excited state of $Ru(bpy)_3^{2+}$ can be produced via three different routes: (1) $Ru(bpy)_3^{+}$ oxidation by $TPrA^{\bullet+}$ cation radicals (Scheme 5); (2) $Ru(bpy)_3^{3+}$ reduction by $TPrA^{\bullet}$ free radicals (Scheme 6); and (3) the $Ru(bpy)_3^{3+}$ and $Ru(bpy)_3^{+}$ annihilation reaction (Scheme 7).

The direct oxidation of TPrA at an electrode plays an important role in the ECL process of the $Ru(bpy)_3^{2+}$/TPrA system and varies with the electrode material and its surface hydrophobicity. For example, in the presence of added small amounts of halide species that could inhibit the growth of the oxide surface on Pt and Au electrodes or low concentrations of surfactants (nonionic and ionic) that could increase the hydrophobicity of the electrode, the oxidation rate of TPrA and hence the ECL intensity increased significantly.[173–176] The effect of room temperature ionic liquids (ILs) on ECL has also been exploited recently.[177–180] Upon addition of 1% (v/v) hydrophilic IL 1-butyl-3-methylimidazolium tetrafluoroborate ($BMImBF_4$) to 5 μM $Ru(bpy)_3^{2+}$/100 mM coreactant [TPrA, 2-(2-aminoethyl)-1-methyypyrrolidine (AEMP),

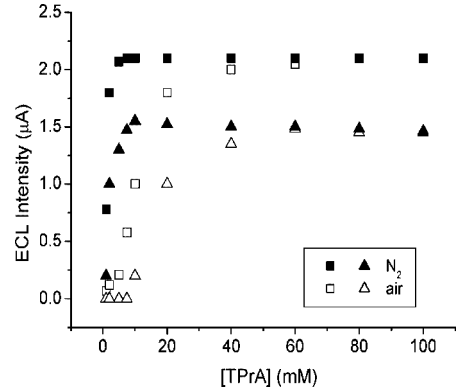

Figure 5. Intensities of the second ECL (squares) and first ECL (triangles) at the GC electrode (3 mm diameter) as a function of TPrA concentration. The electrolyte solution was 0.15 M PBS (pH 7.5) containing 1 μM $Ru(bpy)_3^{2+}$, and the scan rate was 0.1 V/s. Reprinted with permission from ref 182. Copyright 2005 American Chemical Society.

and 4-(dimethylamino)butyric acid (DMBA)] aqueous systems at a GC electrode, different effects of $BMImBF_4$ on coreactants were observed due to the IL adsorption at the electrode surface, which results in a change of the polarity of the electrode surface.[180] Because the sequence for polarity difference between $BMImBF_4$ and the coreactants is AEMP < DMBA < TPrA, the sequence of concentration enrichment of the coreactants at the electrode follows AEMP > DMBA > TPrA. As a result, the ECL efficiency increases in the order AEMP (~10-fold) > DMBA (~5-fold) > TPrA (no obvious change).[180] The potential applications of hydrophobic IL, 1-butyl-3-methylimidazolium hexafluorophosphate ($BMIMPF_6$), however, could be limited, because the IL has very high viscosity and low ionic conductivity. In addition, the solubility of $Ru(bpy)_3^{2+}$ can be reduced due to the association between $Ru(bpy)_3^{2+}$ and PF_6^{-}.[180] Although these ILs are air and moisture stable, both O_2 and water still need to be removed in ion annihilation ECL or they will limit the electrochemical windows.[181]

The ECL intensity for the first and the second waves was also found to be proportional to the concentration of TPrA species over a very large dynamic range (up to 0.10 M).[20,145,169,171,172] Dissolved O_2 could influence the ECL intensity when low concentrations (< 20 mM) of TPrA are used (Figure 5),[182] which is particularly remarkable for the first ECL wave. This behavior can be readily explained on the basis of the ECL mechanisms described in Schemes 5−7: A large excess of intermediate reducing radicals ($TPrA^{\bullet}$) was produced at high [TPrA], and the dissolved O_2 within the ECL reaction layer was completely reduced by these radicals and exerted no quenching effect on the emission. At low [TPrA], however, coreactant oxidation generated a relatively small amount of reducing intermediates, and O_2 acted as an interceptor, destroying the intermediates before they participated in the ECL pathways, which led to the obvious reduction of the emission intensity. In the latter case, the less efficient initial ECL route was more significantly affected.[182]

Up to 2.5 V vs Ag/AgCl anodic potential limit can be reached for neutral aqueous ECL systems at the deposited boron-doped diamond (BDD) electrode.[183] Three ECL waves at 1.2, 2.0, and 2.3 V vs Ag/AgCl for $Ru(bpy)_3^{2+}$/TPrA, which correspond to the oxidation reaction of $Ru(bpy)_3^{2+}$ at the electrode and homogeneous catalytic oxidation of TPrA with electrogenerated $Ru(bpy)_3^{3+}$, the direct oxidation of

TPrA at the electrode, and the electrode oxidation of propylamine formed by preceding dealkylation of TPrA, respectively, were observed. The wide potential window in aqueous solution and the high stability for ECL due to the low adsorption property for reaction products make such a diamond electrode very promising for ECL production of amines with high oxidation potentials. Hydroxyl radical ($OH^{\bullet}$)-related ECL reactions for $Ru(bpy)_3^{2+}$−coreactant (ascorbic acid and alcohols) systems at BDD electrode were also observed in the extremely positive potential region (>2.6 V with a peak potential at ~3.7 V vs Ag/AgCl).[184] It is believed that the coreactant radical was formed through the hydrogen abstraction reaction with the $OH^{\bullet}$ generated during the oxygen evolution reaction. Such behavior was not found at GC or Pt electrode. The formation of $OH^{\bullet}$ at the BDD electrode in the high-potential region (>2.6 V vs Ag/AgCl) was confirmed previously by ESR measurement with the spin-trap method.[185]

The ECL intensity of the $Ru(bpy)_3^{2+}$/TPrA system also strongly depends on the solution pH,[20,48] with dramatic increases at pH >~5.5 and a maximum value at pH 7.5. The exact reason remains unclear, but this may be associated with the deprotonation reactions of $TPrAH^+$ and $TPrA^{\bullet+}$ shown in Schemes 5–7 as well as the stability of the intermediates formed. Solubility decrease of TPrA at high pH could be another reason why TPrA produces the highest ECL intensity at pH 7.5. A recent study regarding the influence of the nature, concentration, and pH of buffer on the rate-determining step of $Ru(bpy)_3^{2+}$/tertiary aliphatic amine systems revealed that deprotonation of the ammonium species is the rate-determining step at pH <5, whereas deprotonation of radical cations is the rate-determining step at pH >5.[186] Usually, pH values higher than 9 should not be used, because $Ru(bpy)_3^{3+}$ generated at the electrode could react with hydroxide ions to produce a significant ECL background signal.

On the basis of the ECL mechanism discussed above, one can readily explain the ECL generation from "magnetic bead" based commercially available ECL instruments such as the original BioVeris M-series analyzers.[66] In the system, the $Ru(bpy)_3^{2+}$-tagged species in an immunoassay are immobilized on 2.8 μm diameter nontransparent magnetic beads that are brought to an electrode by a magnetic field. The high sensitivity of the technique suggests that most of the labels on the beads participate in the ECL reaction (see Scheme 5, the first ECL wave), whereas the direct oxidation of $Ru(bpy)_3^{2+}$ on the beads would occur only for those within electron tunneling distance from the electrode, ~1−2 nm, and its contribution to the overall ECL intensity should be small and negligible.

The ECL behavior of $Ru(bpy)_3^{2+}$/TPrA in MeCN has been also studied, and it is believed the ECL generation in this case is predominately associated with the direct oxidation of $Ru(bpy)_3^{2+}$ at the electrode.[187–190] The cyclic voltammetric and ECL responses of 0.10 μM $Ru(bpy)_3[(B(C_6F_5)_4)]_2$ in MeCN containing 0.10 M $(TBA)BF_4$ electrolyte−0.10 M TPrA coreactant at a Pt electrode with a scan rate of 50 mV/s are shown in Figure 6.[188] Unlike in aqueous solution, where the ECL intensity is proportional to the TPrA concentration, in MeCN a maximum ECL response is found with TPrA concentrations around 30 mM (Figure 7a). ECL intensity is affected by the "acidity" of the solution (Figure 7b), which is unsurprising and consistent with the ECL behavior in aqueous media.

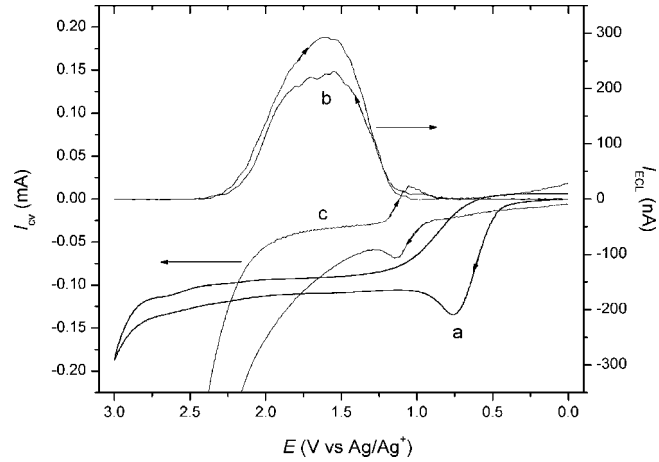

Figure 6. (a) CV and (b) ECL responses obtained from 0.10 μM $Ru(bpy)_3[(B(C_6F_5)_4)]_2$ in MeCN containing 0.10 M $(TBA)BF_4$ electrolyte−0.10 M TPrA coreactant at a 2.2 mm in diameter Pt electrode with a scan rate of 50 mV/s. For comparison, CV of 1.0 mM $Ru(bpy)_3[(B(C_6F_5)_4)]_2$ in MeCN containing 0.10 M $(TBA)BF_4$ in the absence of TPrA is presented in (c), in which the experimental conditions were as in (a) and (b), but the CV current was multiplied by 10. Reprinted with permission from ref 188. Copyright 2004 American Chemical Society.

ECL intensity and stability are affected by the electrode material used, which is, however, different from the data obtained from an aqueous solution, where the GC electrode generally exhibits the strongest ECL response among Au, Pt, and GC electrodes. The relative ECL intensity, obtained from a MeCN solution containing 0.10 μM $Ru(bpy)_3[(B(C_6F_5)_4)]_2$−0.10 M TPrA−0.055 M TFAA−0.10 M $(TBA)BF_4$ during the first potential cycle between 0 and 3.0 V vs Ag/Ag^+ at a scan rate of 50 mV/s, at Au, Pt and GC electrode had a ratio of 100:93:61.[188]

The electrochemistry, UV−vis absorption, PL of $Ru(bpy)_3^{2+}$, and its ECL with TPrA have been reported in a series of hydroxylic solvents such as fluorinated and nonfluorinated alcohols and alcohol/water mixtures.[191] Blue shifts of up to 30 nm in PL and ECL emission wavelength maximums were observed compared to a $Ru(bpy)_3^{2+}/H_2O$ standard due to interactions of the polar excited state [i.e., $Ru(bpy)_3^{2+}*$] with the solvent media. Dramatic increases in ECL efficiencies ranging from 6- (in 5% BuOH) to 270-fold (in 30% 2,2,2-trifluoroethanol) were seen in mixed alcohol/water solutions compared to $Ru(bpy)_3^{2+}$ (0.1 μM)/TPrA (40 mM) in water.

3.2.2.3.2. Other Amine-Related Systems. Similar to the case of TPrA, a wide range of amine compounds can be used as coreactants and take part in ECL reactions with $Ru(bpy)_3^{2+}$. Because amine groups are prevalent in numerous biologically and pharmacologically important compounds including amino acids and peptides, $Ru(bpy)_3^{2+}$/amine coreactant ECL forms the basis of a large number of biorelated species detection and determination, such as those reported with CE-ECL approaches.[60]

Several workers[29,38,40,46,48,50,51,57,58] have tried to correlate the coreactant ECL efficiency with the amine structure. Although there are no strict rules governing ECL activity in amines, as a general rule, the ECL intensity increases in the order primary < secondary < tertiary amines, with tertiary amines having the lowest detection limits.[19,20] As shown in Schemes 5–7, the amine should have a hydrogen atom attached to the α-carbon, so that upon oxidation newly formed radical cation species can undergo a deprotonation process to form a strongly reducing free radical species. Also,

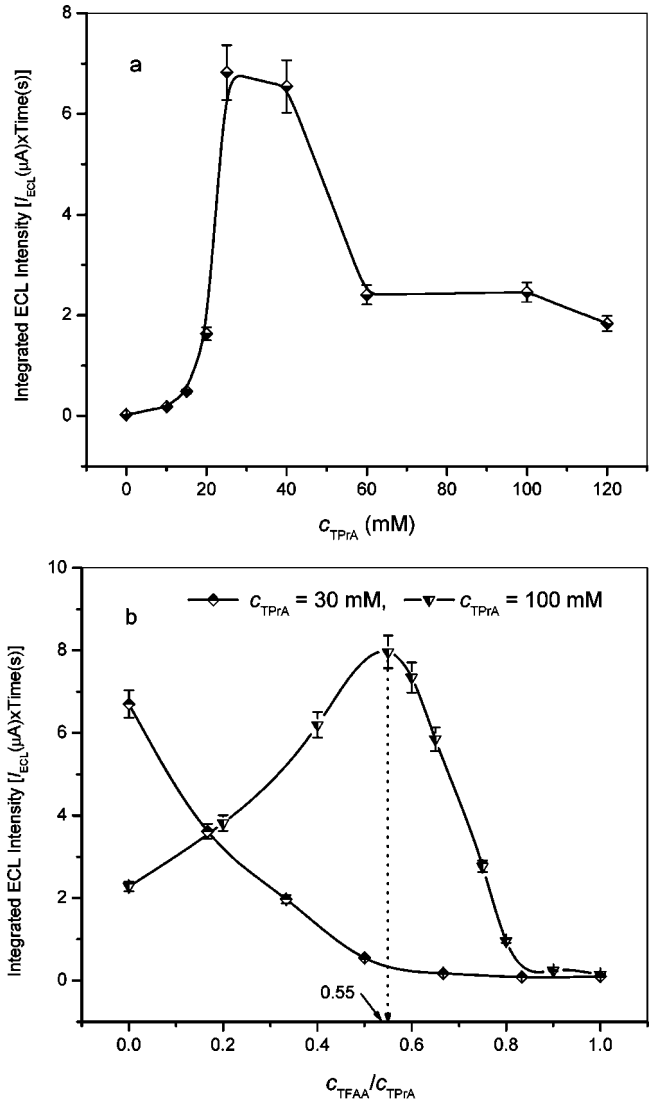

Figure 7. (a) TPrA and (b) TPrA−trifluoroacetic acid (TFAA) concentration effect on ECL intensity. All samples contained 0.10 μM $Ru(bpy)_3[(B(C_6F_5)_4)]_2$ and 0.10 M $(TBA)BF_4$ in MeCN. The working electrode was 2.2 mm in diameter Pt, and the scan rate was 50 mV/s. Reprinted with permission from ref 188. Copyright 2004 American Chemical Society.

the nature of substituents attached to nitrogen or α-carbon on an amine molecule can affect the ECL activity.[48] In general, electron-withdrawing substituents tend to cause a reduction of ECL activity, and electron-donating groups have the opposite effect. Aromatic amines, aromatic substituted amines, and amines with a carbon−carbon double bond that can conjugate the radical intermediates consistently give a very low ECL response. Note that aromatic amines may also quench the emission of the $Ru(bpy)_3^{2+}$* complex, further reducing the ability of these compounds to give an ECL response.[192] Furthermore, amines that have other functional groups that are more readily oxidized than the nitrogen atom may take part in alternative, ultimately non-chemiluminescent, reactions.

The ECL reaction mechanism of $Ru(bpy)_3^{2+}$ with six tertiary aliphatic amines, namely, tri-*n*-butylamine (TBuA), tri-isobutylamine (TisoBuA), TPrA, methyl-di-*n*-propylamine (MeDPrA), triethylamine (TEtA), and trimethylamine (TMeA), in aqueous solution was examined using fast potential pulses at carbon fiber microelectrodes and with simulation techniques with the aim to obtain information on the $E°$ value

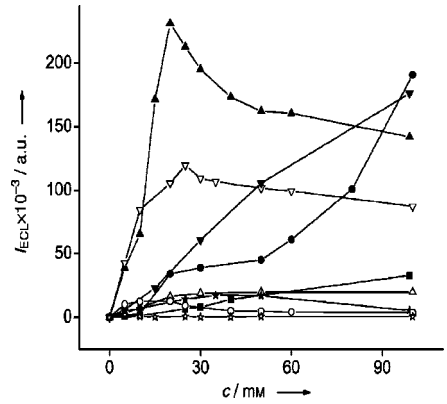

Figure 8. Dependence of the ECL peak intensity on the concentrations of 2-(dibutylamino)ethanol (DBAE, ▲), triethanolamine (▽), *N*,*N*-diethylethanolamine (▼), TPrA (●), triethylamine (■), *N*,*N*-diethyl-*N*′-methylethylenediamine (△), 3-diethylamino-1-propanol (★), nitrilotriacetic acid (○), and ethylenediaminetetraacetic acid (☆), measured at Au electrode in 0.1 M phosphate buffer solution (pH 7.5) containing 1 μM $Ru(bpy)_3^{2+}$. The potential was stepped from 0 to 1.35 V vs Ag/AgCl. Reprinted with permission from ref 193. Copyright 2007 Wiley-VCH.

of the amine redox couples.[186] The experimental approach to estimate the $E°$ values of the amine redox couples consisted of combining electrochemistry and ECL data with TPrA as the reference compound ($E° = 0.88$ V vs SCE[171]). The estimated $E°$ values were as follows: 1.05 ± 0.04 V (TMeA), 0.92 ± 0.04 V (TEtA), 0.91 ± 0.03 V (MeDPrA), 0.79 ± 0.03 V (TBuA), and 0.72 ± 0.03 V vs SCE (TisoBuA).

Very recently, a new coreactant, 2-(dibutylamino)ethanol [$(n\text{-}C_4H_7)_2NCH_2CH_2OH$, DBAE], has been reported for $Ru(bpy)_3^{2+}$ ECL system.[193] The ECL intensity of the $Ru(bpy)_3^{2+}$/DBAE system at Au (Figure 8) and Pt electrodes was found to be approximately 10 and 100 times greater than that of the commonly used $Ru(bpy)_3^{2+}$/TPrA system, respectively, when 25 mM of each coreactant was used in the presence of 0.10 M phosphate buffer (pH 7.5). At the GC electrode, however, the ECL performance of this system was poor; the intensity of ECL first increased with the concentration of DBAE up to 3 mM and then leveled off. The ECL enhancement of DBAE was attributed to the catalytic effect of hydroxyethyl group toward the direct oxidation of DBAE at the electrode. This suggests that not all electron-withdrawing substituents such as the hydroxyethyl group in the current case cause ECL efficiency decrease. Compared to $Ru(bpy)_3^{2+}$/TPrA, the $Ru(bpy)_3^{2+}$/DBAE system exists over a wider dynamic range and has a lower detection limit for $Ru(bpy)_3^{2+}$ at the Au electrode and very sensitive ECL responses at Pt electrode. As a result, DBAE could be a promising coreactant for $Ru(bpy)_3^{2+}$ ECL immunoassays and DNA probe assays.

3.3. ECL from Luminol

The first report on luminol (5-amino-2,3-dihydro-1,4-phthalazinedione) ECL was published in 1954 at a dropping mercury electrode during the reduction of oxygen in an alkaline medium in the presence of luminol.[194] This was followed by the studies of anodic generation of ECL in similar reaction media at a Pt electrode.[195,196] Luminol ECL is often produced in alkaline solution with hydrogen peroxide upon electrochemical oxidation.[58] However, a recent study indicated that oxygen, hydrogen peroxide, or other oxidizing

Scheme 9

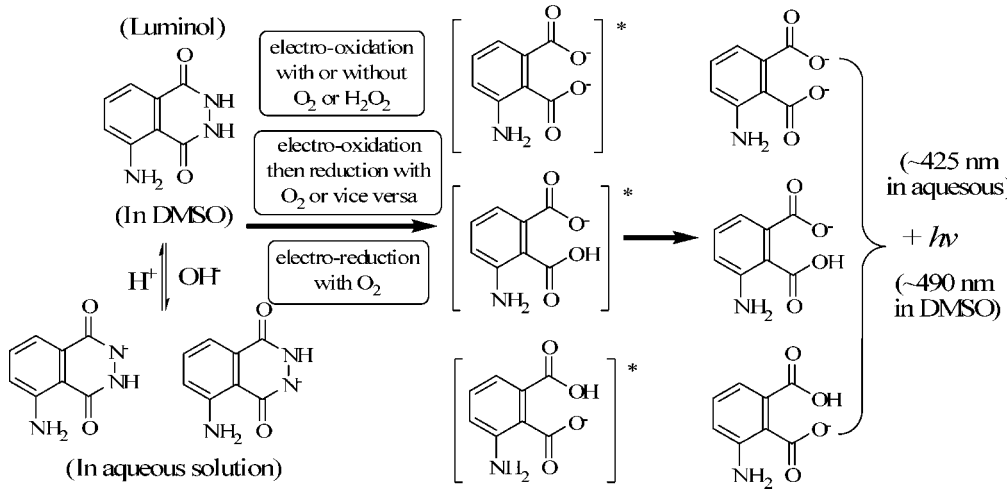

agents are all unnecessary for the anodic generation of luminol ECL at a Pt or graphite electrode in alkaline solution, and the electrogenerated excited monoanionic form of 3-aminophthalic acid is believed to be the origin of the ECL.[197] Because luminol can produce ECL under a wide range of experimental conditions, which include (1) different solvents [aqueous[58] or dimethyl sulfoxide (DMSO)[198]], (2) broad pH ranges (weakly acidic,[199] neutral to high pH[200–206]), (3) the presence and absence of oxygen and/or hydrogen peroxide,[38,196–198,202–204,207–232] (4) different electrodes (Hg,[194] Pt,[195–197] Au,[200,201,206,233–235] graphite and paraffin-impregnated graphite,[197,204] carbon nanotube paste,[236] Cu,[237,238] GC,[200,209,234] indium tin oxide (ITO),[239] and screen-printed graphite containing tetracyanoquinodimethane (TCNQ) electrode][240,241] or electrode modified with nanoparticles,[200–202,206,235,242–245] clay,[213,216] and self-assembled monolayer (SAMs)/multilayer/film,,[218,246] (5) different electrode potential scanning directions and ranges,[202–204] and (6) other coexisting chemical species such as Br^- and Cl^-,[196,200,202,212,235,247] a number of ECL waves located at different potential regions and associated with the excited state monoanionic forms of 3-aminophthalic acid or 3-aminophthalate generated from, for example, the oxidation between luminol, its deprotonated forms, or their electro-oxidized forms and a various oxygen-containing oxidizing species such as $O_2^{\bullet}$ and $HO_2^{\bullet}$ have been observed. Scheme 9 summarizes the generally accepted overall ECL reactions of luminol. The ECL emission of luminol varies slightly with the solvent used, in which the maximum emissions of ~425 nm in water and ~490 nm in DMSO have been reported.[198,203,204] Emission from alkaline solutions generally is much stronger than that obtained from neutral solutions. Electrodes modified with nanoparticles (NPs) such as Au or Ag NPs can enhance the ECL emission by 2–3 orders compared to the original bare electrodes.[206] The size and nature of NPs and the nature of the substrate electrode can also affect the ECL behavior.[200] Much stronger ECL emission was found from Ag NPs/Au substrate electrode than that from Au NPs/Au substrate.[206] Such NP-modified electrodes showed good stability and reproducibility for the oxidation of luminol and the generation of ECL.[200,202,206,235,242] The enhancement of ECL could be due to the increase of the electrode area as well as the catalytic effect of NPs on luminol oxidation hence the ECL production.

Comparative studies between acridan ester (2′,3′,6′-trifluorophenyl 10-methylacridan-9-carboxylate)/H_2O_2, luminol/H_2O_2, and $Ru(bpy)_3^{2+}$/TPrA ECL at transparent ITO electrodes have been reported.[239] Potentials of >1 V vs Ag/AgCl showed a corrosive effect on ITO. The effects of pH and H_2O_2 concentration on ECL detection of the acridan ester and luminol in a planar flow cell were described. The limits of detection (LODs) of the acridan ester and luminol were found to be 65 and 72 pM, respectively.

Mechanistically, the luminol ECL system is very different from the classical ion annihilation or coreactant ECL system discussed in sections 3.1 and 3.2. First, in the luminol system, there are no oxidized and reduced luminol species involved. Second, luminol itself can be directly oxidized at the electrode to produce light. Third, once oxidized, luminol cannot be regenerated upon light emission.

4. ECL Instrumentation

The basic components of an ECL instrument include an electrical energy supply for the ECL reaction at an electrode within an electrochemical cell and an optical detector for the measurement of either the emitted light intensity (as photocurrent or counts/s) or its spectroscopic response.[51,142] Although certain types of ECL instruments are now commercially available (see below), most of the ECL studies reported in the literature were carried out in homemade ECL instruments.

4.1. Nonaqueous Electrochemical Media

Historically, all ECL studies except for luminol systems were carried out in organic media, although modern ECL instruments used for the detection of biorelated species are often run in an aqueous environment. In these cases, the purity of the solvent/supporting electrolyte is very crucial, because trace amounts of water and oxygen can significantly affect the ECL production by either disabling the generation of both reductive and oxidative ECL precursor species at the electrode or quenching the newly formed excited state species. As a result, the ECL experiment is often conducted in an oxygen-free dry box with pure and dry solvent and electrolyte. Detailed discussions on solvent and electrolyte drying and purification[248,249] as well as commonly used solvent-supporting electrolyte systems for ECL study[51,142] can be found in the literature.

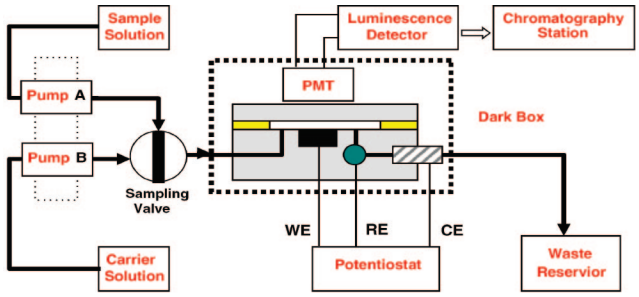

Figure 9. Schematic diagram of a FI-ECL detection system. Reprinted with permission from ref 253. Copyright 2006 Elsevier.

4.2. Cell Design

Different types of ECL cells are used for different types of ECL studies. For ion annihilation ECL, the system needs to remain oxygen- and moisture-free; hence, proper sealing with good electronic connections is required.[51] For general coreactant ECL studies, suitably sized glass vials may be used as a cell, because degassing in this case is often unnecessary. If ECL experiments are carried out with a wafer type electrode, such as ITO, a Au-coated silicon wafer used for the detection of DNA and C-reactive protein (CRP),[187,188,250] and highly oriented pyrolytic graphite (HOPG),[251] the effective area of the electrode exposed to the coreactant solution needs to be carefully controlled and to face the window of the photodetector.

ECL has been widely used as a detector in FIA, liquid chromatography, CE, and microchip CE.[8,60,62,252] Figure 9 shows a schematic diagram of a FI-ECL detection system,[253] in which "Chromatography Station" may be replaced with a computerized data acquisition system. Various types of thin-layer flow-through ECL cells for FIA have been developed, and Figure 10 illustrates two examples of such a cell. These kinds of ECL cells could have several drawbacks,[254] which include (a) large dead volumes that could reduce both the detection sensitivity and separation efficiency of a sample, (b) high IR drops that could decrease the sensitivity of ECL detection, and (c) high flow resistance that could cause significant noise due to difficulties of removing gas bubbles. To overcome the above problems, a new type of ECL flow cell consisted of a capillary inlet, a Pt ring working electrode (WE), and a stainless steel pipe counter electrode (CE) coated with a black plastic jacket to prevent any undesired ECL emission from the electrode has been fabricated and used for the detection of 2-thiouracil in biological samples (Figure 11).[254] In addition to millimeter-order-sized working electrodes, a microelectrode ($w = 2$ μm, $l = 2.5$ cm) was also constructed by sealing a piece of platinum foil between two microscope slides with epoxy into an ECL flow cell.[23] This type of cell has been employed in high-frequency ECL studies. The reduced time scale enables reaction kinetics to be accessed and affords a means for investigating ECL without rigorously purifying solvents or working on a vacuum line or in a dry box.[23]

Two microfluidic ECL cells that combine transparent polydimethylsiloxane (PDMS) microchannels with the electrodes fabricated by using printed circuit board (PCB) technology were tested with luminol−H_2O_2 solutions.[232] The differences between the two cells were the working electrode size (10 mm^2 Au vs 0.09 mm^2 Au) and the ECL detection volume (4 μL vs 4 nL). The "Ag/AgCl" reference electrode was obtained by electrodeposition of Ag on Au, followed by electro-oxidation of Ag in the presence of 0.10 M KCl. No counter electrode was used.

A microfluidic cell designed to transport and mix two different solutions on the chip and generate ECL using $Ru(bpy)_3^{2+}$ as luminophor and amino acids as coreactants was presented recently by Hosono et al.[257] Figure 12A illustrates the basic arrangement of the electrodes. The system is constructed with a glass substrate (20 mm×14 mm) with driving electrodes formed by a thin-film process and a PDMS substrate (14 mm×14 mm) with structures to form microflow channels [40 μm (h) × 300 μm (w) for sample transport and 40 μm (h) × 500 μm (w) for solution mixing]. The electrode system consists of three elongated Au working electrodes formed along the flow channels, two Pt auxiliary electrodes formed in the injection ports, and two Ag/AgCl reference electrodes formed in separate compartments that are filled with photosensitive poly(vinyl alcohol) gel (PVA-SbQ gel) containing 0.1 M KCl and connected to the injection ports with liquid junctions. Additionally, a Pt working electrode (200 μm × 300 μm) at the end of the mixing channel is constructed for the generation of ECL [Figure 12A(c)]. Figure 12B displays the process of the liquid transport in one of the flow channels. At the beginning, the solution in the injection port wets the edge of the working electrode and is not mobilized because the electrode surface is not sufficiently hydrophilic [Figure 12B(a)]. With the application of a potential of −0.9 V vs Ag/AgCl, the surface of the working electrode becomes more hydrophilic, and the solution is transported along the flow channel to the end of the electrode by a capillary action [Figure 12B(b)]. The solution is then confined in a space between the protruding structure and the working electrode due to interfacial tension [Figure 12B(c)]. Because the two flow channels are placed in close proximity and the third Au working electrode is placed between them, solutions that arrive at the mixing area exude through the intervening glass areas and wet the edges of the electrode for mixing. Finally, when a potential (−0.90 V vs Ag/AgCl) is applied at the mixing electrode, the two solutions move over the electrode and mix together. Such a cell requires only 50 nL of analyte solutions for ECL test. One problem of this type of cell, however, is that it cannot distinguish one analyte from another if the sample solution contains several ECL active unknown species.

When ECL detection is combined with CE separation, a number of key factors need to be considered in the design of the ECL cell.[8,60,62] First, the LOD—the elimination or reduction of the electrophoretic current from the ECL current—is generally needed. The electrical current in CE capillaries under the high electric field could significantly affect the ECL reactions at the electrode such as the redox potential change of the emitting species [e.g., $Ru(bpy)_3^{2+}$] and the interference of the electrode potential control of an amperometric controller,[258,259] resulting in high background signals. Several different fashions of CE decoupler have been utilized for the elimination of the electrophoretic current, which include the use of an on-column fracture covered with a Nafion tube,[260,261] a porous polymer junction near the end of the capillary,[262] a section of outside wall-etched capillary,[263] and a porous etched joint capillary.[264] Second, sensitivity—the alignment or arrangement of the working electrode against the detection capillary and the photodetector—is required.[264–266] Ideally, all of the separated analyte should reach the electrode and take part in the ECL reactions that produce light detected completely by the

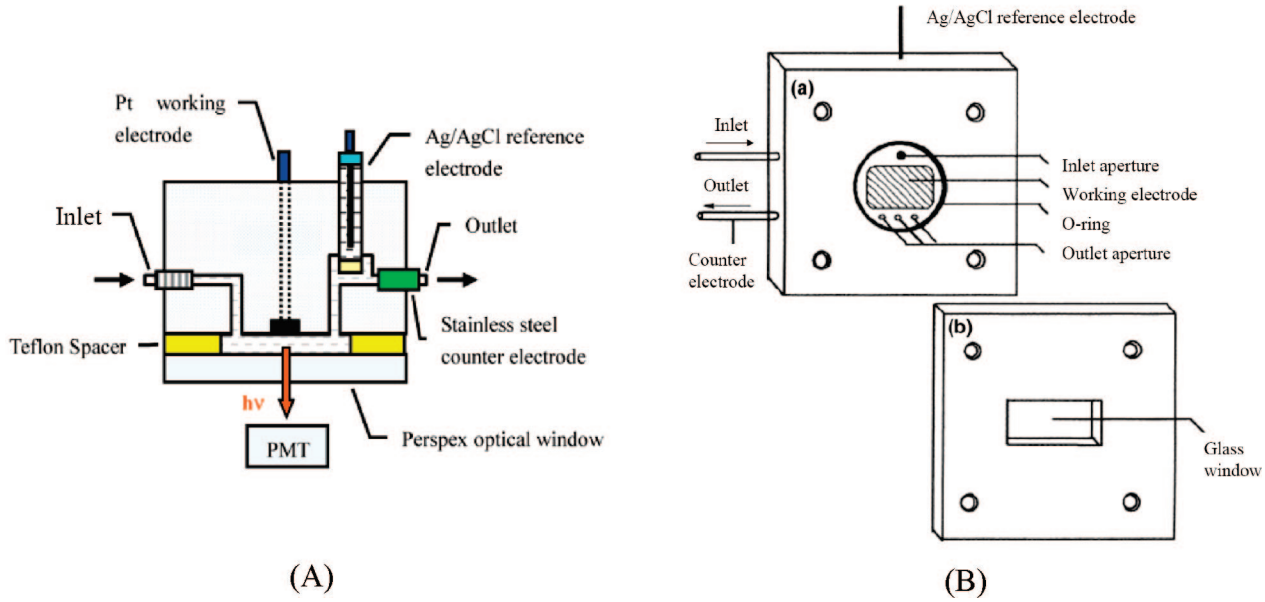

Figure 10. Schematic diagrams of FI-ECL thin-layer flow-through cells from refs 255 (A) and ref 256 (B) in which (a) is the cell body and (b) the cell cover window. Reprinted with permission from refs 255 and 256. Copyright 2007 and 2002, respectively, American Chemical Society.

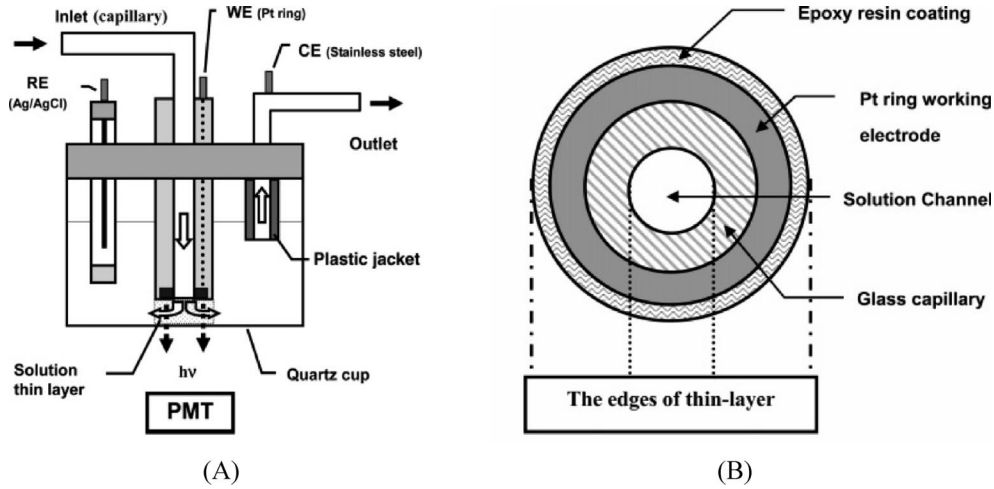

Figure 11. (A) Schematic diagram of a newly designed FI-ECL thin-layer flow-through cell with small dead volume, IR drop, and flow resistance. (B) Distribution of the thin layer at the tip of the Pt ring immobilized capillary shown in (A). Reprinted with permission from ref 254. Copyright 2006 American Chemical Society.

photodetector. The distance between the end of the capillary and the working electrode needs to be optimized; too short a distance would block the $Ru(bpy)_3^{2+}$ diffusion and too long a distance would dilute the analyte concentration at the electrode, resulting in poor sensitivity and reproducibility. Third, selectivity—the CE separation efficiency—is influenced by the length of the detection capillary.[264] Because there is no electric field gradient in the detection capillary, the movement of the sample zone is governed by the pressure generated in the capillary. Thus, band broadening could become problematic when a short length (e.g., a few centimeters) of detection capillary cannot be used. Figure 13 illustrates a schematic diagram of an ECL detection cell used for CE separation, in which the joint was fabricated by etching the capillary wall with hydrofluoric acid after half of the circumference of the polyimide coating in a 2–3 cm section was removed.[264] Compared with previously reported ECL cells,[263] a number of advantages have been noted. The joint was strong enough, which allowed the whole system to be fabricated with no need to fix the joint on a plate. Also, a very short detection capillary of ~7 mm can be used for the cell, which dramatically reduced the band broadening effect and increased the CE efficiency. Moreover, the sample loss is small and the part replacement is relatively easy.

A low-cost miniaturized CE system developed on a chip platform of a glass slide to provide easy interface both with FI sample introduction and with ECL detection was reported (Figure 14).[265] The CE high-voltage effect on ECL detection was effectively eliminated with the falling-drop interface of FI split-flow sample introduction method. As shown in Figure 14c, a plexiglass reservoir at the capillary outlet serves as both the reaction and detection cell for the ECL reaction, with $Ru(bpy)_3^{2+}$ reagent continuously flowing through the cell. An optical fiber is positioned within the reservoir close to the capillary outlet for transferring the ECL emission to the PMT. The performance of the entire system was illustrated by the baseline separation of proline, valine, and phenylalanine with a high throughput of 50 h^{-1} and plate height of 14 μm for proline under 147 V cm^{-1} field strength.

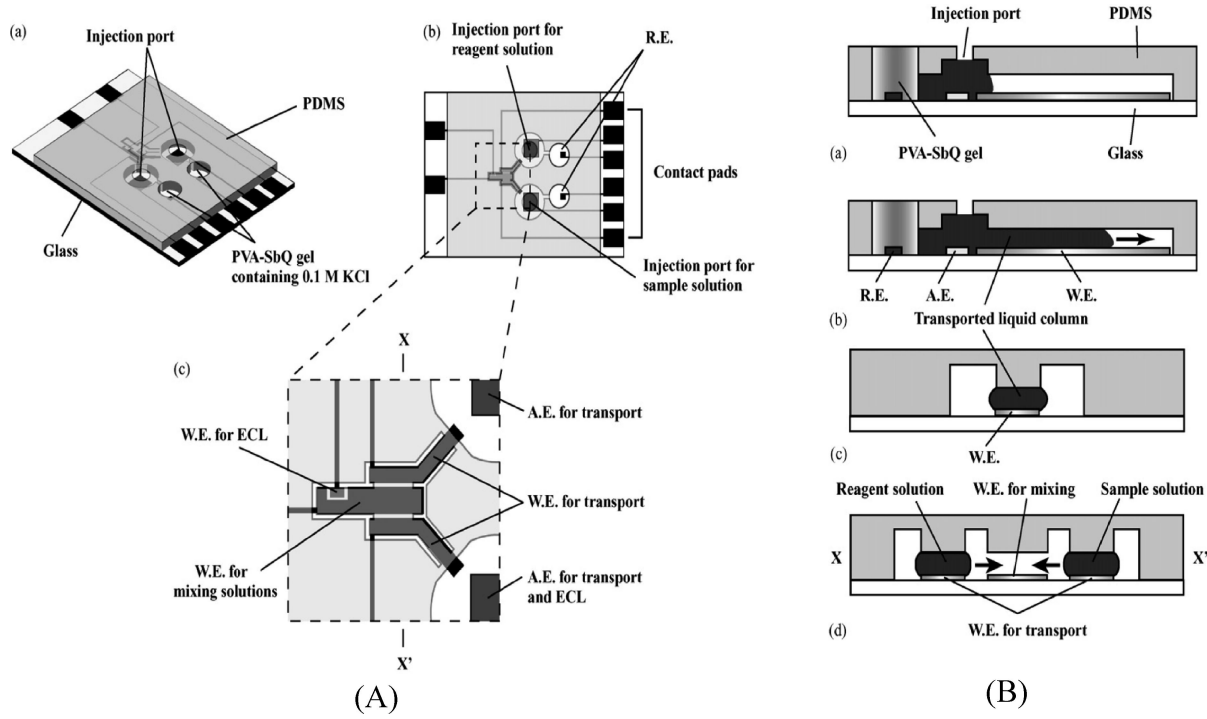

Figure 12. (A) Active microfluidic transport system with integrated components for optical sensing based on ECL: (a) completed chip; (b) planar layout of the entire system; (c) magnified view of the mixing area showing electrodes for the transport, mixing, and generation of the ECL. The dimensions of the chip are 14 mm × 20 mm. W.E., working electrode; R.E., reference electrode; A.E., auxiliary electrode. (B) Basic structure and arrangement for the microfluidic transport system: (a, b) cross section along the flow channel showing the initial status (a) and movement of the solution (b); (c) cross section of the flow channel area viewed from the direction normal to the flow; (d) cross section of the mixing area along line $X-X'$ in (A). Reprinted with permission from ref 257. Copyright 2007 Elsevier.

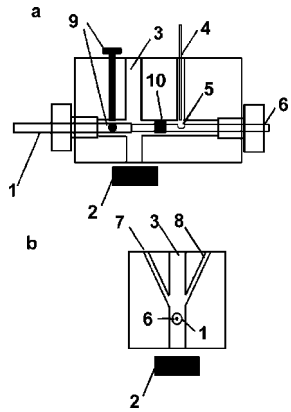

Figure 13. Schematic diagram of the ECL detection cell coupled with capillary electrophoresis (CE) separation (not to scale): (a) front view and (b) side view from $Ru(bpy)_3^{2+}$ solution reservoir [(1) working electrode; (2) photomultiplier tube (PMT); (3) $Ru(bpy)_3^{2+}$ solution reservoir; (4) CE ground electrode; (5) porous section of capillary; (6) separation capillary; (7) for reference electrode; (8) for counter electrode; (9) working electrode alignment screws; (10) seal-on film (to isolate the $Ru(bpy)_3^{2+}$ solution reservoir and CE ground cell and to align the separation capillary]. Reprinted with permission from ref 264. Copyright 2004 American Chemical Society.

Because microchip CE offers a number of advantages over classical CE, including high performance, short analysis time, portability, disposability, and consumption of minute sample and reagent, many efforts have been made in the development of microchip CE based separation with ECL detection.[60,62,267–269] This concept was first demonstrated by Manz et al. in 2001.[270] In their paper, a microfabricated U-shaped floating platinum electrode was placed across the CE separation channel, and its two legs acted as working and counter electrode. ECL reactions occurred at the Pt electrode by the electrical field available in the separation channel during electrophoretic separation in the presence of ECL-emitting species. Direct ECL detection of micromolar levels of ruthenium(II) tris(1,10-phenanthroline) $[Ru(phen)_3^{2+}]$ and $Ru(bpy)_3^{2+}$ and indirect detection of amino acids were provided. Later, Crooks' group reported one-,[271] two-,[272] and three-channel microfluidic sensors[273] that could detect redox reactions indirectly using anodic coreactant ECL [i.e., $Ru(bpy)_3^{2+}$/TPrA system]. As shown at the top of Scheme 10,[273] a one-channel microfluidic device, incorporating either one or two electrodes, is able to detect electrochemical processes at the cathode and report them via light emission at the anode. Similarly, a two-electrode, two-channel microfluidic device (middle of Scheme 10) can be used in the same manner, but with complete chemical separation of the detection and reporting functions. The one- and two-channel methods, however, permit detection only of targets that can be reduced when the $Ru(bpy)_3^{2+}$/TPrA system is used. This problem was overcome by using a multichannel approach, such as the three-channel configuration shown at the bottom of Scheme 10. In this case, channel 1 houses the cathode and a flowing solution of a sacrificial electroactive molecule [e.g., $Ru(NH_3)_6^{3+}$] that can be easily reduced. A solution containing $Ru(bpy)_3^{2+}$/TPrA flows in channel 2, and the oxidizable analyte of interest is present in channel 3. Both of these channels share a common anode. When a sufficiently large potential is applied between the cathode and anode, $Ru(NH_3)_6^{3+}$ is reduced to $Ru(NH_3)_6^{2+}$, whereas $Ru(bpy)_3^{2+}$ and TPrA are oxidized. In the absence of a redox-active analyte in channel 3, maximum light emission is observed at the anode. However, when an oxidizable analyte is present in channel 3, it competes with the ECL reactions in channel 2 to provide electrons for the cathodic reduction in channel 1. This results in a decrease in light intensity from the

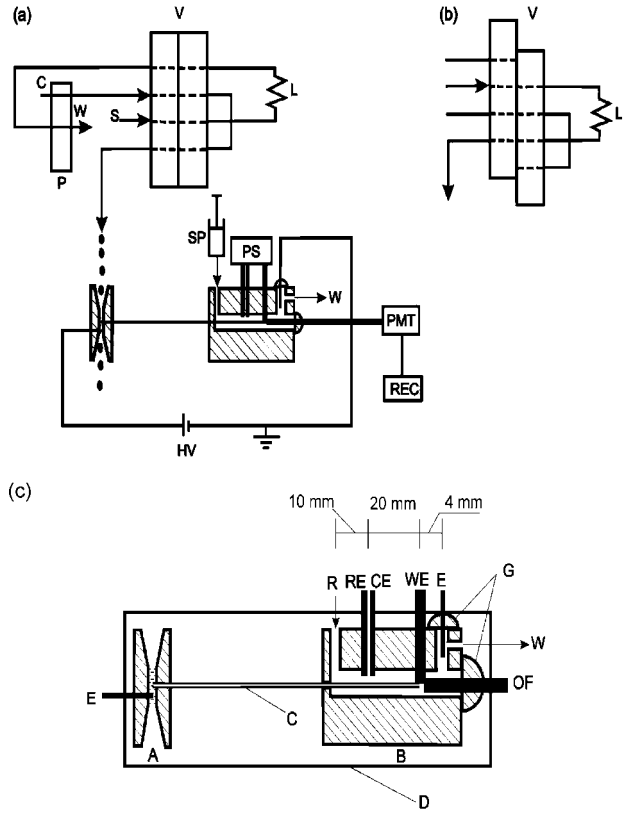

Figure 14. Experimental setup of the miniaturized CE system with FI sample introduction and ECL detection: (a) sample loading; (b) injection. S, sample; C, carrier; W, waste; P, peristaltic pump; SP, syringe pump; V, 8-channel 16-port valve; L, sample loop; HV, high-voltage supply; PS, potentiostat. (c) Schematic diagram of the microfluidic device (not to scale). A, falling-drop interface (inlet tubular reservoir); B, ECL reaction and detection cell (outlet reservoir); C, separation capillary; D, chip baseplate; E, Pt wire electrodes for high-voltage supply connections; RE, Ag/AgCl reference electrode; CE, counter electrode; WE, Pt working electrode; G, epoxy glue; OF, optical fiber; R, ECL reagent [$Ru(bpy)_3^{2+}$] inlet; W, waste. Dimensions not to scale. Reprinted with permission from ref 265. Copyright 2002 Elsevier.

electrode in channel 2, indicating the presence of the target analyte. Reducible analytes can be also detected with this three-channel method. For example, if only buffer is present in channel 3 and the analyte is present in channel 1, then the device is essentially identical to the two-channel device shown in Scheme 10. All three proposed approaches rely on charge balance between the anode and cathode. In other words, the current at the cathode must equal the current at the anode. Accordingly, there is a correspondence between the number of electrons consumed at the cathode and the ECL photon flux at the anode.

An integrated ITO electrode-based $Ru(bpy)_3^{2+}$ ECL detector for a PDMS microchip CE device (Figure 15) was first reported by Wang's group in 2003.[269] The microchip CE-ECL system utilizes an ITO-coated glass slide as the chip substrate with a photolithographically fabricated ITO electrode located at the end of the CE separation channel. The high separation electric field of CE was found to have no significant influence on the ECL detector; hence, no decoupler was needed in this microchip CE-ECL system. This system was used for the rapid analysis of lincomycin in a urine sample without pretreatment[274] and for the study of the interaction between biotin and avidin based on the separation of a mixture of 2-(2-aminoethyl)-1-methylpyrrolidine (AEMP) and biotinylated AEMP.[275] A simultaneous

Scheme 10[a]

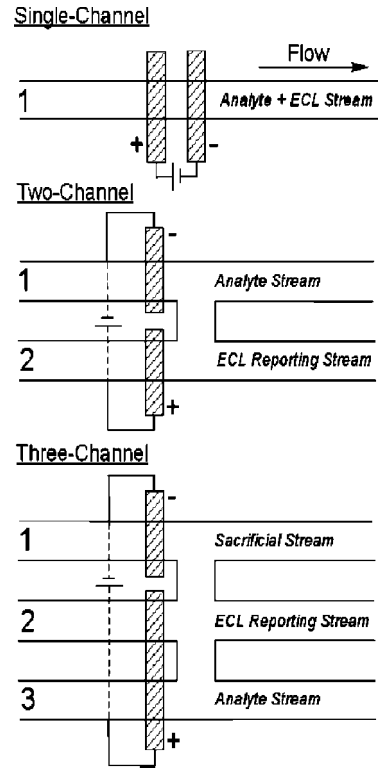

[a] Reprinted with permission from ref 273. Copyright 2003 American Chemical Society.

electrochemical (EC) and ECL dual detection to microchip CE, in which $Ru(bpy)_3^{2+}$ was used as an ECL reagent as well as a catalyst [in the formation of $Ru(bpy)_3^{3+}$] for EC detection was also reported.[276] Chen's group constructed a simple and universal wall-jet configuration for the microchip CE-ECL detection system, to which both precolumn and postcolumn detection modes were applied to determine TPrA, tramadol, and lidocaine.[267] In contrast to the above CE-ECL devices, in which solution phase $Ru(bpy)_3^{2+}$ was either added to the running buffer or placed in the detection reservoir, solid state ECL detectors coupled with microchip CE by immobilizing $Ru(bpy)_3^{2+}$ into either Eastman AQ55D–silica–carbon nanotube composite thin film on a patterned ITO electrode[268] or zirconia−Nafion composite on a GC disk electrode[277] have been constructed and used for the detection of proline[268] and pharmaceuticals of tramadol, lidocaine, and ofloxacin.[277] Detailed fabrication of the second solid state ECL detector can be found in ref 278.

A flow cell system based on BioVeris (BV) technology for ECL assays employing magnetic beads is shown in Figure 16.[66] The sample, reagents such as $Ru(bpy)_3^{2+}$ and TPrA buffer, and magnetic beads are combined in microwells, incubated, and aspirated into the detection module (flow cell system), followed by the collection of modified magnetic beads on the top of the working electrode with a magnet. After application of the electrochemical potential to the electrode, coreactant ECL signals are generated and measured with a photodetector such as a photodiode or a PMT located above the electrode.

4.3. Light Detection

Among three commonly used photodetectors, namely, avalanche photodiodes (APD), photomultiplier tubes (PMTs),

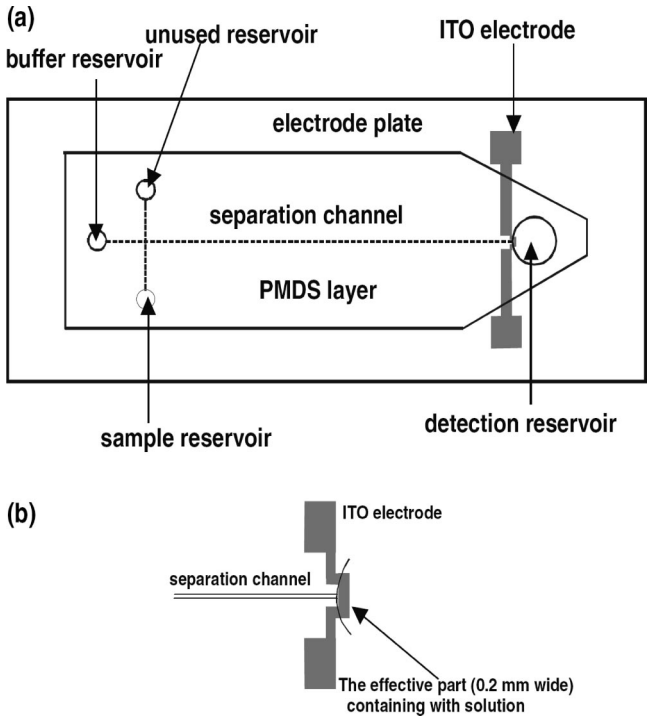

Figure 15. Schematic of a microchip CE-ECL device. (a) Top view of the polydimethylsiloxane (PDMS) layer and electrode plate. Separation channel dimensions: 15 μm deep × 48 μm wide at the bottom and 60 μm wide at the top × 45 mm from the intersection to the detection reservoir, and 5 mm from the intersection to the sample, buffer, and unused reservoirs. (b) Enlargement of the detection region. Distance between the separation channel outlet and the ITO electrode is 30 μm. Reprinted with permission from ref 269. Copyright 2003 American Chemical Society.

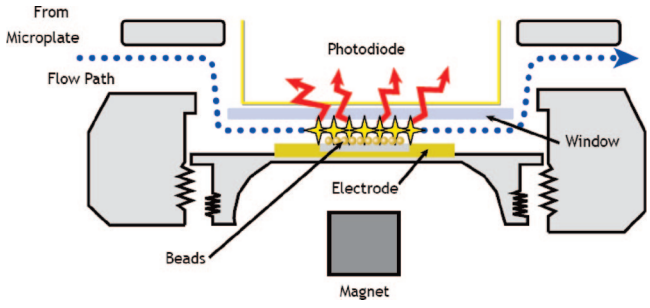

Figure 16. Schematic diagram of a flow system based on BioVeris technology using magnetic beads as a solid support for binding reactions and ECL measurements. Reprinted with permission from ref 66. Copyright 2007 Roche Diagnostics.

and charged coupled device (CCD) cameras, PMTs provide the most sensitive means of detecting light and are capable of detecting single photons. Table 4 compares the performances of these popular choices with those of other common photodetectors.[279] For quantitative analysis of a given analyte (emitter) or its related species, ECL intensity measurements are normally required, whereas ECL spectral recording is usually used for qualitative analysis.

The most popular PMTs used for ECL study are probably Hamamatsu[280] R4240 and R928 PMTs with spectral response ranges of 185–710 and 185–900 nm, respectively. Both PMTs feature extremely high cathode sensitivity, low dark current, and good S/N ratio. For the detection of ECL generated from $Ru(bpy)_3^{2+}$ species, R928 PMT may be better than R4220, because the $Ru(bpy)_3^{2+}$ ECL spectrum covers a spectral range of about 550−800 nm with a maximum emission at ~620 nm. The Hamamatsu H7421-40 metal package photon counting PMT has been recently reported in the application of ECL study.[284] The PMT uses a GaAsP photocathode that shows an exceptionally high quantum efficiency of 40% at 580 nm and very low dark count of ~100–300/s. For extremely weak ECL measurements, such as in the ECL spectral recording experiments, the photodetector, such as a PMT or CCD camera, often needs to be operated under low temperatures, so that the dark current can be reduced. Detailed discussions of this aspect can be found in refs 51 and 285.

4.4. Commercial ECL Instruments

The first commercial ECL instrument was produced by Igen International, Inc. (now BioVeris, part of Roche Diagnostics Corp.)[66] in 1994,[286] which is adapted to measure ECL labels [$Ru(bpy)_3^{2+}$ or its derivatives] present on the surface of magnetically responsive beads in the presence of TPrA (Figure 16). Three models of M-series ECL analyzers are currently available from BioVeris Corp.: M1M, M1MR, and M-384. The analyzers are either single-channel (M1M and M1MR) or multichannel (M-384, eight channels) flow-based detection instruments designed to meet the throughput needs of pharmaceutical research, industrial, academic, and government research laboratories. All analyzers employ an on-line automated separation to reduce nonspecific interferences and improve precision for enhanced assay performance. The M1MR analyzer is the M1M instrument with research software installed. It is an open system used for assay development. The M-384 analyzer, however, was designed mainly for industrial use. It contains two main components: (1) a sample handling and detection unit and (2) a built-in computer with application-specific software for instrument control and data handling. Figure 17 shows several examples of commercial flow cell-based (A−G) or imaging-based (H−L) ECL instruments.[51,168]

The Sector Imager and Sector PR Reader ECL instruments developed by Meso Scale Discovery (MSD)[65] (Figure 17H,I) use disposable screen-printed carbon ink electrodes within the wells of multiwell plates. Each well contains several binding domains (MULTI-SPOT) that react with specific targets. ECL is generated using $Ru(bpy)_3^{2+}$ analogues–$Ru(bpy)_3^{2+}$-(4-methyl sulfonate) NHS ester label (MSD SULFO-TAG) and TPrA or similar coreactants, and the light is collected with either an ultralow-noise CCD camera for ultimate sensitivity, wide dynamic range, and rapid read times (Sector Imager) or a photodiode array for fast and efficient detection (Sector PR Reader). Figure 18 shows a schematic diagram of a multispot plate assay for four human cytokines.

A commercial CE-ECL system developed at the Changchun Institute of Applied Chemistry, Chinese Academy of Sciences, and manufactured by Xi'an Remax Electronic Co. Ltd., (Xi'an, China) has been recently reported (Figure 19).[8,259]

4.5. Other ECL Setups for Emitted Light Intensity Measurements

A typical homemade ECL instrument for ECL intensity measurement would include a potentiostat, an electrochemical cell, a light detector, and a data acquisition system. Many modern computer-based potentiostats, such as CH660A (CH Instruments, Austin, TX)[288] and Autolab PGSTAT100 (Autolab Electrochemical Instruments, The Netherlands),[289] come with external signal recording functions, which can

Table 4. Comparison of Photodetectors ($T = 25$ °C)[a]

device type	gain	spectral response range (nm)	responsivity	response time (ns)	dark current (nA)	refs
photomultiplier	$10^5-2\times10^7$	115−1400	10^3–10^6 A/W	0.15–13	0.015–200	280
p-n photodiode	1 or less	190−1650	0.06–0.4 A/W	~1000	0.001–0.2	280, 281
silicon *p-n* photodiode	1 or less	190−1100	0.3–0.6 A/W	150–2500	0.002–0.2	280
p-i-n photodiode	1 or less	190−1100	0.14–0.7 A/W	10–10^6	0.001–10	281
silicon APD	50–100	400−1000	15–50 A/W	>0.003	0.05–30	280
bipolar phototransistor	10^2	400−1100	50–100 A/W	0.02	<100	282
bipolar photodarlington	$10^4-5\times10^4$	400−1100	200–400 A/W	$2.5\times10^6-5\times10^6$	<100	282
CCD	1 or less	200−1200	0.60–2 μV/e	$2\times10^6-1.4\times10^8$	1000−4000 e/pixel/s	280, 283

[a] Modified from ref 279.

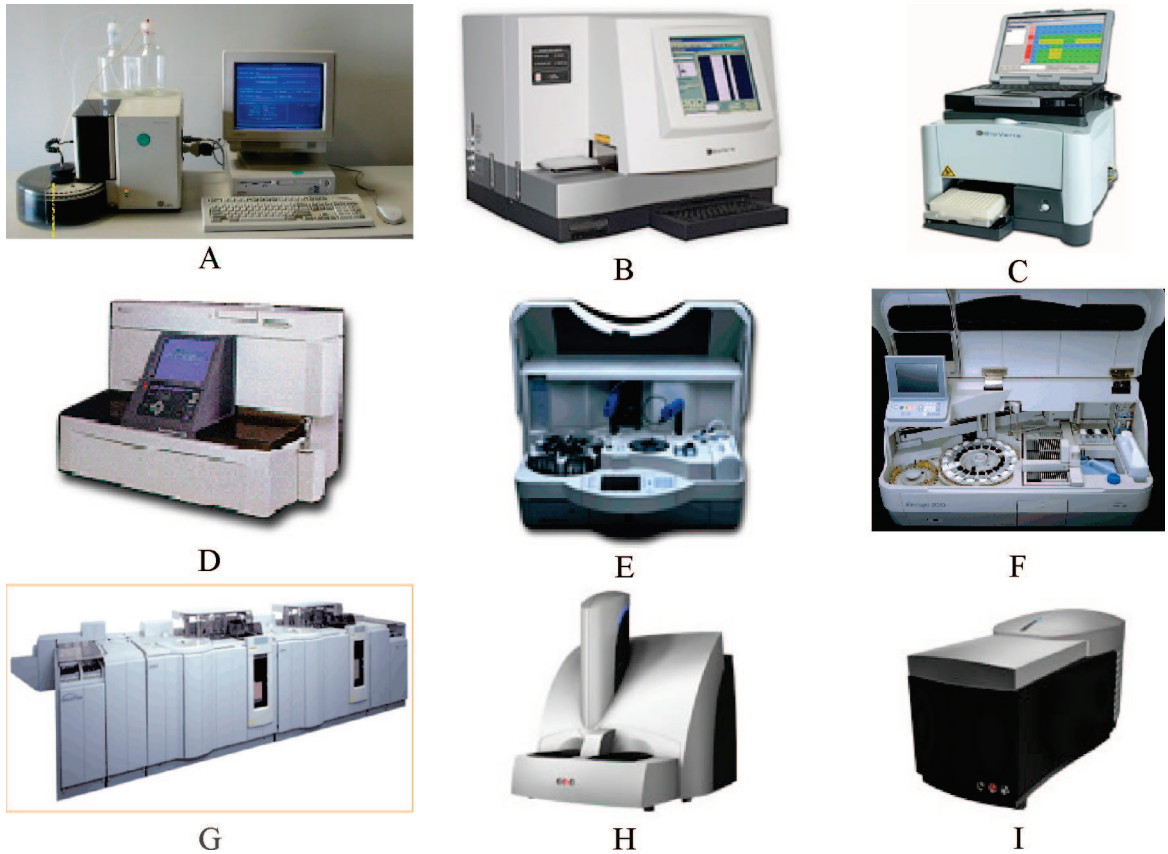

Figure 17. Commercial flow cell-based (A−G) or imaging-based (H−I) ECL instrumentation: (A) ORIGEN 1.5; (B) M series M-384 analyzers by BioVeris Corp.;[66] (C) M1M analyzers by BioVeris Corp.; (D) PicoLumi by Eisai, Japan; (E) Elecsys 1010; (F) Elecsys 2010 and (G) MODULAR system containing E-170 immunoassay module by Roche Diagnostics;[66] (H) Sector Imager 6000 and (I) Sector PR Reader 400 by Meso Scale Discovery.[65] Modified from refs 51, 65, 66, and 68.

be used to simultaneously record/collect the ECL and electrochemical signals. Light detection can be made by a bare PMT (e.g., Hamamatsu R4240 or R928[280]) biased at a high voltage (from ~−500 to −1000 V) with a high-voltage power supply (e.g., Brandenburg Photomultiplier Power Supply). The light signal (as photocurrent) can be measured with a highly sensitive electrometer (e.g., Keithley 6517, 6514 electrometer, Keithley, Cleveland, OH[290]) and converted to a voltage (normally in the range of ±2 V) that is collected/recorded to the computer. The PMT and the electrochemical cell must be placed in a light-tight box to avoid any environmental light interference. Figure 20 shows a set of homemade ECL instruments fabricated in this author's research laboratory.[291]

Wilson et al.[120,224] recently reported a flow injection electrochemiluminometer either with (Figure 21) or without a magnet in the flow cell for enzyme immunoassays of explosives 2,4,6-trinitrotoluene (TNT) and pentaerthyritol tetranitrate (PETN). Also, a fully automated sequential injection analyzer for simultaneous ECL and amperometric detection has been described.[292] The instrument is composed of a peristaltic pump, a multiposition selection valve, a homemade potentiostat, a thin-layer electrochemical/optical flow-through cell, and a light detector (Figure 22).

5. ECL Luminophores

In the past several years, a number of new ECL-emitting species were synthesized and their ECL properties were investigated. Driving forces of these kinds of studies include (a) finding new luminophores with higher ECL efficiencies and (b) modifying a moiety of the emitter so that it can be used for labeling of biomolecules. All luminophores discussed in the following section are classified into three categories: (a) inorganic systems, which mainly contain organometallic complexes; (b) organic systems, which cover polycyclic aromatic hydrocarbons (PAHs); and (c) semiconductor nanoparticle systems.

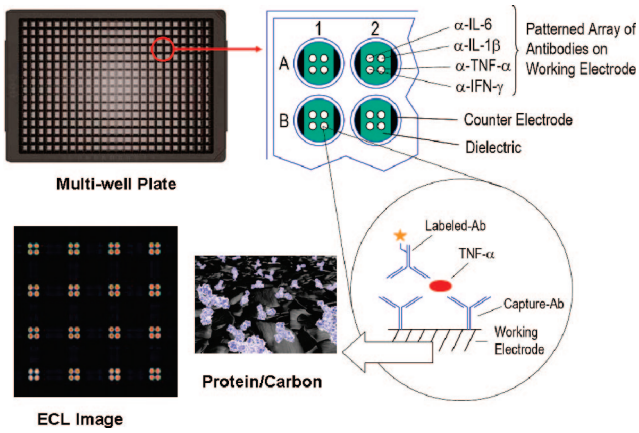

Figure 18. Schematic diagram of a multispot plate assay for four human cytokines. Each spot within each well of the multiwell plate contains capture antibody specific for one cytokine. (Inset) Images of the ECL emitted from assays and protein immobilized on carbon electrode surface. Modified from Meso Scale Discovery.[65]

Figure 19. MPI-A capillary electrophoresis−electrogenerated chemiluminescent analyzer developed at the Changchun Institute of Applied Chemistry, Chinese Academy of Sciences, and manufactured by Xi'an Remax Electronic Co. Ltd. (Xi'an, China). Reprinted with permission from refs 8 and 287. Copyright 2004 Elsevier.

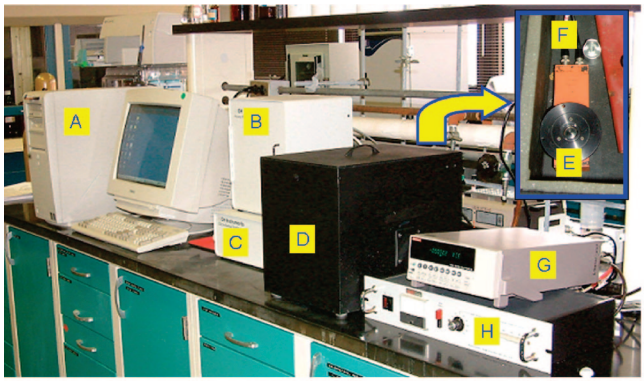

Figure 20. Homemade ECL instrumental setup from Dr. Wujian Miao's research laboratory in the Department of Chemistry and Biochemistry at the University of Southern Mississippi: (A) computer system; (B) Faraday cage; (C) potentiostat; (D) light-tight metal box containing (E) PMT and (F) sample holder; (G) electrometer; (H) high-voltage power supply.

5.1. Inorganic Systems

Because of their excellent properties in photochemistry, electrochemistry, and ECL, $Ru(bpy)_3^{2+}$ and its derivatives comprise one of the most extensively studied classes of

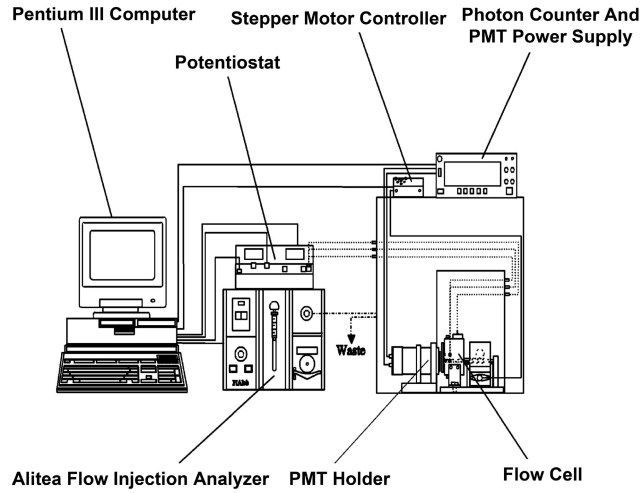

(a)

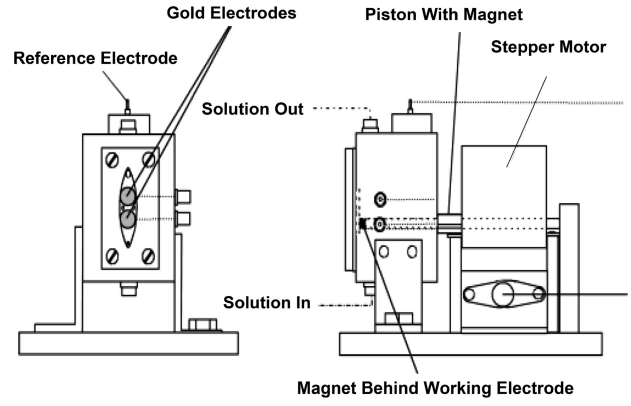

(b)

Figure 21. (a) Flow injection electrochemiluminometer and (b) flow cell with a magnet concentrator. Reprinted with permission from ref 120. Copyright 2003 American Chemical Society.

coordination complexes.[7,33,58,162] Many attempts have been made in designing or modifying the ligands of the complexes so as to improve both the light-emitting and the electron transfer performances of such systems. A very recent effort in this field was the synthesis and thorough characterization of a new family of mono- and dinuclear Ru(II) polypyridyl complexes containing 5-aryltetrazolate ligands such as the deprotonated form of 4-(1*H*-tetrazol-5-yl)benzonitrile (4-TBNH) and bis(1*H*-tetrazol-5-yl)benzene (BTBH2) (Figure 23).[293] The electrochemistry of the complex $[Ru(4\text{-}TBN)]^+$ in MeCN showed four one-electron reduction processes and a one-electron oxidation. The first two reductions were completely reversible, whereas the successive two were affected by chemical follow-up reactions associated with probably the deprotonation, either by the solvent or by the electrolyte, of one of the tetrazolate nitrogens. As shown in Figure 24, the voltammetric curve of the dinuclear $[Ru(4\text{-}TBN)Ru]^{3+}$ complex shows five reduction peaks and two oxidation ones. The two oxidation peaks are both reversible one-electron processes, and the first one is centered on the Ru(II) bound to the tetrazolate moiety of the bridge ligand. The electrochemical behavior of the dinuclear $[Ru(BTB)Ru]^{2+}$ complex is very similar to that of mononuclear $[Ru(4TBN)]^+$ one with one oxidation and four reduction processes, except that two-electron transfer reactions for each peak are involved. ECL spectra of the complexes were produced by ion annihilation reactions and are displayed in

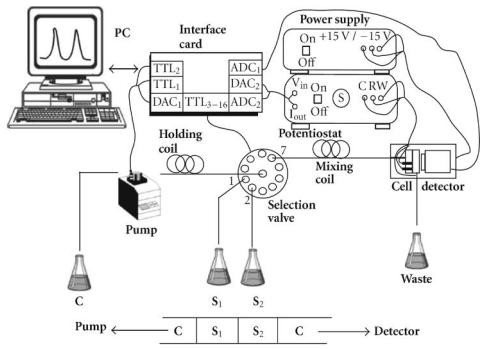

(a)

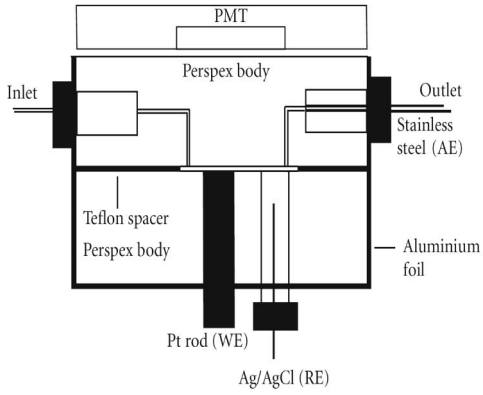

(b)

Figure 22. (a) Experimental configurations of the sequential injection analyzer for ECL detection. S_1, sample containing oxalate or H_2O_2; S_2, 5 mM $Ru(bpy)_3^{2+}$ in PBS buffer (pH 6) or 0.1 mM luminol in 10 mM NaOH; C, carrier (10 mM KCl). (b) Schematic diagram of the electrochemical/optical flow-through cell. Reprinted with permission from ref 292. 2006 Hindawi.

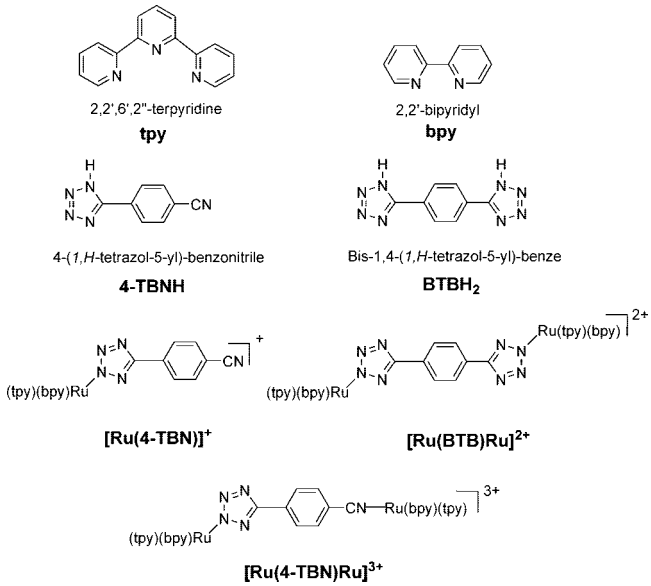

Figure 23. Ligands, complexes, and acronyms used in ref 293.

Figure 25. An exceptionally high ECL efficiency of 150% for the dinuclear $[Ru(4\text{-}TBN)Ru]^{3+}$ complex has been observed with respect to that of $Ru(bpy)_3^{2+}$, which has an absolute ECL efficiency of 0.05 in MeCN.[294–296] This result suggests that the yield for the formation of the excited states is close to 100%, which is promising for a future development of the species in ECL devices. Previously, ECL in

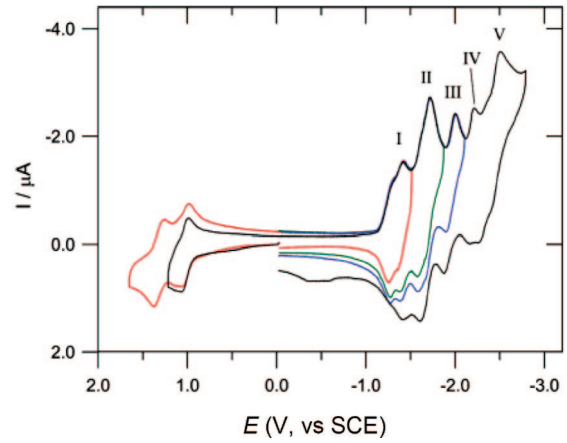

Figure 24. Cyclic voltammetric curve of 1 mM of dinuclear complex $[Ru(4\text{-}TBN)Ru]^{3+}$ in 0.05 M $(TBA)PF_6$/MeCN solution: working electrode, 1.25 mm diameter Pt disk; reference electrode, SCE; *T*, 25 °C; scan rate, 1 V/s. Reprinted with permission from ref 293. Copyright 2006 American Chemical Society.

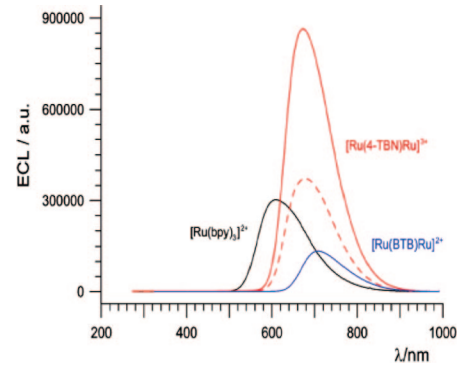

Figure 25. ECL spectra of the reference compound $Ru(bpy)_3^{2+}$ (black trace), $[Ru(BTB)Ru]^{2+}$ (blue trace), and $[Ru(4\text{-}TBN)Ru]^{2+}$ (red traces). The dashed red line for $[Ru(4\text{-}TBN)Ru]^{2+}$ is the spectrum obtained by annihilation of one-electron-oxidized and -reduced forms; the full red line is obtained for the doubly oxidized and reduced forms of complex. All ECL spectra were collected for 1 mM MeCN solutions and $(TBA)PF_6$ as supporting electrolyte, 25 °C, and accumulation time 4 min. Reprinted with permission from ref 293. Copyright 2006 American Chemical Society.

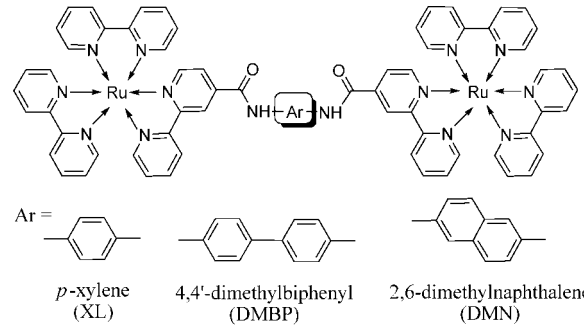

Figure 26. Aryl-diamide-bridged binuclear $Ru(bpy)_3^{2+}$ complexes reported in ref 298.

solution and solid state of several Ru(II) complexes containing tetrazolate groups was reported from the same research group.[297]

The synthesis and photophysical, electrochemical, and ECL properties of three symmetrical aryl-diamide bridged binuclear $Ru(bpy)_3^{2+}$ complexes (Figure 26) have also been presented.[298] All complexes showed characteristic metal-to-ligand charge transfer (MLCT) transition adsorption and similar redox behavior. No or very weak interactions between

the two Ru(II) centers were found, and their ECL emission maxima were red-shifted by ca. 65 nm compared to their fluorescence spectra. Strong ECL emissions [1−11.5 vs 1.0 of $Ru(bpy)_3^{2+}$] of the binuclear complexes, which may be related to the polarity and the conjugation of the entire molecules, indicate that this type of Ru(II) compound could be very useful in light-emitting devices and ECL-based biomolecule analysis.

A note on the synthesis, electrochemistry, spectroscopy, and ECL of five $(bpy)_2Ru(II)(L)(PF_6)$ complexes has been appeared,[299] where L represents different acetylacetonate ligands including (a) benzoylacetonate (BA), (b) thenoyltrifluoroacetonate (TTFA), (c) 4,4,4-trifluoro-1-phenyl-1,3-butanedionate (TFPB), (d) 1,1,1-trifluoro-2-4-pentanedionate (TFPD), and (e) dibenzoylmethide (DBM). All complexes presented absorptions in the UV−vis regions of the spectra, with visible absorptions ranging from 350 to 700 nm, typical of MLCT transitions. Depending on the nature of the acetylacetonate ligand, PL emission maxima of 575−600 nm were observed, which is also characteristic of MLCT transitions. Much lower ECL efficiencies ($\varphi_{ECL} \sim 0.013$–0.051) of the complexes than a $Ru(bpy)_3^{2+}$ standard ($\varphi_{ECL} = 1.0$) obtained from TPrA coreactant reactions suggest that electron-withdrawing substituents could dramatically decrease the ECL efficiencies of bipyridine Ru(II) complexes.

Systematic studies of the ligand effects on the ECL efficiencies of a series of 2,2′-bipyridyl-[300,301] and *o*-phenanthroline[302] (*o*-phen or phen)-substituted Ru(II) complexes containing different α-diimine ligands, such as 2-(2-pyridyl)-benzimidazole (PBIm-H), 2-(2-pyridyl)-*N*-methylbenzimidazole (PBIm-Me), 4,4′-dimethyl-2,2′-bipyridyl (dmbpy), and 4-carboxymethyl-4′-methyl-2,2′-bipyridyl (mbpy-CH_2COOH), have found a good correlation between the donor ability of the ligand and the number of substitutions and the ECL properties of the complexes. The ECL efficiency generally increases as fewer electron-donating ligands are introduced to the complexes. In other words, a strong donor ligand in a Ru(II) complex could cause a decrease in ECL emission. Because the donor property of the ligands increases in the order phen < bpy < dmbpy ≪ PBIm-Me < PBIm-H, the ECL efficiency of the Ru(II) complexes decreases in the order phen > bpy > dmbpy > PBIm-Me > PBIm-H (Table 5).

The studies of dendrimers peripherally functionalized with polypyridyl Ru(II) complexes have now been extended. Previously, enhanced ECL was observed for a dendrimer attached with multiple $Ru(bpy)_3^{2+}$ complex units.[303] When polyamidoamine (PAMAM) and polyamine dendrimers were used as carriers for covalent bonding of a series of Ru(II) complexes, such as $Ru(L)_2(L')$ [L = bpy, phen; L′ = bpy-CO-, mbpy-$(CH_2)_3$CO-, and phen-Cl], four and three identical units can be attached to the dendrimer, respectively.[304,305] Although free $Ru(phen)_3^{2+}$ has an ECL efficiency of 1.94 vs $Ru(bpy)_3^{2+}$ standard (Table 5), about half of the ECL intensity was obtained with respect to its counterpart when Ru(II) complexes were linked to the dendrimer network. In addition, the length of the spacer connected to the dendrimer from the complex significantly affected the ECL intensity; an alkyl chain spacer with at least three carbons seems to be needed for intense ECL production. Finally, much stronger ECL emissions were found when Ru(II) complexes were attached to polyamine rather than PAMAM dendrimers. It must be noted, however, that all dendrimer molecules contain a number of tertiary and secondary amine groups, which can act as coreactants and react with attached Ru(II) complexes

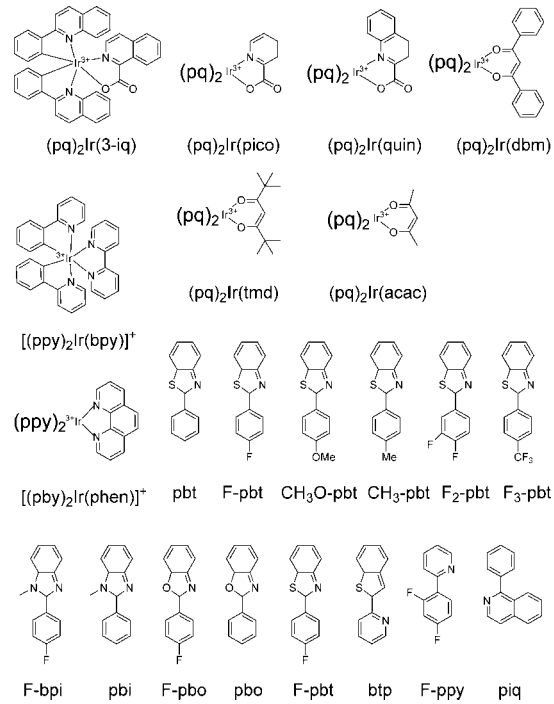

Figure 27. Cyclometalated iridium(III) complexes and ligands used. See section 10 for ligand abbreviations.

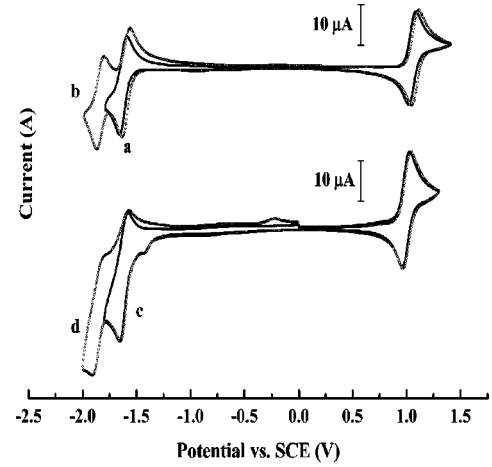

Figure 28. Cyclic voltammograms of 1 mM $(pq)_2Ir(pico)$: (a) scan to −1.8 V; (b) scan to −2.0 V and 1 mM $(pq)_2Ir(acac)$; (c) scan to −1.8 V; (d) scan to −2.0 V in the MeCN solution. Scan rate, 0.2 V/s; supporting electrolyte, 0.1 M $(TBA)PF_6$. Reprinted with permission from ref 307. Copyright 2007 American Chemical Society.

when sufficient anodic potential is applied (section 3.2.2.3). Consequently, strong background ECL can be generated in the absence of added coreactant.

Comparative study of seven $Ru(bpy)_3^{2+}$ derivatives with one or more mono-/bisubstituents at 4- and/or 4′-position(s) of bipyridine ring(s) has been carried out to examine the relationship between their PL and ECL efficiencies (Table 5).[306] ECL measurement in $Ru(bpy)_3^{2+}$ derivative/TPrA aqueous PBS buffer solutions (pH 6.8 with added nonionic surfactant) at the Pt electrode has led to a conclusion that due to the complexity of the ECL generation process, the PL efficiency cannot be used to predict ECL intensity and there is no obvious relationship between the PL quantum yield and the ECL intensity. For example, compared with $Ru(bpy)_3^{2+}$, the ethoxycarbonyl-substituted derivative, [Ru(b-

Table 5. Spectroscopic and ECL Properties of Inorganic Luminophores[a]

complex/reactant	coreactant	solvent for ECL	λ_{em} (nm)	λ_{ECL} (nm)	φ_{em}	φ_{ECL}[b]	refs
		Ruthenium					
$Ru(bpy)_3^{2+}$		MeCN	608	608	0.062	1.0[c]	[d]
$Ru(bpy)_3^{2+}$	TPrA	H_2O (PBS) or MeCN with electrolyte		610−620		1.0	[d]
$Ru(bpy)_3^{2+}$	$S_2O_8^{2-}$	H_2O-MeCN or MeCN with electrolyte		610−620		1.0	[d]
$[Ru(4\text{-}TBN)]^+$		MeCN (0.1 M $(TBA)PF_6$)	672		0.003		293
$[Ru(4\text{-}TBN)Ru]^{3+}$		MeCN (0.1 M $(TBA)PF_6$)	676	680	0.008	1.50	293
$Ru(BTB)Ru]^{2+}$		MeCN (0.1 M $(TBA)PF_6$)	680	710	0.003	0.40	293
$[Ru(bpy)_3CONH]_2$(XL)		MeCN (0.05 M $(TBA)PF_6$)	642	569	0.053	4	298
$[Ru(bpy)_3CONH]_2$(DMBP)		MeCN (0.05 M $(TBA)PF_6$)	638	570	0.081	0.5	298
$[Ru(bpy)_3CONH]_2$(DMN)		MeCN (0.05 M $(TBA)PF_6$)	636	570	0.058	6	298
$(bpy)_2Ru(BA)^+$		MeCN/0.2 M KH_2PO_4 (50:50, v/v)	600	∼600	0.022	0.032	299
$(bpy)_2Ru(DBM)^+$	TPrA	MeCN/0.2 M KH_2PO_4 (50:50, v/v)	600	∼600	0.012	0.051	299
$(bpy)_2Ru(TTFA)^+$	TPrA	MeCN/0.2 M KH_2PO_4 (50:50, v/v)	580	∼580	0.014	0.018	299
$(bpy)_2Ru(TFPB)^+$	TPrA	MeCN/0.2 M KH_2PO_4 (50:50, v/v)	600	∼600	0.0088	0.017	299
$(bpy)_2Ru(TFPD)^+$	TPrA	MeCN/0.2 M KH_2PO_4 (50:50, v/v)	580	∼580	0.014	0.013	299
$(bpy)_2Ru(phen\text{-}PPA\text{-}COOH)^{2+}$	TPrA	H_2O (0.2 PBS)/0.8 mM Triton X-100, 4 mM Tween 20	584				310
$(bpy)_2Ru(phen\text{-}BA\text{-}COOH)^{2+}$	TPrA	H_2O (0.2 PBS)/0.8 mM Triton X-100, 4 mM Tween 20	584				310
$Ru(PBIm\text{-}H)_3$	TPrA	H_2O (0.05 M PBS, pH 7)				0	300, 301
$Ru(bpy)(PBIm\text{-}H)_2$	TPrA	H_2O (0.05 M PBS, pH 7)				0	300, 301
$Ru(bpy)_2(PBIm\text{-}H)$	TPrA	H_2O (0.05 M PBS, pH 7)				0.04	300, 301
$Ru(PBIm\text{-}Me)_3$	TPrA	H_2O (0.05 M PBS, pH 7)				0	300, 301
$Ru(bpy)(PBIm\text{-}Me)_2$	TPrA	H_2O (0.05 M PBS, pH 7)				0.04	300, 301
$Ru(bpy)_2(PBIm\text{-}Me)$	TPrA	H_2O (0.05 M PBS, pH 7)				0.28	300, 301
$Ru(dmbpy)_2(PBIm\text{-}Me)$	TPrA	H_2O (0.05 M PBS, pH 7)				0.17	300, 301
$Ru(dmbpy)_3$	TPrA	H_2O (0.05 M PBS, pH 7)				0.48	300, 301
$Ru(bpy)(dmbpy)_2$	TPrA	H_2O (0.05 M PBS, pH 7)				0.60	300, 301
$Ru(bpy)_2(dmbpy)$	TPrA	H_2O (0.05 M PBS, pH 7)				0.93	300, 301
$Ru(bpy)_2$ $(mbpy\text{-}CH_2COOH)$	TPrA	H_2O (0.05 M PBS, pH 7)				0.85	300, 301
$Ru(phen)_3$	TPrA	H_2O (0.05 M PBS, pH 7)				1.94	300, 301
$Ru(phen)_2(PBIm\text{-}H)$	TPrA	H_2O (0.05 M PBS, pH 7)				0	302
$Ru(phen)(PBIm\text{-}Me)_2$	TPrA	H_2O (0.05 M PBS, pH 7)				0.11	302
$Ru(phen)_2(PBIm\text{-}Me)$	TPrA	H_2O (0.05 M PBS, pH 7)				0.28	302
$Ru(phen)(dmbpy)_2$	TPrA	H_2O (0.05 M PBS, pH 7)				0.46	302
$Ru(phen)(bpy)_2$	TPrA	H_2O (0.05 M PBS, pH 7)				1.33	302
$Ru(phen)_2(dmbpy)$	TPrA	H_2O (0.05 M PBS, pH 7)				0.94	302
$Ru(phen)_2(bpy)$	TPrA	H_2O (0.05 M PBS, pH 7)				1.62	302
$Ru(phen)_2$ $(mbbpy\text{-}CH_2COOH)$	TPrA	H_2O (0.05 M PBS, pH 7)				1.36	302
$Ru(phen)_2$ $(mbbpy\text{-}(CH_2)_3COOH)$	TPrA	H_2O (0.05 M PBS, pH 7)				1.69	302
$PAMAM\text{-}[Ru(bpy)_2$ $(mbpy\text{-}(CH_2)_3CO\text{-})]_4$	TPrA	H_2O (0.05 M PBS, pH 7)	590			2.54[e]	304
$PAMAM\text{-}[Ru(mbpy\text{-}(CH_2)_3CO\text{-})$ $(phen)_2]_4$	TPrA	H_2O (0.05 M PBS, pH 7)	585			0.67[e]	304
$PAMAM\text{-}[Ru((bpy)_2(bpy\text{-}CO\text{-})]_4$	TPrA	H_2O (0.05 M PBS, pH 7)	615			0.37[e]	304
$PAMAM\text{-}[Ru(phen)_2(bpy\text{-}CO\text{-})]_4$	TPrA	H_2O (0.05 M PBS, pH 7)	613			0.19[e]	304
$Dend\text{-}[CO\text{-}(CH_2)_3\text{-}mbpy\cdot Ru(bpy)_2]_3$	TPrA	H_2O (0.05 M PBS, pH 7)	606			4.32[e]	305
$Dend\text{-}[CO\text{-}(CH_2)_3\text{-}mbpy\cdot Ru(phen)_2]_3$	TPrA	H_2O (0.05 M PBS, pH 7)	596			2.52[e]	305
$Dend\text{-}[CO\text{-}(CH_2)_3\text{-}mbpy\cdot Ru(phen\text{-}Cl)_2]_3$	TPrA	H_2O (0.05 M PBS, pH 7)	608			1.45[e]	305
$Dend\text{-}[CO\text{-}(CH_2)_3\text{-}mbpy\cdot Ru(DTDP)_2]_3$	TPrA	H_2O (0.05 M PBS, pH 7)	600			3.90[e]	305
$Ru[bpy\text{-}(COOEt)_2]_3^{2+}$	TPrA	PBS, pH 6.8, with nonionic surfactant added	632		0.112	0.029	306
$Ru[bpy\text{-}(COOH)_2]_3^{2+}$	TPrA	PBS, pH 6.8, with nonionic surfactant added	622		0.150	0.091	306
$[Ru(bpy)_2(bpy\text{-}COOH)]^{2+}$	TPrA	PBS, pH 6.8, with nonionic surfactant added	627		0.109	1.22	306
$[Ru(bpy)_2(mbpy\text{-}COO\text{-}NHS\ ester]^{2+}$	TPrA	PBS, pH 6.8, with nonionic surfactant added	624		0.135	1.24	306
$[Ru(bpy)_2(bpy\text{-}O(CH_2)_7CH_3)]^{2+}$	TPrA	PBS, pH 6.8, with nonionic surfactant added	619		0.109	0.089	306
$[Ru(bpy\text{-}(COOH)_2)_2$ $(bpy\text{-}O(CH_2)_7CH_3)]^{2+}$	TPrA	PBS, pH 6.8, with nonionic surfactant added	637, 660		0.092	0.56	306

Table 5. Continued

complex/reactant	coreactant	solvent for ECL	λ_{em} (nm)	λ_{ECL} (nm)	φ_{em}	φ_{ECL} [b]	refs
		Iridium					
$(pq)_2Ir(quin)$		MeCN (0.1 M $(TBA)PF_6$)	571		0.28	0.69	307
	TPrA	MeCN (0.1 M $(TBA)PF_6$)		~595		18	307
	$S_2O_8^{2-}$ (10 mM)	MeCN (0.1 M $(TBA)PF_6$)				18	307
$(pq)_2Ir(pico)$		MeCN (0.1 M $(TBA)PF_6$)	571	~595	0.27	18	307
	TPrA	MeCN (0.1 M $(TBA)PF_6$)		~595		28	307
	$S_2O_8^{2-}$ (10 mM)	MeCN (0.1 M $(TBA)PF_6$)				25	307
$(pq)_2Ir(3\text{-}iq)$		MeCN (0.1 M $(TBA)PF_6$)	572	~595	0.18	12	307
	TPrA	MeCN (0.1 M $(TBA)PF_6$)		~595		38	307
	$S_2O_8^{2-}$ (10 mM)	MeCN (0.1 M $(TBA)PF_6$)				8.6	307
$(pq)_2Ir(acac)$		MeCN (0.1 M $(TBA)PF_6$)	589[f]	609	0.10[f]	3.1	307
	TPrA	MeCN (0.1 M $(TBA)PF_6$)		609		77	307, 311
	$S_2O_8^{2-}$ (10 mM)	MeCN (0.1 M $(TBA)PF_6$)				26	307
$(pq)_2Ir(tmd)$		MeCN (0.1 M $(TBA)PF_6$)	~590[f]	~615	0.10[f]	16	307
	TPrA	MeCN (0.1 M $(TBA)PF_6$)		615		~48	307, 311
	$S_2O_8^{2-}$ (10 mM)	MeCN (0.1 M $(TBA)PF_6$)				26	307
$(pq)_2Ir(dbm)$		MeCN (0.1 M $(TBA)PF_6$)	588		0.03	0.46	307
	TPrA	MeCN (0.1 M $(TBA)PF_6$)		~610		6.5	307
	$S_2O_8^{2-}$ (10 mM)	MeCN (0.1 M $(TBA)PF_6$)				0.21	307
fac-$Ir(ppy)_3$	TPrA	MeCN (0.1 M $(TBA)PF_6$)	510,[f] 517[f]	517	0.40[f]	0.33	311, 321
$[(ppy)_2Ir(bpy)]^+$	TPrA	MeCN (0.1 M $(TBA)PF_6$)	606[f]	606	0.04[f]	2	311
$[(ppy)_2Ir(phen)]^+$	TPrA	MeCN (0.1 M $(TBA)PF_6$)	606[f]	606	0.14[f]	4	311
$(F\text{-}pbt)_2Ir(acac)$/DCN		MeCN/dioxane (1:1, v/v) (0.1 M $(TBA)PF_6$)	545	~550	0.54	6	308, 314
$(F\text{-}pbt)_2Ir(acac)$/ABN		MeCN/dioxane (1:1, v/v) (0.1 M $(TBA)PF_6$)		~550		7.4	314
$(CH_3O\text{-}pbt)_2Ir(acac)$/DCB		MeCN/dioxane (1:1, v/v) (0.1 M $(TBA)PF_6$)	548	~550	0.46	7.6	314
$(CH_3\text{-}pbt)_2Ir(acac)$/DCB		MeCN/dioxane (1:1, v/v) (0.1 M $(TBA)PF_6$)	560	~560	0.41	4.4	314
$(F_2\text{-}pbt)_2Ir(acac)$/DCN		MeCN/dioxane (1:1, v/v) (0.1 M $(TBA)PF_6$)	562	~560	0.46	7	314
$(pbt)_2Ir(acac)$/DCN		MeCN/dioxane (1:1, v/v) (0.1 M $(TBA)PF_6$)	566	~565	0.44	5.4	308, 314
$(pbt)_2Ir(acac)$/DCB		MeCN/dioxane (1:1, v/v) (0.1 M $(TBA)PF_6$)		~565		6.4	308, 314
$(F_3\text{-}pbt)_2Ir(acac)$/DCN		MeCN/dioxane (1:1, v/v) (0.1 M $(TBA)PF_6$)	576	~580	0.32	5.8	314
$(F\text{-}pbi)_2Ir(acac)$/DCBP		MeCN/dioxane (1:1, v/v) (0.1 M $(TBA)PF_6$)	485	~485	0.27	4	308
$(pbi)_2Ir(acac)$/DCBP		MeCN/dioxane (1:1, v/v) (0.1 M $(TBA)PF_6$)	489	~490	0.47	1.4	308
$(pbi)_2Ir(acac)$/CPA		MeCN/dioxane (1:1, v/v) (0.1 M $(TBA)PF_6$)		~490		6.2	308
$(pbi)_2Ir(acac)$/CNL		MeCN/dioxane (1:1, v/v) (0.1 M $(TBA)PF_6$)		~490		6.8	308
$(ppy)_2Ir(acac)$/DCBP		MeCN/dioxane (1:1, v/v) (0.1 M $(TBA)PF_6$)	526	~526	0.72	11	308
$(F\text{-}pbo)_2Ir(acac)$/DCB		MeCN/dioxane (1:1, v/v) (0.1 M $(TBA)PF_6$)	516	~515	0.44	5	308
$(pbo)_2Ir(acac)$/DCB		MeCN/dioxane (1:1, v/v) (0.1 M $(TBA)PF_6$)	542	~540	0.38	6.8	308
$(btp)_2Ir(acac)$/DCB		MeCN/dioxane (1:1, v/v) (0.1 M $(TBA)PF_6$)	613	~610	0.12	1.6	308
$(piq)_2Ir(acac)$/DCN		MeCN/dioxane (1:1, v/v) (0.1 M $(TBA)PF_6$)	642	~640	0.31	4.2	308
$(piq)_2Ir(acac)$/DCB		MeCN/dioxane (1:1, v/v) (0.1 M $(TBA)PF_6$)		~640		4	308
Lead							
$Pb_4Br_{11}^{3-}$	TPrA	MeCN (0.1 M TBABr)	~550			0.0026	317
Boron							
$(pS\text{-}1)_2$[g]		CH_2Cl_2 (0.2 M $(TBA)PF_6$)	537[h]	~565	0.52[h]		319
DHA-DBP		CH_2Cl_2 (0.2 M $(TBA)PF_6$)	~540	550	0.67		320

[a] See section 10 for ligand abbreviations. ECL was generated via ion annhihilation if no coreactant is given (eq 3). If the annhiliation ECL was produced from a "mixing system",[122] the second reactant as the precursor of electrogenerated radical anion is listed after the backslash. [b] All ECL efficiencies (φ_{ECL}) are relative to $Ru(bpy)_3^{2+}$ systems; the absolute efficiency can be estimated using the listed φ_{ECL} value × 0.05 if the ECL was produced via annihilation. [c] The absolute ECL efficiency is 0.05 in MeCN by ion annihilation.[294–296] [d] Assigned value of 1.0 for comparison purpose. If possible, the same experimental conditions should be used for the studied system and the standard. [e] Data are for an entire unit, and the ECL efficienty for each Ru(II) complex should be the given value divided by the overall number of complexes included (e.g., 4 or 3). [f] Values obtained in thoroughly degassed CH_2Cl_2 solution using Rhodamine 6G in ethanol ($\varphi_{em} = 0.95$) as a standard.[311] [g] See Scheme 11 for the structure. [h] Measured in MeCN.

py-$(COOEt)_2)_3]^{2+}$, one of the most efficient luminophores under photoexcitation, did not generate reasonably intense ECL, whereas luminophores with lower PL quantum yields demonstrated higher ECL. A similar conclusion was also reached for iridium(III) complexes under both annihilation and coreactant ECL conditions.[307,308]

Although a number of $Ru(bpy)_3^{2+}$-based ECL labels are commercially available for amine, carbohydrate, carboxylic acid, thiol, and DNA linkage,[66,168,309] several new −COOH-functionalized derivatives of $Ru(bpy)_3^{2+}$ have been recently published[306,310] (Table 5), which can be used to tag proteins or species with primary amine groups.

Extremely efficient ECL from cyclometalated Ir(III) complexes has been recently reported,[307,308,311–313] in which the ECL efficiency values from some chelates were even higher than PL efficiencies.[307] The first group of complexes have a common formula of $(pq)_2Ir(L)$, in which pq is a 2-phenylquinoline anion and L is a monoanionic bidentate ligand [e.g., acetylacetonate (acac), picolinate (pico), see Figure 27].[307] Their electrochemical and spectroscopic behaviors are similar to those of $Ru(bpy)_3^{2+}$. In MeCN, both one-electron oxidation around 1.0−1.1 V vs SCE and the first reduction ranging from −1.45 to ∼−1.70 V vs SCE are reversible in most cases. The maximum ECL emissions are around 600–615 nm, which is about 20 nm red shifted from their PL emissions. ECL efficiencies were measured in three ways: ion annihilation, oxidative-reduction ECL with TPrA as the coreactant, and reductive-oxidation ECL with $S_2O_8^{2-}$ as the coreactant. Most of the complexes in this group exhibited exceptionally efficient ECL efficiencies. For example, $\varphi_{ECL} = 0.88$ for $(pq)_2Ir(pico)$ was observed in the annihilation process, which is ∼17 times higher than that of $Ru(bpy)_3^{2+}$. Under the same experimental conditions, up to 77 and 26 times higher ECL efficiencies with respect to a $Ru(bpy)_3^{2+}$ standard were observed for $(pq)_2Ir(acac)$/TPrA and $(pq)_2Ir(tmd)$ (tmd = 2,2,6,6-tetramethyl-3,5-heptanedione)/$S_2O_8^{2-}$ systems, respectively. As expected, the ECL intensity depends primarily on the electrochemical stability of the redox precursors of $(pq)_2Ir(L)$. For example, $(pq)_2Ir(acac)$, which shows irreversible reduction, has produced efficient ECL during the oxidative-reduction process but less intense ECL during both the annihilation and reductive-oxidative processes (Figure 28 and Table 5). In contrast, redox species generated from $(pq)_2Ir(pico)$ are very stable. Consequently, highly efficient ECL is produced in all three processes.

The second group of Ir(III) complexes can be formulated as $[(ppy)_2Ir(L)]^+$, where ppy = 2-phenylpyridine anion and L = bpy and phen.[311] Maximum emissions from PL and ECL are all close to 605 nm, and TPrA coreactant ECL intensities are 2 and 4 times that of the $Ru(bpy)_3^{2+}$/TPrA system, respectively (Table 5).

A common formula for the third group of Ir(III) complexes can be expressed as $L_2Ir(acac)$, where L are different organic ligands (see Figure 27) able to coordinate Ir(III) ions of the covalent metal−nitrogen and the ionic metal−carbon bonds.[308,314] Extremely high ECL efficiencies [up to 0.55, 15 times of that from $Ru(bpy)_3^{2+}$] were observed via ion annihilation between one-electron oxidized Ir(III) complex $L_2Ir(acac)^+$ and one-electron reduced aromatic nitrile species A^- (Table 5). Most of the $L_2Ir(acac)$ complexes can be also reversibly reduced to form monoanion and dianion species, but their first reduction waves were more negative than that from added aromatic nitriles (A). ECL spectra exhibited traces of vibronic structures, and their emissions depended on the nature of ligand L. Colors from fairly green (∼490 nm) to deep red (∼640 nm) were observed, which may be useful for the fabrication of display devices and multiplexing analysis based on ECL. It is believed that the bright ECL emission is attributed to the formation of strongly emissive triplet excited $^3L_2Ir(acac)^*$ species from the reaction of

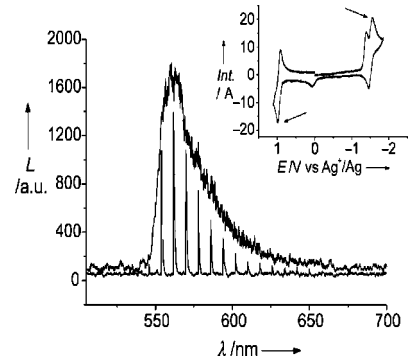

Figure 29. ECL spectra $(pS\text{-}1)_2$ (see Scheme 11 for structure) in CH_2Cl_2 [0.1 M $(TBA)PF_6$], with switch times of 1 s^{-1} (discrete lines) and 50 ms^{-1} (curve). (Inset) Corresponding CV, with the applied potentials indicated by the arrows. Reprinted with permission from ref 319. Copyright 2006 Wiley-VCH.

$$L_2Ir(acac)^+ + A^- \rightarrow {}^3L_2Ir(acac)^* + A \qquad (25)$$

ECL from Nafion and poly(9-vinylcarbazole) (PVK) bound Ir(III) complexes has also been investigated using TPrA as a coreactant in aqueous (0.2 M PBS, pH 8) and MeCN [0.10 M $(TPA)PF_6$ media].[315] Significant and reproducible ECL was observed for $Ir(ppy)_3$ and $(btp)_2Ir(acac)$ complexes when bound in PVK in MeCN, and $(F\text{-}ppy)_2Ir(pico)$ (Figure 27) displayed ECL in both aqueous and MeCN solutions when bound in Nafion and PVK, respectively.

Photoluminescence detection of Pb(II) in nanomolar concentrations[316] has led to the ECL study of Pb(II)−bromide complexes.[317] Weak ECL was obtained from a $Pb_4Br_{11}^{3-}$ cluster formed in situ by reaction of Pb(II) and bromide ions in MeCN (0.1 M TBABr) with TPrA as a coreactant. The ECL mechanism of this system is unclear, and the ECL based LOD of Pb(II) was around micromolar levels.

Because boron-based dipyrromethene (BDP) complexes have been used as laser dyes due to their high PL QYs, a number of studies have examined the ECL behavior of several selected BDP dyes in an attempt to use these molecules as either luminophore labels or molecular switches.[318–320] As shown in Figure 29 and Scheme 11, ECL spectra with the maximum emission at ∼565 nm are observed for *m*-phenyl-substituted BDP disulfide $(pS\text{-}1)_2$ when alternating potentials are applied to oxidize and reduce the dye.[319] Similar behavior was obtained for dihydroazulene–BDP dye (Table 5)[320] and several other BDP dyes.[318]

5.2. Organic Systems

A number of series of donor−acceptor type luminophores have recently been synthesized in an attempt to understand the effect of structure on their spectroscopic, electrochemical, and ECL behaviors. The first five series of luminophores include 32 compounds (Table 6, **1**−**32**) with quinoline and isoquinoline acceptors and aryl donors linked by a triple bond.[322,323] All of the compounds showed blue-green fluorescence in acetonitrile and more strongly in dichloromethane. Low Stokes shifts in the range of 25–88 nm were

Scheme 11. Mechanism of ECL Generation by Annihilation in (pS-1)$_2$[a]

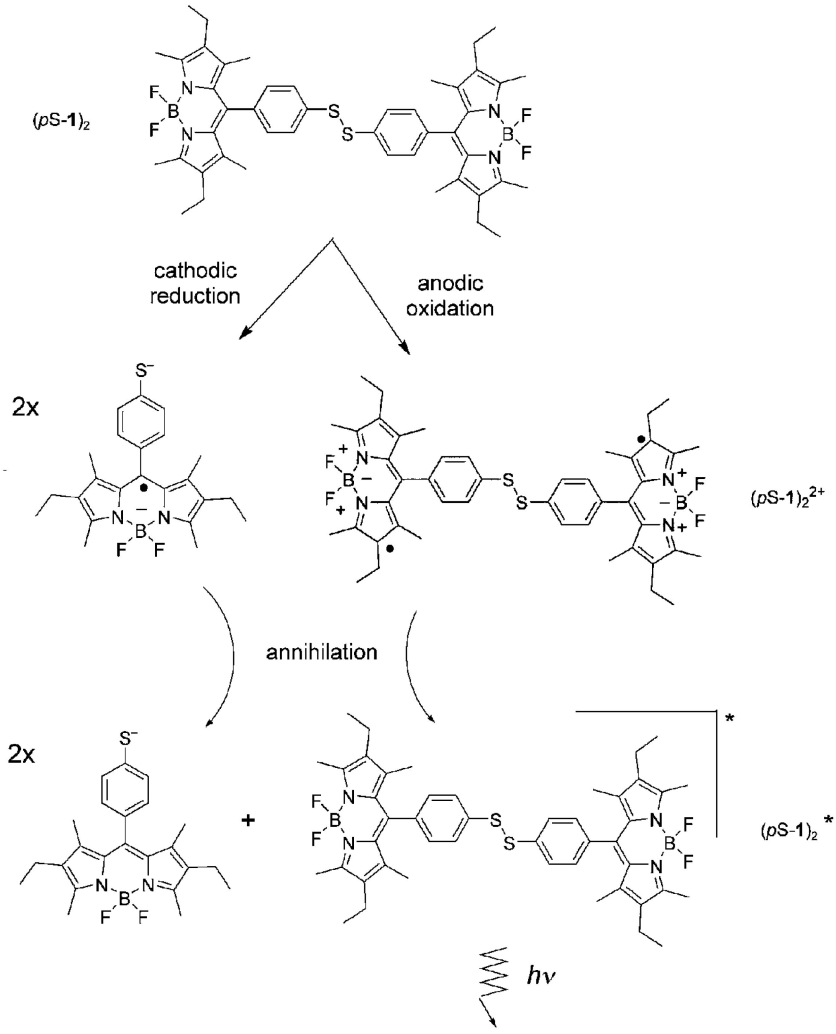

[a] The involvement of (pS-1)$_2^-$ as a minority electron donor cannot be ruled out. Reprinted with permission from ref 319. Copyright 2006 Wiley-VCH.

observed for compounds bearing no or weak donors (−H, −Me, −OMe), and those bearing strong donors revealed larger Stokes shifts in the range of 150–188 nm, consistent with intramolecular charge transfer (ICT).[324] Very similar CVs were obtained for all compounds, which showed a reversible reduction in the range of −0.80 to −2.16 V vs Ag/AgCl and an irreversible oxidation process from 0.55 to 2.16 V vs Ag/AgCl. The first reduction and oxidation waves were ascribed to reduction at the quinolinyl acceptor moiety and oxidation at the donor-substituted phenyl moiety, respectively. Among the five series, the first group (compounds **1**–**7**) proved to be the most difficult for reduction. With respect to oxidation, compounds with weaker electron-donating groups generally exhibited higher oxidation potentials. ECL emissions were well observed for those compounds with ethynyl-bridged donor groups attached at the carbon that has an ortho- and para-like relationship with respect to the ring nitrogen heteroatom in the quinolinyl/isoquinolinyl moiety, whereas very weak to no ECL was observable for those compounds in which the donors are linked through the triple bond with a meta-like relationship. The ECL for weak donor-substituted compounds [1–3,9,10,15–17,21,22,27–29] is believed to be from the normal excimer formed by annihilation of radical ions generated electrochemically due to the planar nature of these molecules (E-route, eq 7, and Scheme 12a). Compounds with strong donor groups (**4**–**8**, **31**) produced ECL from their ICT states through direct annihilation of radical ions due to the large twist angle between the plane of the quinoline moiety and the donor-bearing phenyl moiety (Scheme 12b). In general, ICT ECL can be generated only by those systems with polar charge separation and low orbital overlapping between the donor and acceptor moiety. A special aggregation of H-type excimer[325] formation in **18**–**20** is believed to be responsible for the observed blue shift of ECL in comparison with their solution fluorescence maxima. Only the 4-quinolinyl systems show such H-type excimers in which two quinolinyl moieties are stacked face to face with donor-bearing phenyl groups projecting perpendicularly away from each other (Schemes 12c and 13). Additionally, ECL for compounds **1**–**8** is believed to follow the S-route (eq 3a), and the rest (**9**–**32**) follow the T-route (eq 3b). This is because, only in the former case, the annihilation enthalpy changes estimated from CVs (eq 5) are sufficiently larger than their singlet energies estimated from FL emissions.

Table 6. Spectroscopic and ECL Properties of Organic Luminophores[a]

compounds	R	code	λ_{em} (nm)	φ_{em}[b]	λ_{ECL} (nm)	φ_{ECL}	refs
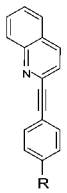	-H	**1**	361	0.013	463	1.3[c]	323
	-Me	**2**	364	0.0022	472	0.5[c]	323
	-OMe	**3**	405	0.0060	479	37.8[c]	323
	-NMe_2	**4**	527	0.24	540	2.0[c]	323
	-NEt_2	**5**	528	0.027	539	7.6[c]	323
		**6**	533		547		322
		**7**	531	0.040	527	7.5[c]	323
		**8**	359		531		322
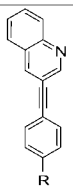	-H	**9**	354	0.082	448	0.1[c]	323
	-Me	**10**	370	0.24	460	0.1[c]	323
	-OMe	**11**	406	0.25	too weak		323
	-NMe_2	**12**	534	0.030	too weak		323
	-NEt_2	**13**	532	0.037	too weak		323
		**14**	534	0.027	too weak		323
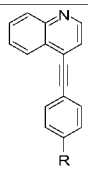	-H	**15**	378	0.0005	451	5.0[c]	323
	-Me	**16**	374	0.0033	449	4.8[c]	323
	-OMe	**17**	422	0.045	450	15[c]	323
	-NMe_2	**18**	538	0.0027	448	2.8[c]	323
	-NEt_2	**19**	536	0.0039	500	3.6[c]	323
		**20**	540	0.0013	481	1.0[c]	323
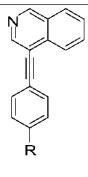	-H	**21**	372	0.017	463	1.0[c]	323
	-Me	**22**	382	0.10	553	1.0[c]	323
	-OMe	**23**	414	0.24	too weak		323
	-NMe_2	**24**	534	0.025	too weak		323
	-NEt_2	**25**	534	0.030	too weak		323
		**26**	536	0.017	too weak		323
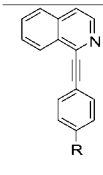	-H	**27**	372	0.0012	440	6.5[c]	323
	-Me	**28**	376	0.0018	524	7.2[c]	323
	-OMe	**29**	404	0.028	457	22.0[c]	323
	-NMe_2	**30**	530	0.013	525	12.0[c]	323
	-NEt_2	**31**	528	0.018	527	0.9[c]	323
		**32**	530	0.013	too weak		323
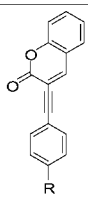	-H	**33**	406	0.88	439	0.60[d]	326,327
	-Me	**34**	416	0.73	456	0.03[d]	326,327
	-OMe	**35**	456	0.55	438	0.20[d]	326,327
	-$OCHMe_2$	**36**	464	0.43	451	0.50[d]	326,327
	-NMe_2	**37**	550	0.009	505	0.06[d]	326,327
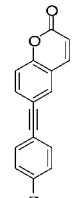	-H	**38**	364	0.011	456	0.008[d]	326,327
	-Me	**39**	440	0.016	448	0.005[d]	326,327
	-OMe	**40**	465	0.029	454	0.003[d]	326,327
	-$OCHMe_2$	**41**	470	0.034	455	0.004[d]	326,327
	-NMe_2	**42**	438	0.009	478	1×10^{-4}[d]	326,327
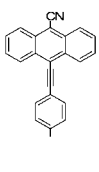	-H	**43**	460	0.58[e]	542		328
	-Me	**44**	466	0.73[c]	541		328
	-OMe	**45**	496	0.64[c]	536		328
	-NMe_2	**46**	603	0.10[e]	556		328
	-NEt_2	**47**	604	0.08[e]	550		328
		**48**	608	0.05[e]	540		328
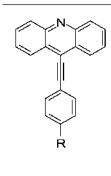	-H	**49**	431	0.16	473	0.044[d]	329
	-Me	**50**	434	0.27	482	0.022[d]	329
	-OMe	**51**	464	0.59	480	0.09[d]	329
	-$OCHMe_2$	**52**	469	0.53	487	0.012[d]	329
	-$OCH_2CH(Et)(n\text{-}C_4H_9)$	**53**	466	0.62	479	0.021[d]	329
	-NMe_2	**54**	569	0.043	534	0.01[d]	329

compounds	R	code	λ_{em} (nm)	φ_{em}[b]	λ_{ECL} (nm)	φ_{ECL}	refs
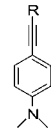	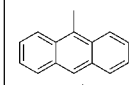	**55**	563	0.18[e]	537		330
	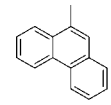	**56**	488	0.26[e]	no ECL		330
		**57**	484	0.24[e]	441		330
	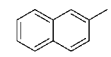	**58**	472	0.35[e]	no ECL		330
	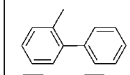	**59**	447	0.25[e]	457		330
	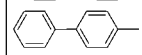	**60**	472	0.43[e]	517		330
	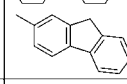	**61**	452	0.59[e]	No ECL		330
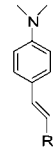		**62**	451		545		331
		**63**	484		509		331
		**64**	441		461		331
		**65**	468		484		331
		**66**	483		471		331
	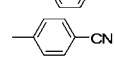	**67**	519		521		331
		**68**	522		530		331
		**69**	536		540		331
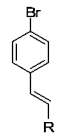	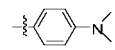	**70**	452	0.229[f]	460[g]		338
	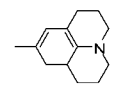	**71**	479	0.075[f]	490[g]		338
	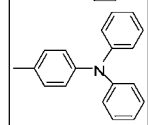	**72**	464	0.175[f]	469[g]		338
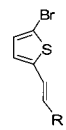	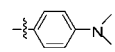	**73**	460	0.135[f]	564[g]		338
		74	473				338
		75	600	0.095[f]	523[g]		338
		76	600	0.279[f]	577[g]		338
		77	633	0.233[f]	614[g]		338
		78	594	0.264[f]	570[g]		338

Table 6. Continued

compounds	R	code	λ_{em} (nm)	φ_{em} [b]	λ_{ECL} (nm)	φ_{ECL}	refs
	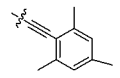	**79**	522	0.300[h]		0.01[j]	332
	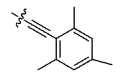	**80**	529	0.630[h]	~529[i]	0.1[j]	332
	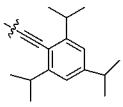	**81**	507	0.560[h]	~507[i]	0.1[i]	332
		**82**	548	0.183[h]	~548[i]	0.001[j]	332
		**83**	584	0.016[h]		0.01[i]	332
	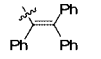	**84**					332

compounds	R	code	λ_{em} (nm)	φ_{em} [b]	λ_{ECL} (nm)	φ_{ECL}	refs
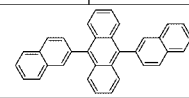		**85**	422	0.86[k]	430	0.90[l]	337
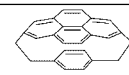		**86**	422	0.38[m]	(430, 590)[o]	no ECL[n]	133
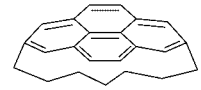		**87**	423	0.37[m]	(439, 603)[o]	no ECL[n]	133
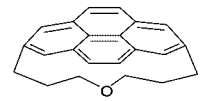		**88**	429	0.19[m]	(444, 607)[o]	no ECL[n]	133
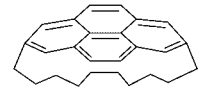		**89**	397	0.54[m]	(414, 587, 681)[n] (420, 589)[o]	very weak[n] bright[o]	133
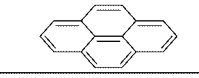		**90**	393	0.60[m]	(513, 644)[n] (418, 514)[o]	very weak[n]	133

[a] All ECL were generated in dried degassed MeCN (0.05 M TBAP) via ion annihilation, unless otherwise stated. [b] Unless otherwise stated, all φ_{em} data were measured in CH_2Cl_2 with reference to coumarin 1. [c] Relative to $Ru(bpy)_3^{2+}$/oxalate system (φ_{ECL} = 100%). [d] Relative to $Ru(bpy)_3^{2+}$ (φ_{ECL} = 1.0). [e] φ_{em} data were determined in MeCN using coumarin 334 as stardard. [f] φ_{em} data were measured in MeCN with reference to quinine sulfate. [g] Annihilation ECL was obtained from PhH/MeCN (1:1)−0.05 M (TBA)PF_6 solutions. [h] Determined with respect to fluorescein. [i] Annihilation ECL was obtained from PhH/MeCN (1:1)−0.1 M TBAP solutions. [j] Represents the fraction of a DPA cell under similar conditions (accurate to about an order of magnitude). [k] Measured in PhH/MeCN (1:1) with reference to DPA. [l] Measured in PhH/MeCN (1:1)−0.1 M (TBA)PF_6 with respect to DPA. [m] Measured in MeCN compared to pyrene (**90**) as a standard (φ_{em} = 0.60 in PhH[339]). [n] Obtained from annihilation ECL in PhH/MeCN (1:1)−0.1 M (TBA)PF_6. [o] Obtained from coreactant ECL with benzoyl peroxide as the coreactant.

Scheme 12. ECL emission of donor (D)−acceptor (A) type luminophores from (a) excimers, (b) intramolecular charge transfer (ICT) systems, and (c) H-type excimers promoted by $\pi-\pi$ interactions between the two A's

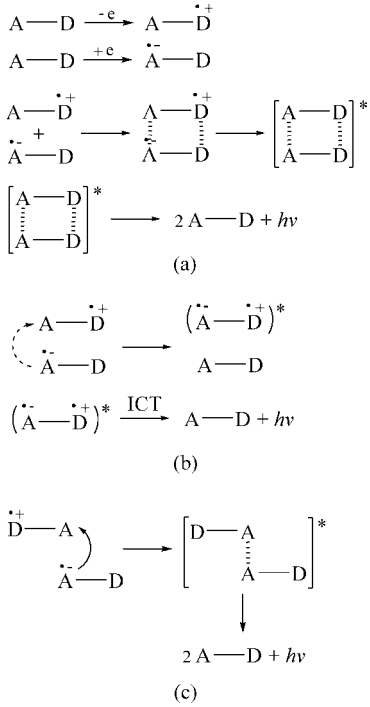

Another two series of luminophores displayed in Table 6 (**33**–**42**) are donor-bearing phenylethynylcoumarins.[326,327] Compounds **33**–**37** are 3-isomers with a planar geometry, whereas **38**–**42** are 6-isomers with a twisted geometry. Most probably, very weak electronic coupling between donor and acceptor subunits in the 6-isomers, contrary to the 3-isomers, is responsible for the different UV−vis spectroscopic properties of the investigated coumarin derivatives. Consequently, lack of additional charge-transfer bands in the 6-isomers makes their UV−vis spectra similar to that of unsubstituted coumarin.

Scheme 13. Proposed Structure of the H-type Dimer of 20[a]

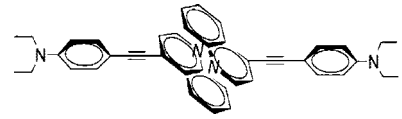

[a] Reprinted with permission from ref 323. Copyright 2004 Royal Society of Chemistry.

The PL φ_{em} values for **33**–**36** are much higher than those of **38**−**42**. The φ_{em} decreases with the increase of the donor strength and is highest for **33** and lowest for **37** (and for **42**). Possible quenching by ICT from the *N*,*N*-dimethylanilino group to the coumarin of the neighboring molecule or even the strong excited state ICT itself could be the reason for this reduction in quantum yield. The positions of ECL maxima for **33**–**36** and **38**–**41** are close and in the range of 438–456 nm, which is only slightly affected by the presence of strong donors such as the $-NMe_2$ group on the phenyl moiety linked through the C−C triple bond. All compounds are believed to show ECL emission via the TTA pathway (eq 6) as deduced from their lower annihilation reaction enthalpy, and the formation of excimers and the H-type aggregates is also involved as discussed earlier for compounds **1**–**32**.

Fluorescent emission could be tuned from 460 to 610 nm when a set of donors was attached to the phenylethynylanthronitrile moiety (Table 6, **43**–**48**).[328] Surprisingly, all of the compounds emitted ECL at almost the same maxima centered at 545 nm regardless of the nature of the donor subunits. That is, the ECL maxima for **43**–**45** were red-shifted by 40–80 nm, and for compounds **46**–**48** the ECL maxima were blue-shifted by 40–68 nm when compared with

Scheme 14. H-excimer or Trans Excimer Formation Proposed for the ECL-Emitting State of Compounds 43–48 in Table 6[a]

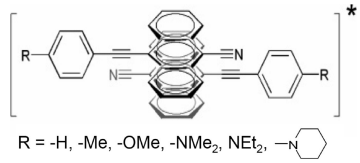

[a] Reprinted with permission from ref 328. Copyright 2005 American Chemical Society.

their fluorescence maxima. Moreover, although the ECL was produced in high-polarity MeCN, no PL was observed in the same solvent for **46–48**. These data suggest that the ECL-emitting state was different from the PL state as described previously[136,326] and that all of the ECL emission could be from the same excited state species as proposed in Scheme 14.

To examine the effect of donor steric hindrance and strength on ECL, a series of donor−acceptor ethynes with acridine as acceptor and several donor-substituted phenyl groups have been synthesized at the donor site (Table 6, **49–54**).[329] All of the compounds exhibited ECL from the annihilation of the radical anions and radical cations via the T-route. Compounds with weak donors (**49–53**), irrespective of whether they were sterically capable of causing hindrance or not, emitted excimer ECL, whereas compound **54**, which has the strongest donor (−NMe_2) in the group, resulted in blue-shifted ECL. This demonstrates that the excimer ECL (and perhaps the monomeric ECL as well) are determined by the strength of the electron-donating group rather than steric hindrance at the donor site.

As discussed in section 5.1, although highly efficient ECL is often produced from highly fluorescent species, there is no direct correlation between PL QYs and φ_{ECL} due to the complexity of ECL generation from either annihilation or coreactant modes. This has been confirmed by the PL and ECL studies of a family of aryl−π-donor−aryl molecules (Table 6, **55–61**).[330] All of the compounds showed high fluorescence quantum yields (φ_{em} = 0.18–0.59) in solution, and their bright solid state photoluminescence was also observed. Electrochemically, all seven compounds displayed very close behavior in MeCN (50 mM TBAP), with a reversible reduction at ∼−0.90 V vs Ag/AgCl and an irreversible oxidation at ∼1.60 V vs Ag/AgCl. Their ECL behavior, however, was very different. Compounds **55** and **57** showed blue-shifted ECL emission, probably originated from the H-type aggregates compared to their photoluminescence. Compound **59** revealed monomeric ICT ECL and **60** showed excimer ECL emission. Unexpectedly, no ECL activity for **56**, **58**, and **61** was obtained. This may be due to the instability of radical ions, especially the radical anion, of compounds **56**, **58**, and **61**. Also, for **61**, even though the fluorenyl moiety is rigid and planar, the bend caused by the rigidification due to the methylene bridge likely prevents ICT, and hence no ECL was observed.

ECL studies on a series of donor−acceptor stilbenoid systems (Table 6, **62**−**69**)[331] bearing an *N*,*N*-dimethylamino group as donor and pyridine, thiophene, quinoline, and substituted phenyl groups as acceptors indicate that most of the compounds in the group (**63–69**) showed ICT ECL (Scheme 12b) through direct annihilation of the radical ions. For the weaker ICT compound (**62**), however, excimer ECL was produced from the excimer. Because thiophene is less electron withdrawing and makes compound **62** less polar in the excited state, more delocalization of charge in the radical ions occurs, which makes excimer formation more favorable.

Compounds **70–78** listed in Table 6 are donor−acceptor−π-conjugated luminophores with a phenylvinyl or thienylvinyl unit as the bridge, a bromide or aldehyde group as the acceptor moiety, and the rest as the donor. All compounds showed good electrochemical stability, exhibiting two successive one-electron oxidation waves with the first one reversible and the other irreversible. On the other hand, one quasi-reversible or irreversible one-electron reduction wave was observed. Three different categories of ECL mechanisms for each of the three families of compounds were proposed. Compounds **70–72** produced typical and simple monomer ECL emission resulting from the annihilation of their radical cations and radical anions, because their ECL maxima were in good agreement with their fluorescence maxima. The ECL emission of compounds **73–75** was ascribed as an excimer emission, where significant red-shifted ECL maxima from their fluorescence maxima by 50–104 nm were observed. Finally, compounds **76–78** exhibited an H-type excimer-like aggregate ECL emission, which was consistent with their blue-shifted ECL emissions with respect to their fluorescence maxima. These assignments were supported by X-ray crystal structures of some of the compounds studied.

Electrochemistry, spectroscopy, and ECL of two sets of six silole-based luminophores (Table 6, **79–84**) have been reported recently.[332] The first set (**79–81**) and the second set (**82–84**) of compounds are ethynyl- and ethylene-substituted siloles, respectively. Different trends were observed in their electrochemical and photophysical behaviors. Because the ethynyl-substituted siloles (**70–81**) were more sterically rigid, they showed higher PL QYs (0.3–0.63 with fluorescein as a standard) than the ethylene-substituted siloles (**82–84**, φ_{em} < 0.183), but the unprotected triple bonds resulted in poor oxidative behavior. By adding *tert*-butyl groups to the silicon, the bonds were more protected from secondary homogeneous reactions. As a result, compounds **80** and **81** exhibited higher fluorescence quantum efficiencies (φ_{em} = 0.63, 0.56 for **80** and **81**, respectively, vs φ_{em} = 0.30 for **79**) and produced intense ECL on radical ion annihilation. To reduce steric stress in **83** and **84**, the 2,5-substituents were forced to rotate out of the plane of the silole moiety, whereas **82** can remain completely planar. Thus, the luminophores of **83** and **84** were with less protected from secondary reactions upon oxidation or reduction. Consequently, their radical ions were less stable, and they showed lower fluorescence quantum yields than **82** and poor ECL.

As in the case of luminol (section 3.3), blue intense ECL emission was reported to be produced in alkaline solutions after electrochemical oxidation of an acridan phosphate ester [9-(phenylthiophosphoryloxymethylidene)-10-methylacridan disodium salt] in the presence of H_2O_2 or dissolved molecular oxygen.[333] This compound could be employed as a label in aerated sample solution for automated biomolecule analysis without the addition of H_2O_2.

9,10-Bis(2-naphthyl)anthracene (**85** in Table 6) and its polymers, known to be new emitting materials in light-emitting devices (LEDs), have proved to generate efficient and stable blue light emission with low turn-on voltages.[334–336] In PhH/MeCN (1:1) solution, it showed a high fluorescence quantum yield of 0.86 with respect to DPA.[337] Strong, intense ECL was also observed in the same solvent containing 0.1 M TBAP when pulsing between the potentials for the first

Table 7. Spectroscopic and ECL Properties of Semiconductor Nanoparticles in Solution

NP (diameter, in nm)	capping agent	ECL medium	λ_{em} (nm)	λ_{ECL} (nm)	refs
Si (~2–4)	octanol, octene, and octanethiol	(a) MeCN (0.1 M THAP) (b) 2.5 mM $C_2O_4^{2-}$/MeCN (0.1 M THAP) (c) 6 mM $S_2O_8^{2-}$/DMF (0.1 M THAP)	420	640	25
Ge (4.5)	C_8 hydrocarbon chains	DMF (0.1 M TBAP)	500	700	344
CdS (~4)	thioglycerol			no ECL	345
CdS (~5)	uncapped	(a) MeCN (0.1 M TBAP) (b) 0.1 M NaOH (0.1 M KNO_3)	616	700	346
CdS (~7) nanotubes		0.1 PBS (pH 8)/0.1 M KCl/0.01 M $K_2S_2O_8$		500, 640	347
CdSe (3.2)	TOPO	CH_2Cl_2 (0.1 M TBAP)	545	740	348
CdSe (~2.5)	octadecanamine	CH_2Cl_2 (0.1 M TBAP)		510, 663	349
CdSe/ZnSe	dodecylamine	CH_2Cl_2 (0.1 M TBAP)	580	580, 740	341
CdTe (4)	TOPO	CH_2Cl_2 [0.1 M (TPA)PF_6] CH_2Cl_2 may act as a coreactant	635	638	342
CdTe (2.0–3.5)	MAA	0.10 M KCl	562		350
Bi_2Te_3 nanoflaks (10–150)		(a) 0.05 M $K_2S_2O_8$/0.1 M KOH/0.1 M KCl (b) H_2O_2 and dissolved O_2 can be also acted as coreactants		2 ECL waves along with CV	351
ZnS (5-7) ZnS/$Zn(OH)_2$ (7−11)		(a) 0.10 M NaOH (b) (a) + 10 mM $K_2S_2O_8$	440	~460	352

oxidization and reduction of the compound. Consistent with its fluorescence, ECL emission maximum at 430 nm with an ECL efficiency of 0.90 with reference to DPA was measured. Fully reversible one-electron oxidation and reduction to the radical ions were attributed to electron transfers to the anthracene core. Immediately after the second reduction of the core, which was a one-electron irreversible process, a fast protonation reaction occurred. The third and fourth electron transfers were said to occur on the two naphthyl groups.

The photophysical, electrochemical, and ECL studies of a family of nonplanar pyrene derivatives ("pyrenophanes", Table 6, **86**–**89**) have been published.[133] Overall, pyrenophanes with a shorter bridge across the 2- and 7-positions showed less positive peak potentials for oxidation and more negative reduction potentials. The nonplanarity in these compounds resulted in a considerable decrease in PL QY as well as a slight red shift in both the absorption and emission spectra when compared to pyrene (**90**), the planar molecule. Additionally, unlike pyrene, no excimer emission was evident in the fluorescence spectra even at concentrations as high as 1 mM. The instability of the cation as well as the anion in some systems gave rise to a lack of ECL or low ECL intensity upon radical ion annihilation. However, the ECL spectra of all four pyrenophanes, produced by generating the anion radical in the presence of benzoyl peroxide as a coreactant, showed broad "excimer-like" emission in addition to the monomer emission observed at shorter wavelengths.

Finally, the electrochemistry and ECL of two linear, stereoregular, and structurally defined PPV derivatives, poly[distyrylbenzene-*b*-(ethylene oxide)]s, with respective to 12 and 16 ethylene oxide repeat units in the backbone, have been studied.[291] In CH_2Cl_2, a one-electron transfer, reversible oxidation at ~0.75 V vs Ag/Ag^+, was observed for both polymers. ECL responses with a maximum emission at ~1.10 V vs Ag/Ag^+ were obtained with the polymer cast films in MeCN (0.10 M TBAP) in the presence of TPrA after both TPrA and film were oxidized.

5.3. Semiconductor Nanoparticle Systems

The ECL study of semiconductor nanoparticles (NPs, also known as nanocrystals, quantum dots) was first reported in 2002 for Si NPs, where ECL was generated from both annihilation and coreactant oxalate and persulfate systems in MeCN.[25] In addition to elemental semiconductors (e.g., Si and Ge), many compound semiconductors (e.g., CdS, CdSe, and CdTe) can also produce ECL (Table 7). A common feature of ECL behavior obtained from NPs is their considerable red-shifted ECL maxima with respect to their photoluminescence, suggesting that the emitting states are different. It is believed that PL spectroscopies mainly probe the interior of the particle and provide information about the electronic transition (band gap) of material, whereas electrochemistry and ECL studies mainly probe the particle surface, because ECL emission generally is not sensitive to NP size and capping agent used but depends more sensitively on surface chemistry and the presence of surface states.[340] This model (Figure 30) was further verified via the ECL study of CdSe/ZnSe core/shell type NPs.[341] CdSe NPs that were well-passivated with a shell of ZnSe showed a large ECL peak at the wavelength of band-edge PL plus a red shift by ~200 nm from the PL peak. This ECL spectrum suggested that completely passivated NPs were present along with nonpassivated NPs, demonstrating that ECL is an effective probe of surface states on semiconductor NPs.

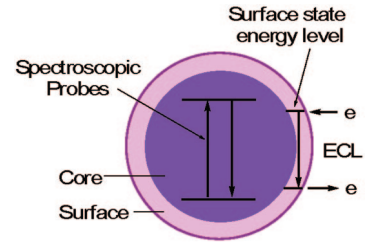

Figure 30. Schematic representation of PL and ECL in semiconductor NPs. Modified with permission from ref 341.

The ECL mechanism of semiconductor NPs follows the general annihilation and coreactant ECL reaction pathways as discussed in sections 3.1 and 3.2. Note that a new coreactant, CH_2Cl_2, was proposed during the ECL study of CdTe in CH_2Cl_2 containing 0.1 M (TBA)PF_6.[342] In this case, a large ECL signal was detected at the first negative potential, which cannot be explained by the annihilation of redox species of NPs, because there were only reduced particles; there were no oxidized particles to act as electron acceptors. Much weaker ECL signals were detected when the reaction

Scheme 15

$$CH_2Cl_2 + e \rightarrow CH_2Cl_2^{\bullet -} \rightarrow CH_2Cl^{\bullet} + Cl^- \quad (26)$$

$$(CdTe)_{NP}^{\bullet -} + CH_2Cl^{\bullet} \rightarrow (CdTe)_{NP}^{*} + CH_2Cl^- \quad (27)$$

medium was changed to a mixture of benzene−MeCN at the first negative potential, which was attributed to some impurities in the cell. Previously, $CH_2Cl^{\bullet}$ radicals produced under irradiation of CH_2Cl_2 were proposed to act as electron acceptors to oxidize aromatic hydrocarbons.[343] On the basis of this reference, $CH_2Cl^{\bullet}$ was proposed as the oxidant in the system. The reduced CH_2Cl_2, $CH_2Cl_2^{\bullet -}$, decomposes into $CH_2Cl^{\bullet}$ and Cl^-, and the oxidant, $CH_2Cl^{\bullet}$, accepts an electron from the reduced NPs to form the emitting state (Scheme 15).[342]

In addition to the above-discussed solution phase NPs ECL, several papers on NPs film ECL have also been published. For example, films of octadecyl-capped Si NPs (~3.4 nm) on ITO showed ECL for both cathodic and anodic potential sweeps in KOH solutions containing persulfate.[353] The ECL exhibited a relatively broad spectrum (FWHM = 160 nm) with a peak wavelength of ~670 nm, similar to the PL spectra. Other studies on NP films include PbSe,[354] CdSe thin film and single monolayers of CdSe in molecular organic devices,[355–358] and CdSe/ZnS,[359] ZnS/CdSe, and CdSe/CdS core/shell type films.[360] Such studies are important because NPs may find applications in optoelectronic systems or as components in future nanoelectronic devices. Besides, semiconductor NP thin films may also offer better electrochemical and ECL signals, because the solution phase NPs often suffer from low solubility, low concentration, and small diffusion coefficient.

For a deep discussion of the electrochemical and ECL behaviors of semiconductor NPs in solutions and in films, readers are referred to a very recent comprehensive review[340] of this field.

6. Immobilization of $Ru(bpy)_3^{2+}$ on the Surface of Electrode for Solid State ECL Detection

Earlier studies on the immobilization and ECL detection of $Ru(bpy)_3^{2+}$ and its derivatives on the electrode surface began in 1980s; ECL-emitting species were attached to the electrode via either cation-exchange polymer Nafion[361,362] or directly electropolymerized onto the electrode.[16] This was followed by the monolayer immobilization of ruthenium complexes and their surface ECL detection.[363–365] Significant research interest in this area has been recently promoted, because ECL can be used as a sensitive detector for FIA, HPLC, and CE systems, and the use of $Ru(bpy)_3^{2+}$ in traditional solution phase ECL detection, where $Ru(bpy)_3^{2+}$ is added in running buffer or kept in the detection reservoir, is very costly, complicates the experimental design, and makes the miniaturization of the instrument difficult. On the other hand, enhanced ECL signal may be obtained from a well-designed surface-confined ECL detector. A number of approaches have been employed to immobilize ruthenium complexes to the electrode surface (Table 8), which include the incorporation of Ru(II) molecules to (1) various types of sol−gel-based composite films,[366–377] (2) ion exchange polymer (e.g., Nafion) based composite films,[277,278,378–384] (3) NP-based composite films,[385–390] and (4) others.[179,391–394] Several factors need to be considered for the construction of a good solid state ECL detector. First, a sufficient amount of ruthenium complex should be attached to the electrode surface, because ECL intensity is generally proportional to the concentration of the emitting species. This may be achieved by using ion-exchange polymers, silica, or other small-sized particles. Second, the composite films or Ru(II)-containing paste should be sufficiently conductive, which will allow fast electron transfers occurring between the electrode, ruthenium complexes, and the ECL coreactant or analytes. Introduction of carbon nanotubes or Au or Pt NPs into the composite films can significantly increase the film conductivity as well as the amount of Ru(II) complexes incorporated. Third, there can be no leaching of the emitting species from the film in a wide range of reaction media over a long period of time, because the leaching can cause low stability, poor reproducibility, and reduced sensitivity. Strong electrostatic interactions between positively charged ruthenium complexes and the negatively charged cation-exchange Nafion polymer network or silica particles make both Nafion and silica very popular in the preparation of solid state ECL detectors (Table 8). Covalent attachment of ruthenium complexes to the electrode has been found to give no leaching to the solution,[367] and the sol−gel-derived Ru(II)−titania−Nafion composite films are stable in high contents of organic solvents (30%, v/v).[382] Finally, good adhesion between the electrode and the composite films is needed, which sometimes requires the pretreatment of the electrode surface.[385,387,389] Table 8 lists recently published approaches for the immobilization of ruthenium complexes on various electrode surfaces for solid state ECL detection, in which, when appropriate, the reaction media, the stability of the composite films, and analytes detected and their limits of detection are included. Clearly, the solid ECL detectors are very sensitive to many biomolecules' detection.

7. Biorelated Applications

Biorelated applications of ECL technology are predominately based on $Ru(bpy)_3^{2+}$/TPrA (or other amines) coreactant ECL systems and have been largely accelerated by the use of commercially available ECL instruments (section 4.4).

7.1. CE, HPLC, and FIA-ECL Systems

Two common features of these three systems are that (a) very small amounts of samples (from nano- to microliters) can be used and (b) analytes or their derivatives act as coreactants in the ECL detection cell. As a result, all analytes or their derivatives are generally required to have secondary or tertiary amine groups with an α-carbon hydrogen so that efficient ECL can be produced in the presence of $Ru(bpy)_3^{2+}$. Simultaneous detection of analytes can be realized when different analytes are separated via CE or HPLC prior to ECL detection. There are basically three modes for the introduction of the ECL reagent to CE-ECL systems: inclusion of reagent in the running buffer or in the end-column reservoir and coaxial reagent merging. In the first mode, $Ru(bpy)_3^{2+}$ reagent is incorporated in the CE running buffer and oxidized to $Ru(bpy)_3^{3+}$ at the working electrode of the detection cell.[8,60,252] This approach could be plagued with problems affecting the electroosmotic flow in CE separation due to the adsorption of $Ru(bpy)_3^{2+}$ on the capillary walls.[260] In the end-column mode, $Ru(bpy)_3^{2+}$ reagent is contained in an end-column reservoir. Variations

Table 8. Immobilization of $Ru(bpy)_3^{2+}$ on the Surface of Electrode for Solid State ECL Detection

type of immobilization	measurement conditions and electrode stability	analytes and LOD values	refs
sol−gel composites/fluorine doped tin oxide glass slide	FIA	oxalic acid, 1 μM	368
carbon nanotube −organically modified silicate films/GC	FIA, 0.1 M phosphate buffer, pH 9	herring sperm DNA, LOD 2.0 $\times 10^{-7}$ g/mL	366
carbon nanotube/Nafion composite films/GC	10 mM acetate buffer, 50 mM NaCl, pH 5.50	salmon testes DNA, 34.4 nM; p53 gene at 0.393 nM	380
Nafion−silica composite film/GC	10 mM acetate buffer/50 mM KNO_3, pH 5.0	TPrA, 0.1 μM; Oxalate, 2 μM	395
PPS−silica−Triton X-100 composite thin film/GC	FIA	oxalate, 0.1 μM; TPrA, 0.1 μM; NADH, 0.5 μM	370
PPS−silica−composite thin film/GC	FIA, stable over 6 months in air	TPrA, 0.1 μM; proline etc.	371
[Clay NPs/$Ru(bpy)_3^{2+}$]$_n$ multilayer films/ITO		TPrA, 20 nM; oxalate, 100 nM	385
zirconia−Nafion composite films/graphite	CE, phosphate solution, stable in phosphate for 90+ h	TPrA, 5 nM; lidocaine, 10 nM; proline, 10 μM	278
zirconia−Nafion composite films/graphite	microchip CE-ECL	tramadol, 25 μM lidocaine, 5 μM ofloxacin, 10 μM	277
titania−Nafion membrane/GC		chlorphenamine meleate, 6 nM	378
titania sol−gel membrane/GC	FIA, 0.1 M phosphate, pH 7.4	oxalate, 5.0 μM proline, 4.0 μM	396
sol−gel-derived titania/Nafion composite films/GC	50 mM phosphate buffer, pH 7.0; HPLC, stable in high content of organic solvent (30%, v/v)	TPrA, 0.1 μM oxalate, 1.0 μM erythromycin from urine, 1.0 μM	382
sol−gel-derived titania/Nafion films/Pt	HPLC	human urine samples: promazine, 0.529 μM chlorpromazine, 0.833 μM triflupromazine, 1.64 μM tthioridazine, 1.71 μM trifluoperazine, 2.94 μM erythromycin, 1.11 μM	374
TMOS−DiMe−DiMOS−PSS silicate film/GC	FIA, 0.1 M phosphate buffer/0.20 M KNO_3, pH 7.5	codeine, 5 nM morphine, 30 nM	369
TMOS−DiMe−DiMOS−PSS silicate film/GC	(1) FIA, pH 9.5	berberine, 5 μM trigonelline, 8 μM allantoin, 20 μM betaine, 50 μM	373
	(2) FIA, 0.1 M phosphate buffer, pH 8.0, 5% decrease in ECL for 10 μM methamphetamine over 10 days	methamphetamine, 20 μM	375
Ru(4-methyl-4′-vinyl-2,2′-$bpy)_3^{2+}$ electropolymized/Pt	200 regeneration cycles over 6 months, 0.1 M acetate buffer, pH 6.5, and pH 11	tested with oxalate, ethylamine, diethylamine, and triethylamine	394
electrostatic attachment of Ru(II) to benzenesulfonic acid monolayer /GC	FIA, 0.1 M phosphate buffer, pH 8.0, stored dried in 1 week with no ECL decrease	TPrA, 1 μM	393
sol−gel-derived ceramic carbon−Nafion electrode	analyte was pre-extracted into the electrode, 50 mM phosphate buffer, pH 7.0	dioxopromethazine, 0.66 nM	384
metallopolymer $[Ru(bpy)_2(PVP)_{10}]^{2+}$			391
Pt NPs/Eastman AQ55D composite films	50 mM PBS, pH 7.5	TPrA, 1 fM	386
organosilicate functionized Ru(II)/ITO	50 mM phosphate, pH 7.0 stored at RT more than 6 months, ~10% ECL loss, film not dissolved in organics solvents	tested with TPrA, tartaric acid, ascorbic acid, promazine, NADH, oxalate, proline, etc.	377
sol−gel−chitosan−PSS−alcohol dehydrogenase composite films/GC	0.1 M phosphate buffer, pH 7.5, stored at 4° C for 10 days, ECL unchanged	alcohol, 9.3 μM	376
alcohol dehydrogenase−Au NPs aggregates/ITO	0.25 M NAD^+-phosphate buffer, pH 7.5, stable for 4 weeks at 4 °C	alcohol, 3.33 μM	387

Table 8. Continued

type of immobilization	measurement conditions and electrode stability	analytes and LOD values	refs
citrate-capped Au NPs-Ru(II) aggregates/ITO	50 mM phosphate buffer, pH 9.2	tested with 0.5 mM TPrA	389
Eastman AQ55D−carbon nanotube composite films/GC	phosphate buffer, pH 7.6, in air for 2 weeks, oxidation current of Ru(II) changed <5%	TPrA, 30 pM	381
Ru(II)-doped SiO_2 at MWNTs coaxial nanocable/ITO	phosphate buffer, pH 7.56	TPrA, 39 pM	392
MWCNs−Nafion composite films/GC	phosphate buffer, pH 7.0	NADH, 0.82 μM	383
SiO_2 NPs/Ru(II) multilayer films/ITO	phosphate buffer, pH 8.2	TPrA, 10 nM	390
supramolecular microstructures self-assemblyformed from Ru(II) and H_2PtCl_6/ITO	50 mM phosphate buffer, pH 9.2	tested with 25 μM TPrA	388
sol−gel covalently bound with Ru(II)/GC	$Ru(bpy)_3^{2+}$ derivative with hydrolyzable linkers, air stable >8 months, no leaching from sol−gel films	tested with 1 mM codeine	367
sulfonic-functionalized MCM-41 silica−ionic liquid-based carbon paste electrode	0.1 phosphate buffer, pH 7.5	TPrA, 7.2 nM	179
Nafion−magnetic Fe_3O_4 NPs/Pt (magnet)	50 mM phosphate buffer, pH 7.0, stability better than Nafion and titania−Nafion modified composites	TPrA, 1 μM	397
zeolite Y modified carbon past electrode	FIA, 0.10 phosphate buffer, pH 6.3, stable in air for 15 days and up to100 potential cycles in phosphate buffer	heroin, 1.1 μM	398

Scheme 16. Derivatization Reactions of Amino Acids with Acetaldehyde[a]

[a] Reprinted with permission from ref 424. Copyright 2006 American Chemical Society.

in the concentration of $Ru(bpy)_3^{2+}$ due to dilutions from the column effluent and evaporation of the solution in the reservoir are problematic. Hence, periodic replacement of the electrolyte medium is needed.[399–401] An alternative approach is to use ECL detectors with $Ru(bpy)_3^{2+}$ immobilized on the electrode surface, as outlined in section 6 and summarized in Table 8. In the coaxial flow mode, either the $Ru(bpy)_3^{3+}$ can be generated upstream of the reaction/detection zone in a pumped stream[402] or the separation capillary is immersed in a coaxial flow of $Ru(bpy)_3^{2+}$, and $Ru(bpy)_3^{2+}$ is oxidized to $Ru(bpy)_3^{3+}$ at the end of the capillary and renewed by a syringe pump at a low flow rate.[260,265] This mode could also facilitate the integration of ECL into the microfluidic CE system, as demonstrated in ref 265. Table 9 lists the recent applications of $Ru(bpy)_3^{2+}$ ECL in CE, in which many analytes are pharmaceutical-related.

When $Ru(bpy)_3^{2+}$ ECL detection is combined with HPLC or CE separation, $Ru(bpy)_3^{3+}$ generated either in the detection cell[425–427] or upstream of the detection cell[428–430] has been used. Because tertiary amines can produce sensitive ECL responses (section 3.2.2.3), efforts have been made to introduce such groups to initially less or non-ECL sensitive analytes, such as amino acids[424,429] and fatty acids.[429,430] Derivatization of amino acids with acetaldehyde (Scheme 16) gave a 20–70 times increase in ECL intensity.[424] Other derivatization agents useful for ECL enhancement of primary amines include *N*-methyl-L-proline (NMP), 3-(diethylamino)propionic acid (DEAP), and 4-(dimethylamino)butyric acid (DMBA)[429] (Figure 31a).[431] Previously, two reagents, dansyl chloride[432] and divinyl sulfone (DVS),[48] were reported for the ECL system, with the detection limits of dansyl and DVS derivatives of 2 pmol for amino acids and 1–30 pmol for primary amines, respectively. Two groups of derivatization agents have been used for selective and sensitive carboxylic acid HPLC separation−ECL detection. The first group of compounds are 2-(2-aminoethyl)-1-methylpyrrolidine (AEMP) and *N*-(3-aminopropyl)pyrrolidine (NAPP),[429] and the second compound is 3-isobutyl-9,10-dimethoxy-1,3,4,6,7,11b-hexahydro-2*H*-pyrido[2,1-*a*]isoquinolin-2-ylamine (IDHPIA)[430] (Figure 31b). The derivatives obtained from 10 free fatty acids were completely separated by reversed phase HPLC under isocratic elution conditions. The on-column detection limits were 70 and 0.5 fmol for myristic acid when NAPP and IDHPIA were used as the derivatization agents, respectively.[429,430] The data suggest that IDHPIA is 100-fold more selective than NAPP as a derivatization agent for carboxylic acid detection. Applications of the two group derivatization agents were further demonstrated by the determination of free fatty acids in human plasma and serum samples.[429,430]

Table 9. Applications of $Ru(bpy)_3^{2+}$ ECL in Capillary Electrophoresis

analyte	separation channel (l × i.d.)	matrix	limit of detection	ECL detection system	refs
heroin	45 cm × 25 μm	banknotes	50 nM	5 mM $Ru(bpy)_3^{2+}$−50 mM phosphate−acetate buffer, pH 7.2	403
cocaine			60 nm		
chlorpheniramine	50 cm × 25 μm	urine	0.5 μM	5 mM $Ru(bpy)_3^{2+}$−50 mM phosphate−buffer, pH 8.0	404
sinomenine	50 cm × 25 μm	Chinese herb *Sinomenium acutum*	2.0 ng/mL	5 mM $Ru(bpy)_3^{2+}$−75 mM phosphate−buffer, pH 8.0, chemically modified Pt with europium(III)-doped Prussian blue analogue as working electrode	405
atenolol	45 cm × 25 μm	spiked urine	75 nM	5 mM $Ru(bpy)_3^{2+}$−0.10 M phosphate−buffer, pH 7.5	406
metoprolol			5 nM		
TPrA[a]	50 cm × 75 μm	standard solution	0.14 nM	$Ru(bpy)_3^{2+}$ with phosphate buffer	407
TPrA	50 cm × 75 μm	urine	50 pM	5 mM $Ru(bpy)_3^{2+}$−0.10 M phosphate−buffer, pH 9.5	266
lidocaine			20 nM		
TPrA	50 cm × 50 μm	standard solution	2 nM	0.1 M phosphate, pH 9.5, $Ru(bpy)_3^{2+}$ immobilized	408
proline			2 μM		
anabasine[b]	60 cm × 75 μm	urine	4.7 μM	5 mM $Ru(bpy)_3^{2+}$, 10 mM borate buffer−10% Triton X-100, pH 8.0	401
nicotine		tobacco extracts	1.6 μM		
proline			0.66 μM		
disopyramide enantiomers	65 cm × 50 μm	racemic drug in spiked plasma	80−100 nM	5 mM $Ru(bpy)_3^{2+}$−0.10 M phosphate buffer, pH 6.5	409
disopyramide	45 cm × 50 μm	extracted from urine	25 nM	5 mM $Ru(bpy)_3^{2+}$−50 mM phosphate buffer, pH 7.5	410
sulpiride	50 cm × 25 μm	plasma urine	29 nM	5 mM $Ru(bpy)_3^{2+}$−50 mM phosphate buffer, pH 8.0	411
sulpiride	50 cm × 25 μm	urine	10 nM	5 mM $Ru(bpy)_3^{2+}$−50 mM phosphate buffer, pH 6.0	412
tiapride			15 nM		
thebaine	50 cm × 25 μm	Chinese medicine opium poppy	0.25 μM	5 mM $Ru(bpy)_3^{2+}$−50 mM phosphate buffer, pH 9.18	178
codeine			0.25 μM		
morphine			1 nM		
narcotine			1 μM		
TEtA	50 cm × 75 μm		24 nM	5 mM $Ru(bpy)_3^{2+}$−15 mM borate buffer, pH 8.0	413
TPrA			20 nM		
TBuA			32 nM		
lidocaine		urine	1.0 μM		
anisodamine	50 cm × 25 μm	*Flos daturae*	10 nM	5 mM $Ru(bpy)_3^{2+}$−50 mM phosphate buffer, pH 7.0	414
atropine			16 nM		
scopolamine			0.2 μM		
atropine	50 cm × 25 μm	*Flos daturae*	50 nM	5 mM $Ru(bpy)_3^{2+}$−50 mM phosphate buffer, pH 7.48	415
scopolamine			1.0 μm		
dioxopromethazine	38 cm × 25 μm	rat serum	50 nM	5 mM $Ru(bpy)_3^{2+}$−50 mM phosphate buffer, pH 7.14	399
		urine			
hypaconitine	50 cm × 25 μm	*Aconitum* plant	20 nM	5 mM $Ru(bpy)_3^{2+}$−50 mM phosphate buffer, pH 8.4	416
aconitine			0.17 μM		
mesaconitine			0.19 μM		
ethamsylate	50 cm × 25 μm	urine	8.0 nM	5 mM $Ru(bpy)_3^{2+}$−50 mM phosphate buffer, pH 9	414
tramadol			16 nM		
lidocaine			10 nM		

Table 9. Continued

analyte	separation channel (l × i.d.)	matrix	limit of detection	ECL detection system	refs
putrescine	50 cm × 25 μm	urine	0.19 μM	5 mM $Ru(bpy)_3^{2+}$−0.20 M phosphate buffer, pH 11.0	417
cadaverine			0.19 μM		
spermidine			7.6 nM		
spermine			7.6 nM		
TEtA	58 cm × 21 μm	standard solution	5 μM	3.5 mM $Ru(bpy)_3^{2+}$−15 mM borate buffer, pH 9.5	259
TPrA			5 μM		
proline hydroxyproline			2 μM		
			2 μM		
reserpine	50 cm × 25 μm	urine	70 nM	5 mM $Ru(bpy)_3^{2+}$−0.1 M borate buffer, pH 9.0	418
proline hydroxyproline	50 cm × 25 μm	urine	2 μM	5 mM $Ru(bpy)_3^{2+}$−50 mM phosphate buffer, pH 8.0	419
			4 μM		
bupivacaine	50 cm × 25 μm	plasma	3 ng/mL	5 mM $Ru(bpy)_3^{2+}$−50 mM phosphate buffer, pH 6.5	420
diphenhydramine	50 cm × 25 μm	rabbit plasma urine	20 nM	5 mM $Ru(bpy)_3^{2+}$−0.25 M phosphate buffer, pH 8.5	421
mefenacet	? cm × 25 μm	seedling soil	4 nM	5 mM $Ru(bpy)_3^{2+}$−phosphate buffer, pH 7.38	400
procaine	50 cm × 25 μm	plasma	0.24 mM	5 mM $Ru(bpy)_3^{2+}$−20 mM phosphate buffer, pH 8.0	422
N,*N*-diethylethanolamine			20 nM		
chloroquine phosphate	50 cm × 25 μm	standard solution	0.3 μM	5 mM $Ru(bpy)_3^{2+}$−50 mM phosphate buffer, pH 8.0	423
arginine[c]	50 cm × 25 μm	standard solution	0.1 μM	5 mM $Ru(bpy)_3^{2+}$−50 mM phosphate buffer, pH 8.0	424
proline			80 nM		
valine			1 μM		
leucine			1.6 μM		
proline	6.8 cm × 50 μm	standard solution	1.2 μM	5 mM $Ru(bpy)_3^{2+}$−15 borate buffer, pH 9.2[d]	265
valine			50 μM		
phenylalanine			25 μM		

[a] With discrete wavelets transform for signal denoising. [b] CE with sequential light-emitting diode-induced fluorescence and ECL detection. [c] Amino acids with precolumn derivatization using acetaldehyde. [d] $Ru(bpy)_3^{2+}$ was introduced to the detection cell with a coaxial flow design.

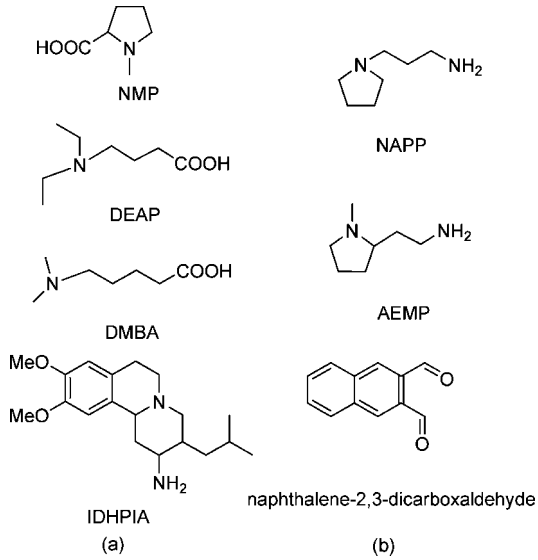

Figure 31. Derivatization reagents used for (a) primary amines and (b) carboxylic acids ECL detection.

Detection of primary amines using naphthalene-2,3-dicarboxaldehyde (Figure 31b) as a derivatization reagent when tri-*p*-tolylamine was used as an electron acceptor for electrogenerated radical anions of naphthalene in the HPLC-ECL system was also reported.[431]

Table 10 lists some of the recent applications of Ru(bpy)$_3^{2+}$ ECL in HPLC for the detection of biomolecules.

Many compounds have been found to be able to quench,[433–438] inhibit,[439–441] or enhance[442,443] the ECL intensities of well-studied coreactant ECL systems such as Ru(bpy)$_3^{2+}$/TPrA and Ru(bpy)$_3^{2+}$/$C_2O_4^{2-}$. For example, phenols,[433,434,438,439] ferrocene,[435] anilinesm[439] and their derivatives can significantly quench the ECL of oxidative-reduction type of coreactant ECL systems via a mechanism involving the energy or electron transfer between Ru(bpy)$_3^{2+}$* and the electro-oxidized species of the quencher.[433–435,438,439] Systematic studies of the quenching effect of 30 phenols and anilines on ECL revealed that the magnitude of ECL quenching was related to the position of the substituting group in the benzene ring and decreased in the order meta > ortho > para.[439] This quenching behavior has been used in FIA for the detection of a large number of phenol and aniline compounds as listed in Table 11, in which the detection limits at $10^{-8}-10^{-9}$ M for the Ru(bpy)$_3^{2+}$/TPrA system and at $10^{-6}-10^{-7}$ M for the Ru(bpy)$_3^{2+}$/$C_2O_4^{2-}$ system were obtained, respectively. A similar strategy has been used in FIA-ECL for the determination of (a) tetracycline (LOD = 4 nM) in a Chinese proprietary medicine and the residues of tetracycline in honey[440] and (b) noradrenaline [LOD = 25 nM for the Ru(bpy)$_3^{2+}$/TPrA system and 7.1 nM for the Ru(phen)$_3^{2+}$/TPrA system] and dopamine [LOD = 15 nM for the Ru(phen)$_3^{2+}$/TPrA system] in commercial pharmaceutical injection samples.[441] The analysis of phenolic compounds, dopamine (LOD = 10 nM) and epinephrine (LOD = 30 nM), has also developed with the CE-ECL method based on the ECL inhibition of the analytes to the Ru(bpy)$_3^{2+}$/TPrA system.[437,444] A very recent study on the ECL inhibition of the Ru(bpy)$_3^{2+}$/TEtA system suggests that the inhibition of Ru(bpy)$_3^{2+}$/tertiary amines ECL by phenols and catechol derivatives in FIA most likely resulted from the electrochemical oxidation of these inhibitors rather than the formation of quenching products, such as quinones.[255]

In contrast to the inhibition behavior discussed above, many compounds have been found to be able to enhance the ECL of Ru(bpy)$_3^{2+}$. For example, melatonin (MT) and its important derivatives, such as 5-methoxyindole-3-acetic acid (MIAA), *N*-acetyl-5-hydroxytryptamine (NAHT), 5-methoxytryptamine (5-MT), and *N*-acetyl-5-methoxy-6-hydroxytryptamine (HMT), are strongly bioactive in humans with regulation actions for genital, endocrine, and immune systems and can enhance the ECL of Ru(bpy)$_3^{2+}$ in a strong alkaline buffer solution (pH ~11.6) upon anodic potential scanning.[443] This enhancement is proportional to the concentration of the compound with LODs of 1.0, 0.1, 1.0, 50.0, and 10.0 nM for MT, MIAA, 5-MT, NAHT, and HMT, respectively. Both the substituted group on the indole ring and the indole ring itself have shown influence on the enhancement ability for ECL. As proposed in Scheme 17,[443] MT and its derivatives (I) are weakly acidic; the proton on the N_1 position of the indole ring is easily dissociated to produce the anion (II) in alkaline solution. The anion can be oxidized under a certain applied potential (E_1) to form the active free radical intermediate (IV). Meanwhile, the compound (I) is oxidized in the lower potential range of 0.2–0.5 V vs Ag/AgCl to form the free radical cation (III); this free radical cation can also lose a proton to form the active neutral free radical intermediate (IV). However, as the neutral free radical intermediate (IV) is very unstable, if there is no active substance in the system, this acid−base equilibrium tends toward formation of the free radical cation (III), which is further oxidized in the potential range of 0.9–1.0V vs Ag/AgCl to form a cation (V), whereas this process is not followed by ECL. In the presence of Ru(bpy)$_3^{2+}$, the reductive neutral free radical intermediate (IV) is easier to react with the electrogenerated Ru(bpy)$_3^{3+}$ to produce the excited state Ru(bpy)$_3^{2+}$* that emits light.

Similarly, allopurinol, a well-known inhibitor of xanthine oxidase, was detected on the basis of FIA-ECL enhancement for Ru(bpy)$_3^{2+}$ at pH 12 with a detection limit of 5 nM.[445] Also, a detection limit of 50 ng/mL for allantion was obtained at pH 11, in which the ECL emission was believed to result from the reaction between Ru(bpy)$_3^{3+}$ and the hydroxylic radical ion generated from allantion ionization in the strong alkaline solution.[446] On the basis of the enhancement of L-thyroxine on Ru(bpy)$_3^{3+}$−NADH ECL intensity, the determination of L-thyroxine (LOD = 50 nM) in pharmaceuticals was carried out.[442] The detailed reaction mechanism is unclear but may involve the increase of the active intermediate NAD$^{\bullet}$ formation rate by coexisting thyroxine during the oxidation of DADH by electrogenerated Ru(bpy)$_3^{3+}$. Finally, detection of fenoterol (LOD = 0.24 μM), salbutamol (LOD = 0.40 μM),[447] and cefadroxil[448] in pharmaceuticals was performed with FIA-Ru(bpy)$_3^{2+}$ ECL configuration.

The CE-ECL technology also has been applied for the thermodynamic and kinetic studies, for example, of drug–human serum albumin (BSA) binding,[449,450] of paracetamol on prolidase activity in erythrocytes,[451] and in the serum of diabetic patients,[452] with procain hydrolysis as a probe for butyrylcholinesterase by in vitro procain metabolism in plasma with butyrylcholinesterase acting as bioscavenger,[422] and the interaction of chloroquine phosphate with BSA.[423] A number of advantages are offered by CE-ECL with respect to other commonly used separation−detection methods such as HPLC using UV−vis or fluorescent

Table 10. Selected Applications of $Ru(bpy)_3^{2+}$ ECL in HPLC

analyte	matrix	limit of detection	ECL reagent	refs
atenolol	pharmaceutical urine[a]	0.5 μM	1 mM $Ru(bpy)_3^{2+}$−10 mM borate buffer, pH 9.0	425
metoprolol		0.08 μM		
matrine	*Sophora flavescens*	3 ng/mL	0.8 mM $Ru(bpy)_3^{2+}$−50 mM NaOH−NaAc−0.3 M KNO_3	426
sophocarpine		6 ng/mL	buffer, pH 10.0, 0.5 mL/min, 2.0 mL/min	
sophoridine		1 ng/mL		
sophoridine	standard solution	30 pg/mL	0.8 mM $Ru(bpy)_3^{2+}$−50 mM NaOH−NaAc−0.3 M KNO_3	427
matrine		60 pg/mL	buffer, pH 10.0, 0.5 mL/min	
sophocarpine		100 pg/mL		
sophoranol		70 pg/mL		
erythromycin A	rat plasma	<0.05 μg/mL	10 mM H_2SO_4−0.8 mM $Ru(bpy)_3^{2+}$, 0.3 mL/min[b]	428
decladinosylerythromycin A	urine	<0.5 μg/mL		
erythromycin B				
ibuprofen[c]	human plasma[d]	45 fmol	10 mM H_2SO_4−0.8 mM $Ru(bpy)_3^{2+}$, 0.5 mL/min[b]	429
myristic acid		70 fmol		
palmitic acid		70 fmol		
histamine		70 fmol		
phenylbutylic acid[c]	human serum[d]	0.6 fmol	10 mM H_2SO_4−0.8 mM $Ru(bpy)_3^{2+}$, 0.3 mL/min[b]	430
myristic acid		0.5 fmol		
palmitic acid		70 fmol		

[a] Sotalol, nadolol, and pindolol were also separated and detected, but no limits of detection were stated. [b] $Ru(bpy)_3^{3+}$ was generated upstream before mixing with analytes in the detection cell. [c] Analytes were derivatized before ECL detection. [d] Lauric acid, myristoleic acid, α-linolenic acid, palmitoleic acid, arachidonic acid, α-linoleic acid, oleic acid, and stearic acid were also derivatized, separated, and detected, but no limits of detection were stated.

Table 11. Detection Limits of Phenols and Anilines Using (a) $Ru(bpy)_3^{2+}/C_2O_4^{2-}$ and (b) $Ru(bpy)_3^{2+}$/TPrA ECL Systems[a]

	detection limits	
phenols and anilines	$Ru(bpy)_3^{2+}/C_2O_4^{2-}$, pH 5.5, μM	$Ru(bpy)_3^{2+}$/TPrA, pH 8.0, nM
phenol	1.2	60
catechol	0.11	36
resorcinol	0.073	2.0
hydroquinone	0.13	33
4-hydroxy-3-methoxybenzyl alcohol	0.33	96
rutin	0.33	40
o-nitrophenol	0.10	9.0
m-nitrophenol	0..078	7.0
p-nitrophenol	0.34	14
salicylic acid	0.73	11
m-hydroxybenzoic acid	0.053	1.5
p-hydroxybenzoic acid	0.20	52
sulfosalicylic acid	0.84	20
protocatechuic acid	0.75	63
2,4-dihydroxybenzoic acid	0.11	12
3,5-dihydroxybenzoic acid	0.092	3.0
phloroglucin	0.15	1.8
pyrogallol	0.22	42
norepinephrine	0.12	9.2
epinephrine	0.23	11
dopamine	1.1	21
gallic acid	0.15	13
tannic acid	0.12	3.0
4-hydroxy-3,5-dimethoxybenzoic acid	1.0	58
1-naphthol	3.6	10
2-naphthol	1.0	14
aniline	0.70	18
m-phenylenediamine	1.1	45

[a] $[Ru(bpy)_3^{2+}] = 20\ \mu M$, $[C_2O_4^{2-}] = 0.5$ mM, [TPrA] = 0.1 mM, $[NaH_2PO_4-Na_2HPO_4] = 0.1$ M (modified from ref 439).

detection for this kind of study and include very powerful resolving ability, good selectivity, high sensitivity, easy sample preparation, and fast data measurement as generally no sample pretreatment is needed and no interference exists.[423,450,452] Characterization of high-affinity antibodies[453] and rapid estimation of enzyme activity in the hydrolysis of peptides[454] by flow-cell-based $Ru(bpy)_3^{2+}$ ECL have also been recently demonstrated. Moreover, CE-ECL for the quantitative determination of pentoxyverine with gold nanoparticle enhanced ECL detection at an appropriate volume

Scheme 17. Proposed Mechanism for the ECL Reaction of $Ru(bpy)_3^{2+}$ with Melatonin and Its Derivatives[a]

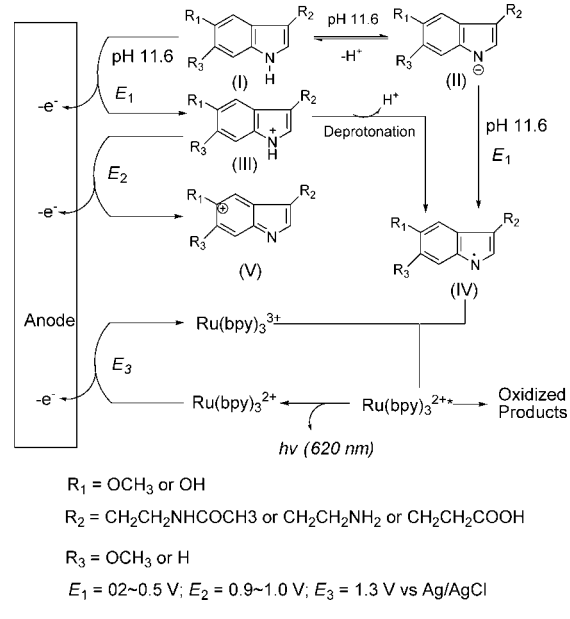

[a] Modified with permission from ref 443.

ratio of nanogold with $Ru(bpy)_3^{2+}$ has been published, in which detection limits of 6 nM and 0.6 μM with or without nanogold were obtained, respectively.[450]

In addition to $Ru(bpy)_3^{2+}$ ECL systems, sensitive luminol-based ECL combined with FIA has also been used for the detection of biorelated species (Table 12). This kind of detection is based on either the enhancing[455–457] or inhibition effect[458] of the analyte on the ECL of luminol or the chemiluminescence reactions of luminol with the electrochemically reduced analyte[459] or with H_2O_2 produced from enzymatic reactions of analytes in the presence of their corresponding oxidases.[460,461]

7.2. Solid Phase ECL Assay Formats

A large number of biomolecules such as proteins, DNAs, and peptides either have no "coreactant function-

Table 12. Applications of Luminol-Based ECL in FIA

analyte	matrix	exptl condition	limit of detection	refs
hydrazine	drinking water waste water	electrooxidation of 60 μM luminol−50 mM borax buffer at pre-anodized Pt, 2.5 mL/min	6.0 nM	456
rifampicin	capsule ocustilla urine	electrooxidation of 4.0 μM luminol−20 mM borax buffer at Pt, 2 mL/min	8.0 nM	457
epinephrine	epinephrine injection solution	electrooxidation of 8.0 μM luminol−50 mM borax buffer at Pt, 2.5 mL/min	28 nM	455
catechol DHBA[a] chlorogenic acid	cigarettes	electrooxidation of 0.25 mM luminol−0.10 M KCl, pH 12.4 at GC, 3.5 mL/min	12 nM 21 nM 5.2 nM	458
vanadium (II)	water	electroreduction of 0.10 mM luminol−1.2 mM $Na_2C_2O_4$ at hollow carbon electrode	0.2 ng/mL	459
norfloxacin oxfloxacin ciprofloxacin pefloxacin enoxacin	pharmaceutical samples	electrooxidation of 0.4 μM luminol−0.10 M Na_2CO_3−$NaHCO_3$ at Pt, 2.0 mL/min	4.0 ng/mL 2.0 ng/mL 10 ng/mL 8.0 ng/mL 0.80 ng/mL	462
choline	standard solution	electrooxidation of 50 μM luminol−30 mM veronal buffer with 30 mM KCl−1.5 mM $MgCl_2$, pH 9.0, at GC, 0.5 mL/min, various supports used for the immobilization of choline oxidase	10−300 pmol	461
glycolic	standard solution	electrooxidation of 0.25 mM luminol−50 mM KNO_3, pH 9.0 at carbon paste containing ground spinach leaves, 1.5 mL/min	15 μM	221

[a] DHBA, 3,4-dihydroxybenzoic acid.

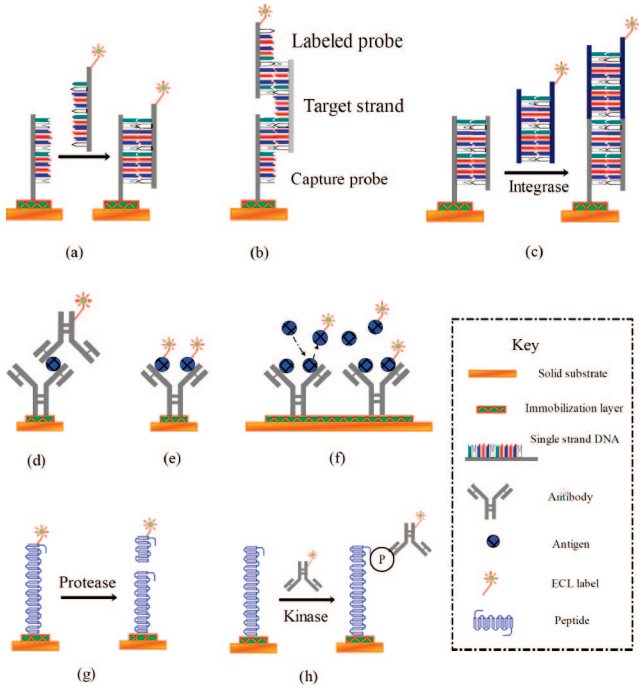

Figure 32. Examples of solid phase ECL assay formats: (a) DNA hybridization assay based on an immobilized ssDNA hybridizes with a labeled target ssDNA; (b) sandwich type DNA biosensor; (c) assay used for integrase activity test with immobilized and free labeled dsDNA; (d) sandwich type immunoassay; (e) direct immunoassay; (f) competitive assay in which analyte competes with labeled analyte for antibody binding sites on immobilized antibody; (g) protease activity assay in which cleavage of the immobilized peptide results in the decrease in ECL emission due to the removal of the ECL label; (h) kinase activity assay using a labeled antibody to recognize the phosphorylated product.

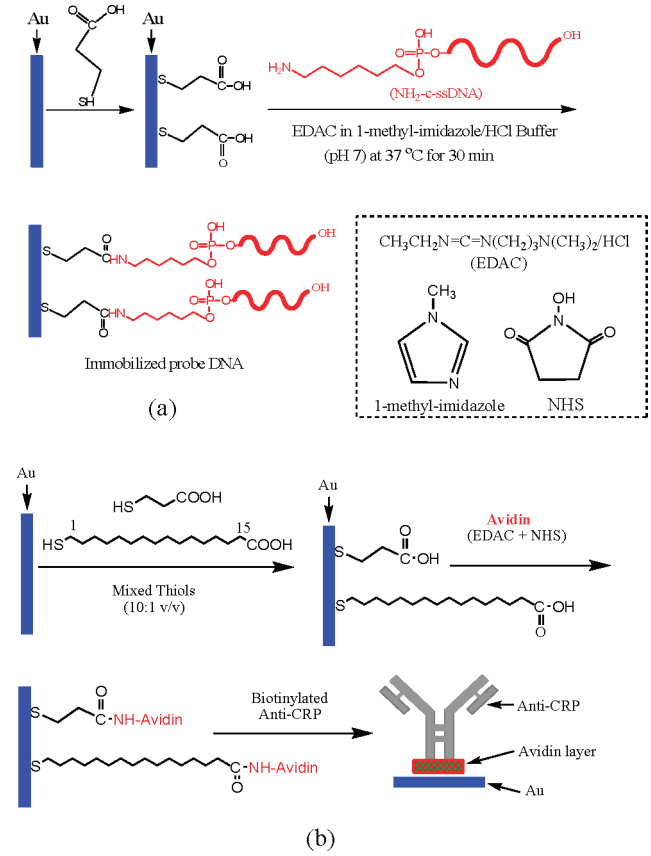

Figure 33. Schematic diagram showing (a) the immobilization of ssDNA (NH_2-c-ssDNA) onto the surface of Au(111)/3-MPA monolayer and (b) the attachment of anti-CRP onto the surface of Au(111)/mixed SAMs/avidin layer. Reprinted with permission from ref 250. Copyright 2003 American Chemical Society.

alities" or have very poor abilities to act as a coreactant; their ECL detections are mainly carried out with solid phase ECL assay formats, in which biomolecules linked with ECL labels [e.g., $Ru(bpy)_3^{2+}$] are immobilized on a solid substrate (e.g., a electrode or a microsized polystyrene bead) and ECL signals associated with the analyte concentration are produced in the presence of an added ECL coreactant, typically TPrA. Figure 32 illustrates eight examples of solid phase ECL assay formats, in which panels a−c, d−f, and g−h are DNA, antibody−antigen, and peptide-related, respectively. In the first case of DNA detection (Figure 32a), a target single-stranded DNA (ssDNA) with an ECL label attached hybridizes with a ssDNA probe that immobilized on a solid substrate.[188,250]

Table 13. Applications of $Ru(bpy)_3^{2+}$ ECL for the Detection of DNA Hybridization

DNA sequence[a]	detection method	comments[d]	refs
5′-SHC_6-22-mer[b]	using DNA-binding intercalator as a reductant of electrogenerated $Ru(bpy)_3^{3+}$ with a throughhole type DNA biosensor	dsDNA intercalated by doxorubicin, daunorubicin, and 4,6-diamidino-2-phenylindole (DAPI), in which DAPI showed efficient ECL	486
5′-NH_2-24-mer	$Ru(bpy)_3^{2+}$-doped silica NPs as ECL labels using assay format of Figure 32a, ECL coreactant: 2.5 mM $H_2C_2O_4$ in PBS, pH 6.6	LR = 0.20 pM−2.0 nM, LOD = 0.10 pM, three-base mismatch and noncomplementary sequences showed almost no ECL	476
5′-21-mer C_6NH_2SH, 5′-NH_2C_6-18-mer, and 42-mer	carbon nanotubes loaded $Ru(bpy)_3^{2+}$ as ECL labels using sandwich type DNA sensor (Figure 32b), ECL in 0.10 M PBS (pH 7.4)−0.10 M TPrA	LR = 24 fM−1.7 pM, LOD = 9.0 fM, discriminated two-base mismatched ssDNA	485
5′-NH_2C_6 23-mer[c]	Au(111)/SAM−DNA using assay format of Figure 32a with $Ru(bpy)_3^{2+}$ tag in 0.10 M $LiClO_4$−0.10 M Tris−0.10 M TPrA (pH 8.0)	a series of electrode treatments (e.g., blocking free −COOH groups and pinholes, washing, and inert gas spraying) were used to reduce the nonspecific adsorption of the labeled species	250
5′-biotin−TEG 23-mer	using $Ru(bpy)_3^{2+}$ loaded PSB as ECL labels, hybridized DNA separated magnetically, ECL in MeCN−0.055 M TFAA−0.10 M TPrA−0.10 M $(TBA)BF_4$	LR = 1.0 fM−10 nM, distinguished two base pair mismatched from noncomplementary DNA hybridization	188
5′ 18-mer−C_3 SH-3′	target ssDNA immobilized on Au electrode hybridized with probe ssDNA labeled with ∼15 nm Au NPs covalently attached with a large number of $Ru(bpy)_3^{2+}$, ECL in 0.10 M PBS (pH 7.4)−0.10 M TPrA	LR = 10 pM−10 nM, LOD = 5.0 pM	487
5′-SH (or NH_2)-19-mer	hybridization on integrated Au chip, light detection with a PIN photodiode detector, assay was based on displacement of DNA hybridization, ECL in phosphate buffer (pH 8.0)−0.10 TPrA	$Ru(bpy)_3^{2+}$ LOD = 0.1 fM	488
15-mer	3′ end of one ssDNA labeled with $Ru(bpy)_3^{2+}$ hybridized with another ssDNA tagged with Cy5 at 5′ end, efficient ECL quenching was observed in ∼0.3 M PBS (pH 7.5)−0.1 M TPrA−SDS (<0.1% w%)	LOD = 30 nM, quenching efficiency = 78%	436
5′-NH_2-15-mer	$Ru(bpy)_2(phen)^{2+}$ derivative as ECL label, assay format of Figure 32a was used, considerably better discrimination of two base pair mismatch was obtained with −0.3 V vs Ag for 300 s, Au chip electrode was used, ECL in 0.3 M PBS (pH 7.8)−0.1 M TPrA−0.1% SDS	LOD = 1 pM in 30 μL of buffer	491
5′-NH_2-18-mer	anodically oxidized GC electrode was used for covalent immobilization of DNA, hybridization detection using labeled $Ru(bpy)_3^{2+}$ was conducted in PBS buffer−4% TPrA	LOD < 1 pM	489

[a] Synthetic DNA sequences were used, unless otherwise stated. [b] Target organism, hepatitis A, B, and C virus, [c] Target organism, *Bacillus anthraci* (Ba813). [d] LR, linear range; LOD, limit of detection.

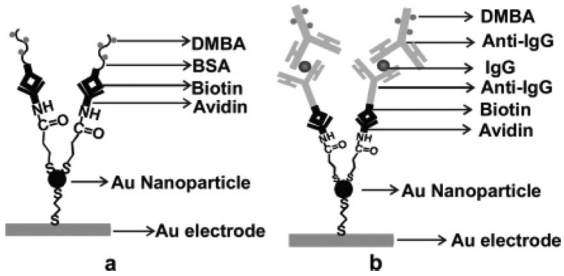

Figure 34. Schematic diagram of immobilization of (a) BSA and (b) IgG on Au electrode with Au nanoparticle amplification. Reprinted with permission from ref 473. Copyright 2005 American Chemical Society.

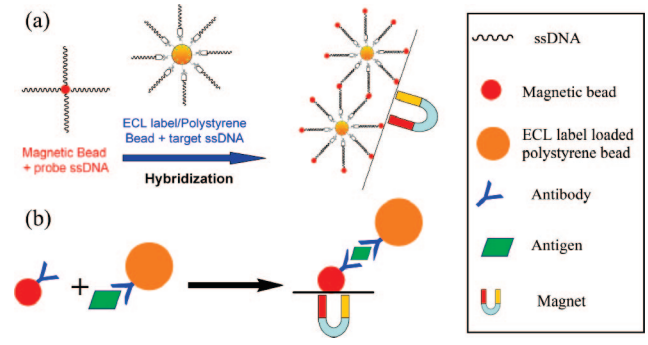

Figure 35. Schematic diagrams of (a) DNA hybridization and (b) sandwich type immunoassay using a polystyrene bead as the ECL label carrier and a magnetic bead for the separation of analyte-containing ECL label/polystyrene beads. Modified with permission from refs 187 and 188.

Under the same experimental conditions, ECL produced from the complementary ssDNA hybridization will be higher than that obtained from a noncomplementary one. Very weak to no ECL signal should be observed if the two ssDNAs are completely mismatched. The minor ECL is often generated from the nonspecific adsorption of the target ssDNA. Figure 32b shows a sandwich hybridization

Table 14. Applications of $Ru(bpy)_3^{2+}$/TPrA ECL Sandwich Type Immunoassays Using Commercial Magnetic Bead-Based Instrumentation[66]

analyte	application	matrix	comments	refs
Clostridium perfringens α toxin	gas gangrene biowarfare	assay buffer urine serum	LOD = 1 ng/mL	510
protective antigen (PA) of anthrax toxins anti-PA	virulence of *Bacillus anthracis*	serum	LOD for free purified PA = 100 pg/mL	507
Clostridium botulinum toxins A, B, E, F	diagnosis of poisoning biological weapon	human serum, urine, assay buffer, and selected foods (milk, beef, eggs, etc.)	LOD for clinical samples = 50 pg/mL for A and E, 100 pg/mL for B, 400 pg/mL for F; LOD for food samples = 50 pg/mL for A, 50−100 pg/mL for B, E, and F	511
Clostridium botulinum type B neurotoxin	diagnosis of poisoning biological weapon	PBS buffer	LOD = 0.39−0.78 ng/mL (vs 1.56 ng/mL with ELISA), ECL assay was 2−4 times more sensitive than the clorimetric ELISA	508
cardiac tropopin T	cardiac disease marker	plasma serum		514
malignant melanona	tumor marker	serum	LOD < 0.02 μg/L	515
antibodies directed against therapeutic human monoclonal antibodies	drug	serum samples (mouse, monkey, rat and human)	LOD = 5−63 μg/L	522
E. coli O157	surface water	raw water samples	LOD = 1 viable water-borne *E. coli* 157 cell/100 mL of surface water	523
β-crosslaps N-MID-osteocalcin intact parathyroid hormone	serum markers of bone metabolism	serum		513
NT-proBNP	marker for various pathologic conditions in pregnancy and the puerperium	plasma		521
	cardiac disease marker neonate cord blood	neonate cord blood mother's blood	11.6-fold higher in the cord blood than in the blood samples from the respective mothers	516
	cardiomyopathy	blood, plasma	LOD = 0.5 pM, LR = 2.60−3540 nM, healthy woman ≫ men, patients with cardiomyopathy ≫ normal subjects, progressively increased with the severity of heart failure	517
sex hormone-binding globulin (SHBG)	regulates the cellular bioavailability of SHBG-boundsteroid hormones, thyroid dysfunction marker	serum	av values, hyperthyroid males, 60 nM; females, 90 nM; healthy males, 30 nM; females, 61 nM	518
parathyroid hormone (PTH)	uremic marker	serum	constant differences in PTH values among immunoassays were observed	519
prolactin	Behcet disease (BD)	serum	prolactinemia was much higher (∼19.34 ng/mL) in BD patients vs controls (∼9.83 ng/mL)	524
adrenocorticotropic hormone (ACTH)	hypothalmic−pituitary−adrenal disorders	plasma	LOD = 1.8 ng/L, subjects without disorders = 7.2−63 ng/L	520

format using a labeled probe and an immobilized probe, each specific for a different sequence of a target ssDNA. This type of format has been employed for the sensitive detection and quantification of DNA and RNA amplification products using nucleic acid sequence-based amplification reactions.[463–465] The ligation activity of HIV integrase can be determined by measuring the ligation of labeled dsDNA to an immobilized dsDNA, as schematically displayed in Figure 32c.[168] The sandwich type format shown in Figure 32d[187,250] is perhaps the most commonly used means of ECL detection of an antigen, although direct interaction between the capture antibody and corresponding labeled antigen is also possible (Figure 32e). One requirement for the direct detection would be the pretreatment of the antigen (analyte) with the ECL label and subsequent separation of the free ECL labels from the antigen−ECL label conjugates. This process could dramatically slow the entire detection progress compared to the sandwich type assays, where both surface-confined and ECL-labeled antibodies can be pre-prepared. However, the direct detection format can be very useful in biology for studying receptor−ligand interactions.[168] In a competition assay format (Figure 32f), unlabeled analyte (usually antigen) in the test sample is measured by its ability to compete with labeled antigen in the immunoassay. The unlabeled antigen blocks the ability of the labeled antigen to bind because that binding site on the antibody is already occupied. Thus, in a competitive

Table 15. Selected Immunoassays Provided Originally by BioVeris (Now Roche Diagnostics[66])

analyte	function	application	assay format
cyclic adenosine monophosphate (cAMP)	indicator of cellular metabolism, cellular function, and modification of cellular pathways	widely used in the discovery and development of new therapeutics	*a*
Campylobacter jejuni	leading cause of bacterial diarrheal illness in the U.S.	detection of raw poultry and other food matrices	*b*
cardiac troponin T (cTnT)	specific protein found only in adult myocardium, a marker of myocardial damage when elevated in serum and plasma	used as an indicator of myocardium damage and for the research and development of novel therapeutics designed to decrease heart disease	*b*
intracellular cGMP	a second messenger, most notably by activating intracellular protein kinases in response to the binding of membrane-impermeable peptide hormones to the external cell surface	detected in crude cell lysates	*a*
DNA polymerases	essential to DNA replication and repair	to determine if a potential "reverse transcriptase inhibitor" inhibits DNA-dependent DNA polymerases leading to increased patient toxicity and side effects	*c*
E. coli O157	major foodborne pathogen	detection and identification in food matrices, water, poultry, and fecal samples	*b*
Clostridium botulinum neurotoxins A, B, E, and F	family of functionally similar, yet antigenically distinct toxins produced by *C. botulinum*, potential use of these toxins as biowarfare	most sensitive antibody pairs can detect <100 pg/mL of homologous toxoid diluted in assay diluent and whole milk	*b*
helicase activity	enzymes that unwind DNA−DNA, DNA−RNA, or RNA−RNA duplexes by disruption of the hydrogen bonds that hold the strands together	to search compounds that inhibit helicases of pathogenic viruses and bacteria which may be important therapeutic molecules for treatment of infectious diseases	*d*
HIV integrase	32 kDa protein produced from the C-terminal portion of the Pol gene product, attractive potential target for new anti-HIV therapeutics	screening potential novel drug candidates for HIV-1 integrase inhibition	Figure 32c
G-protein coupled- receptors (GPCRs) ligand binding	large protein that senses molecules outside the cell and activate inside signal transduction pathways	drug (inhibitor) screening	*e*
Listeria	serious infectious disease caused by eating contaminated food with the bacterium; the disease affects primarily pregnant women, newborns, and adults with weakened immune systems	detecting food contamination by *Listeria*	*b*
Salmonella	consists of a range of very closely related bacteria, many of which cause disease in humans and animals	to detect *Salmonella* at concentrations as low as 1000 cells/mL	*b*
Staphylococcus aureus enterotoxin B (SEB)	represents an antigenically diverse group of toxins with similar biological activities that can be expressed naturally in contaminated foods; the toxicity and stability of SEB make it a prime candidate as a potential bioterrorism agent	detection in food matrices with LOD 10 pg/mL	*b*
tumor necrosis factor α (TNF-α)	17 kDa cytokine that is an important mediator of the inflammatory response, apoptosis, cell proliferation, sepsis, and other immune responses	in therapeutic applications and clinical testing	*b*
tyrosine kinase	enzyme that can transfer a phosphate group from ATP to a tyrosine residue in a protein	measuring tyrosine kinase activity and identifying kinase inhibitors	*f*

[a] Competitive immunoassay. [b] Sandwich immunoassay. [c] Combine DNA polymerase and dNTPs → denature, neutralize, and add excess biotin probe → capture with streptavidin-coated beads → ECL detection. [d] Homogeneous unwinding of helicase substrate DNA → capture of $Ru(bpy)_3^{2+}$–labeled substrate ssDNA with biotinylated capture ssDNA → attachment of biotin−dsDNA to MB → ECL detection. [e] Receptor−ligand assay. [f] Modified direct immunoassay.

immunoassay, less label measured in the assay means more of the unlabeled (test sample) antigen is present. The amount of antigen in the test sample is inversely related to the amount of label measured in the competitive format.

Table 16. Immunoassays Available From Meso Scale Discovery[65]

phosphoprotein and intracellular markers			cardiac markers
Akt	IGF-1R	p70S6K	troponin T
BAD	IR	PARP	troponin I
caspase	IRS-1	PDGFR-b	troponin ITC
Erb-B2	JNK	S6RP	CKMB
ERK1/2	Jun	STAT3	myoglobin
GSK-3α	MAPKAPK-2	Tau	CRP
GSK-3β	MEK	tuberin	myeloperoxidase
HIF-1α	Met	VASP	FABP3
histone 3	NFκB (p65)	VEGFR-2	
HSP27	p38		
HSP70	p53		

vascular markers and growth factors	fertility markers	Alzheimer's disease markers	hypoxia markers
VEGF (165/121)	LH	Aβ38	VEGF (165/121)
sVEGFR1	FSH	Aβ40	EPO
sVEGFR2	progesterone	Aβ42	HIF-1
sVCAM-1	HCG	sAPPα	IGFBP-1
sICAM-1	prolactin	sAPPβ (wt)	
sICAM-3	estradiol	swsAPPβ	
SAA	T3	Phospho-Tau	
thrombomodulin	T4	Tau	
E-Selectin		β-secretase	
P-Selectin			
HGF			
bFGF			
PIGF			
CRP			

toxicology	metabolic markers	bone markers	bioprocess assays
troponin T	insulin	ALP	CHO HCP
troponin I	leptin	sclerostin	MTX
troponin ITC	adiponectin	osteoprotegrin	ProA
FABP3	GLP-1(7-36) amide	osteocalcin	insulin
	GLP-1(7-37)	osteonectin	
	GLP-1(Total)	osteopontin	
	resistin	PICP	
	glucagon	TGF-β1	
	grehlin		

cytokine and chemokine immunoassays			
CRP	IL-6	I-TAC	MMP-1
eotaxin	IL-6R	KC/GRO/CINC (CXCL1)	MMP-2
eotaxin-3	IL-7	LBP	MMP-3
G-CSF	IL-8	MCP-1	MMP-9
GM-CSF	IL-10	MCP-4	MMP-10
IFN-β	IL-12 (total)	M-CSF	Protein C
IFN-γ	IL-12 p40	MDC	RANTES
IL-1α	IL-12 p70	MIG	TARC
IL-1β	IL-13	MIP-1α	TNF-α
IL-2	IL-17	MIP-1β	TNF-RI
IL-4	IL-18	MIP-3α	TNF-RII
IL-5	IP-10		

The solid phase ECL assays can also be used to measure the activity of enzymes (e.g., protease, kinase) as shown in Figure 32g,h. For example, in the presence of protease, the ECL intensity of the immobilized peptides tagged with ECL labels will decrease due to the cleavage of the peptides (Figure 32g). In contrast, an increase in ECL intensity is expected when nonlabeled peptides react with labeled phosphopeptide-specific antibodies in the presence of kinase as a result of peptide−antibody (ECL label) conjugate formation[466] (Figure 32h).

A number of methods can be used for the immobilization of biomolecules onto a solid substrate, which include avidin/biotin interactions,[187,188,250,467] silanization,[468] sol−gel,[469,470] self-assembled thiol−COOH monolayers (SAMs),[250,471–473] polymer films,[474–476] and glyoxyl agarose.[477,478] Although direct adsorption of biomolecules onto a solid substrate via hydrophobic or electrostatic interactions[479,480] is also possible, covalent immobilization and avidin−biotin-based attachment of biomolecules generally offer much more stable, reproducible, and less nonspecific adsorption surfaces for ECL detection. Figure 33 illustrates the immobilization of a ssDNA (NH_2-c-ssDNA) onto the surface of Au(111) modified with a 3-mercaptopropanoic acid (3-MPA) monolayer (Figure 33a) and the attachment of anti-C reactive protein (CRP) onto the surface of Au(111) modified with mixed SAMs/avidin layer (Figure 33b).[250] In this study, the use of a mixed thiol monolayer as a binding layer for avidin was aimed to increase the surface coverage of protein,[472] and the detection of DNA and CRP (1–24 μg/mL) was performed with the assay formats shown in Figure 32a,d, respectively, in the presence of TPrA.

Instead of $Ru(bpy)_3^{2+}$, 4-(dimethylamino)butyric acid (DMBA, Figure 31a), an analogue of TPrA, has been used as an ECL label attached to immobilized BSA and anti-immunoglobulin (anti-IgG) for the determination of BAS and IgG when the electrode was in contact with 1 mM $Ru(bpy)_3^{2+}$ solution and scanned from 0.5 to 1.3 V vs Ag/AgCl.[473] Sensitivity enhancements of 10- and 6-fold were obtained with Au nanoparticle amplification for BAS (linear range = 1–80 μg/mL) and IgG (5–100 μg/mL) over their direct immobilization on an electrode using DMBA labeling (Figure 34).

An ultrasensitive DNA hybridization detection and CRP immunoassay methodology that utilizes polystyrene microspheres/beads (PSB) as the carrier of a large number of hydrophobic ECL labels ($Ru(bpy)_3^{2+}$) has been recently demonstrated.[187,188] As shown in Figure 35a, a known sequence ssDNA (probe ssDNA) is first immobilized on the surface of a magnetic bead (MB). The complementary ssDNA (target ssDNA)-coated PSB bead that contains a large number of ECL labels hybridizes with the probe ssDNA to form a [(probe ssDNA-MB)/(target ssDNA-PSB)] aggregate. Finally, this aggregate is magnetically separated from the reaction mixture and transferred into a MeCN solution, in which the PSBs dissolve and the ECL label is released. Light emission from the released ECL labels is subsequently measured in MeCN in the presence of TPrA at a Pt electrode. A similar approach based on a sandwich type immunoassay can be used for the detection of an antigen (e.g., CRP), as displayed in Figure 35b.

With the above PSB-based "high amplification" technique, a detection limit of 1.0 fM (1.0×10^{-15}M) for a t-ssDNA was achieved,[188] along with a ~100-fold improvement in the sensitivity in CRP determination[187] compared to a previously reported surface-immobilized ECL method.[250] Unlike the usual DNA probes and immunoassays based on, for example, fluorescence[481] or ECL (Figure 32), where only one or a few luminophore molecules are attached directly to a biomolecule, so that self-quenching of the fluorescence and nonspecific adsorption can be avoided and the bioactivity of the biomolecule remains, the present technique does not need the direct attachment of the ECL labels to ssDNA or antibodies, so that the loading capacity of the ECL labels per PSB can be as high as $\sim 10^9$ molecules.[187,188] Thus, there is a very large amplification factor of $Ru(bpy)_3^{2+}$ label molecules for each molecule of analyte, given that a limited number of captured ssDNA or antibody species are attached to one PSB via the immobilization layer (of avidin). The

high selectivity of the technique has been reflected by the well distinguishing in ECL intensity between the complementary, two base pair mismatched, and noncomplementary DNA hybridizations.[188] No complicated treatment to eliminate nonspecific adsorption of $Ru(bpy)_3^{2+}$ was required either. Moreover, because the ECL detection was conducted in solution, high stability and the possibility of multiple measurements of ECL without loss of signal were offered.

With the similar idea but using ~100 nm diameter sized liposomes instead of PSBs as the ECL label carrier, CRP detection (in the 100 ng/mL−10 μg/mL range) in aqueous solution containing TPrA has been reported.[284] The release of the ECL label from liposomes was realized by using 0.1 M TPrA and 0.1 M phosphate buffer (pH 7.6) containing 0.1 M NaCl and 1% (v/v) Triton X-100. This water-based approach could allow the ECL detection of biomolecules at a high amplification to be carried out in current commercial instrumentation (section 4.4).

Aptamers are oligonucleic acid or peptide molecules that bind a specific target molecule.[482] Recently, a novel ECL aptamer-based biosensor for the determination of a small molecule drug has been designed employing cocaine-binding aptamer as molecular recognition element for cocaine as a model analyte and a Ru(II) complex served as an ECL label.[483] An enhanced ECL signal was generated from a gold electrode immobilized with the ECL probe, which was a 5′-terminal cocaine-binding aptamer with the ECL label at 3′-terminus of the aptamer, upon recognition of the target cocaine. This was attributed to a change in the conformation of the ECL probe from random coil-like configuration on the probe-modified film to three-way junction structure, in close proximity to the sensor interface. A detection limit of 1.0 nM cocaine was obtained with the designed sensor.

In addition to the above solid phase ECL assays, approaches have been developed for carrying out ECL binding assays and immunoassays in homogeneous solution formats after the interaction of biomolecules with ECL labels in solution.[59,168] For example, ultrasensitive detection of tumor markers, such as three molecular forms of prostate-specific antigen (PSA), PSA free, PSA complex, and PSA total, was studied using PSA tagged with $Ru(bpy)_3^{2+}$ in the presence of TPrA with a PSA detection limit of 1.7 pg/mL.[484] The solution phase ECL intensity was found to be inversely proportional to their molecular weight ($W^{1/2}$), because the bigger the biomolecules [with small $Ru(bpy)_3^{2+}$ attached], the smaller their diffusion constants were. Likewise, the binding of labeled PSA with its antibody resulted in the decrease in ECL intensity, which was used for the estimation of the affinity constant ($\sim 1 \times 10^{10}$ M^{-1}).[484]

7.3. DNA Detection and Quantification

Most of the recent DNA hybridization detection methods have used the assay format displayed in Figure 32a, although sandwich format assays (Figure 32b) were also reported.[464,465,485] $Ru(bpy)_3^{2+}$ or its derivatives and TPrA have been extensively employed as ECL labels and as a coreactant, respectively. In one paper, however, several dsDNA intercalators were used as reductants of electrogenerated $Ru(bpy)_3^{3+}$ for ECL generation.[486] Oxalate was also chosen as a coreactant for DNA detection.[476] To increase the ECL sensitivity, multiple ECL labels loaded in microsized polystyrene microspheres,[188] silica NPs,[476] and carbon nanotubes[485] or immobilized on Au NPs[487] have been investigated. In addition to millimeter-sized Au electrodes, micrometer-sized Au chips[488] and anodically oxidized GC electrodes[489] have been also used as substrates for covalent immobilization of DNA. Progress in the miniaturization of ECL instrumentation for DNA quantification has been made by the combination of assembled microcell[490] or Au chip electrode[488] with a positive−intrinsic−negative (PIN) photodiode detector. Note that although a silicon PIN diode is typically 2 orders of magnitude less sensitive than a PMT, the noise level is also lower, resulting in a theoretical noise equivalent power ratio of ~20 at room temperature.[490] Efficient ECL quenching of ssDNA−-$Ru(bpy)_3^{2+}$ upon its hybridization with the second ssDNA tagged with Cy5 dye has been demonstrated to be another promising approach for DNA detection and quantification.[436] A study of electric field effect on DNA mismatch discrimination revealed that DNA mismatched discrimination was considerably better when a negative electrode potential of −0.3 V vs Ag was applied for 300 s prior to the ECL detection.[491] Table 13 lists some recent examples of DNA hybridization detection and quantification on the basis of $Ru(bpy)_3^{2+}$ ECL.

Detection of DNA fragments after Polymerase Chain Reactions (PCR) has been mainly performed with sandwich assay format,[492] where the PCR-amplified DNA strands were typically immobilized on the surface of streptavidin-coated MB via biotin-labeled reverse primers and the other ends were linked with $Ru(bpy)_3^{2+}$ molecules. Highly sensitive methods are needed for the detection of PCR products to reduce the number of amplification cycles, as errors are exponentially amplified through multiple cycles toward a plateau phase before sufficient product is generated for analysis.[493] The bead-based PCR-ECL system has been utilized for the detection of anthrax spores using PCR-amplified DNA-aptamers,[494] the detection of various genes from viruses and diseases in human blood and serum[495–498] and plants,[499] genetically modified organisms such as vegetables,[500] and the measurement of DNA helicase activity of *Escherichia coli* DNA.[501]

Other methods of DNA hybridization detection include luminol−H_2O_2-based[502,503] and hot electron-induced ECL.[504] A luminol derivative, *N*-(4-aminobutyl)-*N*-etylisoluminol (ABEI), anchored on a target ssDNA was used for the ECL detection of the hybridization between a complementary probe ssDNA covalently linked to a polypyrrole support and the target ssDNA.[503] In the latter case, thin oxide film coated Al and Si electrodes were modified with an aminosilane layer and derivatized with short, 15-mer DNAs via diisothiocyanate coupling. Target DNAs were conjugated with tetramethylrhodamine dye at their amino modified 5′ end, and hybridization was detected using hot electron-induced ECL of the dye. A limit of detection in picomolar levels and the discrimination of two base pair mismatched hybrids were demonstrated. Furthermore, label-free ECL DNA detection based on catalytic guanine and adenine bases oxidation using $Ru(bpy)_3^{2+}$ modified GC electrode with a cast carbon nanotube/Nafion/ $Ru(bpy)_3^{2+}$ composite film has been recently presented.[380] ECL signals of dsDNA and its thermally denatured counterparts were distinctly discriminated at a low concentration of 30.4 nM for salmon testes DNA, and single-base mismatch detection of p53 gene sequence segment was realized with 0.4 nM. Previously, direct ECL detection of DNA in poly(vinylpyridine) (PVP) ultrathin film using cationic polymer $[Ru(bpy)_2(PVP)_{10}]^{2+}$ or $[Os(bpy)_2(PVP)_{10}]^{2+}$ and also chemically induced damage by

styrene oxide of DNA were demonastrated.[505] This has been extended for the study of DNA damage from benzo[*a*]pyrene metabolites using ECL arrays suitable for genotoxicity screening.[506]

7.4. Detection and Quantification of Other Biorelated Species

Applications of $Ru(bpy)_3^{2+}$ ECL for the determination of amino acids, pharmaceuticals, clinical analytes, and analytes associated with food, water, and biological agents were extensively reviewed by Debad et al.[168] and Richter[58] in 2004. As a result, this section will mainly focus on recent developments of ECL for the detection and quantification of biorelated species that have not been covered in previous reviews and previous sections of this contribution.

The majority of biomolecule detections have been carried out with commercially available magnetic bead-based instruments (Figure 17) using $Ru(bpy)_3^{2+}$ as an ECL label and TPrA as a coreactant. A wide range of analytes have been studied, which include (a) various types of toxins,[507–512] (b) biomarkers for diseases,[513–520] bone metabolism,[513] and various pathologic conditions in pregnancy and the puerperium,[521] (c) antibodies directed against therapeutic human monoclonal antibodies,[522] and (d) bacteria.[523] Matrices used include body fluids, buffer solutions, and food and water samples. Low detection limits of the analytes in the nanograms per milliliter or nanomolar levels have been commonly obtained. Table 14 lists some of the recent applications of $Ru(bpy)_3^{2+}$/TPrA ECL sandwich type immunoassays using commercial magnetic bead-based instrumentation.

An ultrasensitive human CRP detection method based on cathodic hot-electron-induced sandwich type ECL using an isothiocyanate derivative of Tb(III) chelate as a labeling agent for anti-CRP antibodies and disposable, thin insulating film-coated silicon electrodes in fully aqueous solution has been described.[525] With this technique, a low CRP detection limit of 0.3 ng/mL and a calibration curve spanning over ~4 orders of magnitude of concentration were achieved. Moreover, unlike previously discussed surface or solid phase ECL, a homogeneous ECL immunoassay for the determination of anti-digoxin antibody and digoxin hapten (LOD = 0.10 ng/mL) has been recently developed employing $Ru(bpy)_2$(dcbpy)NHS (dcbpy = 2,2′-bipyridine-4,4′-dicarboxylic acid) as an ECL label and BSA as a carrier protein.[526]

Table 15 summarizes the representatives of the immunoassays provided originally by BioVeris[66] in which more than 15 analytes, their functionalities, and applications, as well as their immunoassay formats are briefly explained.

A large number of immunoassays now can be conducted with imaging-based ECL instruments manufactured by Meso Scale Discovery[65] (section 4.4 and Figure 17). As listed in Table 16, the company offers a wide variety of immunoassays, including phosphoprotein and intracellular markers, cardiac markers, vascular markers and growth factors, fertility markers, Alzheimer's disease markers, hypoxia markers, toxicology, metabolic markers, bone markers, bioprocess assays, and cytokine and chemokine immunoassays. A total of ~150 immunoassays are currently available from Meso Scale Discovery. Readers are referred to the company's Website[65] for further description and discussion on the particular immunoassays of interest.

8. Concluding Remarks

The rapid development of ECL in both fundamentals and applications over the past several years has clearly demonstrated that ECL is a powerful tool for ultrasensitive biomolecule detection and quantification. High-throughput, miniaturized biosensors based on ECL technology capable of multiplexing detection with high sensitivity, low detection limit, and good selectivity and stability will continue to attract the interest of the research community. With further understanding of ECL mechanisms, new highly efficient, tunable ECL systems, both emitters and coreactants, will be developed. Approaches based on ECL enhancement as well as quenching may play an important role in designing new methodologies for sensitive biomolecule recognition. Thermodynamic and kinetic studies of biomolecule interactions using ECL are expected to be further expanded. The combination of ECL with other techniques could lead to the development of new instruments or provide valuable insights into molecular structures and intracellular components of biorelated species. Ultimately, detection of single biomolecules will be realized.

9. Acknowledgment

The partial support of this work by grants from NSF-MRSEC (NSF-DMR 0213883) via the University of Southern Mississippi and NSF-OISE 0535467 is gratefully acknowledged.

10. Abbreviations

$(TBA)BF_4$	tetra-*n*-butylammonium tetrafluoroborate
$(TBA)PF_6$	tetra-*n*-butylammonium hexafluorophosphate
4-TBNH	4-(1*H*-tetrazol-5-yl)benzonitrile
5-MT	5-methoxytryptamine
Aβ38	beta amyloid 38
Aβ40	beta amyloid 40
Aβ42	beta amyloid 42
ABEI	*N*-(4-aminobutyl)-*N*-ethylisoluminol
ABN	4-acetylbenzonitrile
acac	acetylacetonate
AEMP	2-(2-aminoethyl)-1-methylpyrrolidine
ALP	alkaline phosphatase
AN	anthracene
APD	avalanche photodioide
AZA-bpy	4-(*N*-aza-18-crown-6-methyl-2,2′-bipyridine
BA	benzoylacetonate, butanaido
BADE	9,9′-bisacridinium-*N*,*N*′-diacetic acid ethyl ester
BDD	boron-doped diamond
BDP	boron-dipyrromethene
bFGF	basic fibroblast growth factor
BL	bioluminescence
$BMImBF_4$	1-butyl-3-methylimidazolium tetrafluoroborate
$BMImPF_6$	1-butyl-3-methylimidazolium hexafluorophosphate
bphb	1,4-bis(4′-methyl-2,2′-bipyridin-4-yl)benzene
BPO	benzoyl peroxide
BPQ-PTZ	3,7-[bis(4-phenyl-2-quinolyl)]-10-methylphenothiazine
bpy	2,2′-bipyridine
bpz	2,2′-bipyrazine
BSA	bovine serum albumin
β-secretase	beta-secretase activity assay
BTA	benzoyltrifluoroacetate
BTBH2	bis(1*H*-tetrazol-5-yl)benzene
Bu_4N^+	tetra-*n*-butylammonium ion
$C_2O_4^{2-}$	oxalate ion

CCD	charged coupled device
CE	capillary electrophoresis, counter electrode
CHO HCP	CHO host cell protein
CKMB	creatine kinase MB fraction
CL	chemiluminescence
CNL	1-cyanonaphthalene
CPA	9-cyanophenantherene
CRP	C-reactive protein
CV	cyclic voltammetric, cyclic voltammetry
dbm	dibenzoylmethane
DBAE	(dibutylamino)ethanol
DCB	1,4-dicyanobenzene
DCBP	4,4′-dicyano-*p*-biphenyl
dcbpy	2,2′-bipyridine-4,4′-dicarboxylic acid
DCN	1,4-dicyanonaphthalene
DEAP	3-(diethylamino)propionic acid
Dend	$N(CH_2CH_2NH)_3$-
DHA	dihydroazulene
$-\Delta H_{ann}$	enthalpy (in eV) for ion annihilation
DHBA	3,4-dihydroxybenzoic acid
DiMe-DiMOS	dimethyldimethoxysilane
DMB	dibenzoylmethide
DMBA	4-(dimethylamino)butyric acid
DMBP	4,4′-dimethylbiphenyl
dmbpy	4,4′-dimethyl-2,2′-dipyridyl
DMF	*N*,*N*′-dimethylformamide
DMN	2,6-dimethylnaphthalene
DMSO	dimethyl sulfoxide
DNA	deoxyribonucleic acid
DPA	9,10-diphenylanthracene
dsDNA	double-stranded DNA
DTDP	1,3-dihydro-1,1,3,3-tetramethyl-7,8-diazacyclopenta-[1]phenanthren-2-one
DVS	divinyl sulfone
$E°$	standard electrochemical potential
EC	electrochemical
ECL	electrogenerated chemiluminescence, electrochemiluminescence, electrogenerated chemiluminescent, electrochemiluminescent
EL	electroluminescence
ELISA	enzyme-linked immunoadsorbent assay
E_p	redox peak potential (in V)
EPO	erythropoietin
E-route	ion annihilation system involving excimer and exciplex formation
E_s	energy gap between the excited singlet state and the ground state
E-Selectin	ELAM-1, endothelium leukocyte adhesion molecule
Estradiol	17β-estradiol
E_t	triplet state energy
FABP3	fatty acid binding protein 3
FIA	flow injection analysis
FSH	follicle-stimulating hormone
GC	glassy carbon electrode
G-CSF	granulocyte colony-stimulatuing factor
GLP-1 (7–36) amide	glucagon-like peptide-1 isoforms 7–36, 9–36, 1–36
GLP-1 (7–37)	glucagon-like peptide-1 isoforms 7–37, 1–37
GLP-1 (Total)	all glucagon-like peptide-1 isoforms (including precursor)
GM-CSF	granulocyte-macrophage colony-stimulating factor
HCG	human chorionic gonadotropin
HGF	hepatocyte growth factor
HIF-1	hypoxia inducible factor 1
HMT	*N*-acetyl-5-methoxy-6-hydroxytryptamine
HOPG	highly oriented pyrolytic graphite
HPLC	high-performance liquid chromatography
HSA	human serum albumin
ICT	intramolecular charge transfer
IFN-β	interferon β
IFN-γ	interferon γ
IGFBP-1	insulin-like growth factor binding protein-1
IgG	immunoglobulin
IgM	immunoglobulin M
IL	ionic liquid
IL-10	interleukin 10
IL-12 (total)	interleukin 12
IL-12 p40	interleukin 12 (40 kDa subunit)
IL-12 p70	interleukin 12 (70 kDa subunit)
IL-13	interleukin 13
IL-17	interleukin 17
IL-18	interleukin 18
IL-1α	interleukin 1α
IL-1β	interleukin 1β
IL-2	interleukin 2
IL-4	interleukin 4
IL-5	interleukin 5
IL-6	interleukin 6
IL-6R	interleukin 6 receptor
IL-7	interleukin 7
IL-8	interleukin 8
IP-10	IFN inducible protein 10
I-TAC	interferon-stimulated T-cell
ITO	indium-doped tin oxide electrode
KC/GRO/CINC(CXCL1)	chemokine (C-X-C motif) ligand 1
LBP	lipopolysaccharide binding protein
LEDs	light-emitting devices
LH	luteinizing hormone
LOD	limit of detection
LR	linear range
Luminol	5-amino-2,3-dihydro-1,4-phthalazinedione
MAA	mercaptoacetic acid
mbpy	4-methyl-2,2′-bipyridine
mbpy-$(CH_2)_3COOH$	4-carboxypropyl-4′-dipyridyl
mbpy-CH_2COOH	4-carboxymethyl-4′-methyl-2,2′-dipyridyl
MCP-1	macrophage chemoattractant protein 1
MCP-4	macrophage chemoattractant protein 4
M-CSF	macrophage colony-stimulating factor
MDC	macrophage-derived chemokine
MeCN	acetonitrile
MeDPrA	methyl-di-*n*-propylamine
MIAA	5-methoxyindole-3-acetic acid
MIG	monokine induced by interferon γ
MIP-1α	macrophage inflammatory protein 1α
MIP-1β	macrophage inflammatory protein 1β
MIP-3α	macrophage inflammatory protein 3α
MLCT	metal-to-ligand charge transfer
MMP-1	matrix metalloproteinase 1
MMP-10	matrix metalloproteinase 10
MMP-2	matrix metalloproteinase 2
MMP-3	matrix metalloproteinase 3
MMP-9	matrix metalloproteinase 9
MT	melatonin
μTAS	micro total analysis
MTX	methotrexate
MWNT	multiwalled nanotubes
NADH	nicotinamide adenine dinucleotide
NAHT	*N*-acetyl-5-hydroxytryptamine
NAPP	*N*-(3-aminopropyl)pyrrolidine
NCs	nanocrystals
NHS	*N*-hydroxysuccinimide ester
NMP	*N*-methyl-L-proline
NPs	brain natriuretic peptide
NSOM	near-field optical scanning microscopy
PAHs	polyaromatic hydrocarbons
PAMAM	polyamidoamine
PBIm-H	2-(2-pyridyl)benzimidazole

PBIm-Me	2-(2-pyridyl)-*N*-methylbenzimidazole
PBS	phosphate buffer solution
PCB	printed circuit board
PCR	Polymerase Chain Reaction
PDMS	polydimethylsiloxane
PETN	pentaerthyritol tetranitrate
phen	1,10-phenanthroline (often referred to as *o*-phen in the literature)
Phospho-Tau	phospho-Tau (Thr 231 or Ser 262)
pico	picolinate
PICP	procollagen type I peptide
PIGF	placenta growth factor
PIN	positive-intrinsic-negative
PL	photoluminescence
PMT	photomultiplier tube
PPA	propioamido
PPS	poly(*p*-styrenesulfonate)
PPV	polyphenylene vinylene
ppy	2-phenylpyridine
pq	2-phenylquinoline
ProA	protein A (immunoassay)
ProBNP	brain natriuretic peptide
PSA	prostate-specific antigen
P-Selectin	PECAM, platelet endothelial cell adhesion molecule
PVA SbQ gel	poly(vinyl alcohol) gel
PVP	poly(4-vinylpydine), poly(*N*-vinyl-2-pyrrolidone)
quin	quinaldate
RANTES	regulated on activation, normal T cell expressed and secreted
RNA	ribonucleic acid
$Ru(phen)_3^{2+}$	ruthenium (II) tris(1,10-phenanthroline)
$S_2O_8^{2-}$	persulfate, peroxydisulfate
SAA	serum amyloid A
SAM	self-assembled monolayer
sAPPα	soluble amyloid precursor protein α
sAPPβ (wt)	soluble amyloid precursor protein β
SCE	saturated calomel electrode
SDS	sodium dodecyl sulfate
SECM	scanning electrochemical microscopy
sICAM-1	secreted intercellular adhesion molecule 1
sICAM-3	secreted intercellular adhesion molecule 3
SL	sonoluminescence
S-route	energy-sufficient ECL system
ssDNA	single-stranded DNA
ST-route	combination of S-route and T route
sVCAM-1	secreted vascular cell adhesion molecule
sVEGFR1	soluble vascular endothelial growth factor receptor-1
sVEGFR2	soluble vascular endothelial growth factor receptor-2
sw sAPPβ	Swedish soluble amyloid precursor protein β
T3	triiodothyronine
T4	thyroxine
TARC	thymus and activation-regulated chemokine
Tau	total Tau
TBAP	tetra-*n*-butylammonium perchlorate
TBuA	tri-*n*-butylamine
TCNQ	tetracyanoquinodimethane
TEtA	triethylamine
TFAA	trifluoroacetic acid
TFPB	4,4,4-trifluoro-1-phenyl-1,3-butanedionate
TFPD	1,1,1-trifluoro-2,4-pentanedionate
TGF-β1	transforming growth factor beta 1
THAP	tetrahexylammonium perchlorate
TisoBuA	tri-isobutylamine
tmd	2,2,6,6-tetramethyl-3,5-heptanedione
TMPD	*N*,*N*,*N*′,*N*′- tetramethyl-*p*-phenylenediamine
TMeA	trimethylamine
TMOS	tetramethoxysilane
TNF-α	tumor necrosis factor α
TNF-RI	TNF receptor I
TNF-RII	TNF receptor II
TNT	2,4,6-trinitrotoluene
TOPO	trioctylphosphine
TPrA	tri-*n*-propylamine
Tris	tris(hydroxymethyl)aminomethane
Triton X-100	poly(ethylene glycol) *tert*-octylphenyl ether
T-route	energy-deficient ECL system
TTA	triplet−triplet annihilation
TTFA	thenoyltrifluoroacetonate
VEGF(165/121)	vascular endothelial growth factor
WE	working electrode
XL	*p*-xylene

11. References

(1) *IUPAC Compendium of Chemical Terminology*, 2nd ed.; McNaught, A. D., Wilkinson, A., Eds.; Blackwell Science: Oxford, U.K., 1997.
(2) Hercules, D. M. *Science* **1964**, *145*, 808.
(3) Visco, R. E.; Chandross, E. A. *J. Am. Chem. Soc.* **1964**, *86*, 5350.
(4) Santhanam, K. S. V.; Bard, A. J. *J. Am. Chem. Soc.* **1965**, *87*, 139.
(5) Dufford, R. T.; Nightingale, D.; Gaddum, L. W. *J. Am. Chem. Soc* **1927**, *49*, 1858.
(6) Harvey, N. *J. Phys. Chem.* **1929**, *33*, 1456.
(7) *Electrogenerated Chemiluminescence*; Bard, A. J., Ed.; Dekker: New York, 2004.
(8) Yin, X.-B.; Dong, S.; Wang, E. *Trends Anal. Chem.* **2004**, *23*, 432.
(9) Maus, R. A. *J. Phys. Chem.* **1965**, *43*, 2654.
(10) Feldberg, S. W. *J. Phys. Chem.* **1966**, *70*, 3928.
(11) Feldberg, S. W. *J. Am. Chem. Soc.* **1966**, *88*, 390.
(12) Faulkner, L. R.; Bard, A. J. *J. Am. Chem. Soc.* **1969**, *91*, 209.
(13) Tokel, N. E.; Bard, A. J. *J. Am. Chem. Soc.* **1972**, *94*, 2862.
(14) Chang, M.-M.; Saji, T.; Bard, A. J. *J. Am. Chem. Soc.* **1977**, *99*, 5399.
(15) Rubinstein, I.; Bard, A. J. *J. Am. Chem. Soc.* **1981**, *103*, 512.
(16) Abruna, H. D.; Bard, A. J. *J. Am. Chem. Soc.* **1982**, *104*, 2641.
(17) White, H. S.; Bard, A. J. *J. Am. Chem. Soc.* **1982**, *104*, 6891.
(18) Ege, D.; Becker, W. G.; Bard, A. J. *Anal. Chem.* **1984**, *56*, 2413.
(19) Noffsinger, J. B.; Danielson, N. D. *Anal. Chem.* **1987**, *59*, 865.
(20) Leland, J. K.; Powell, M. J. *J. Electrochem. Soc.* **1990**, *137*, 3127.
(21) Blackburn, G. F.; Shah, H. P.; Kenten, J. H.; Leland, J.; Kamin, R. A.; Link, J.; Peterman, J.; Powell, M. J.; Shah, A.; Talley, D. B. *Clin. Chem.* **1991**, *37*, 1534.
(22) Bard, A. J.; Whitesides, G. M. U.S. Patent 5,221,605, 1993.
(23) Collinson, M. M.; Wightman, R. M. *Anal. Chem.* **1993**, *65*, 2576.
(24) Horiuchi, T.; Niwa, O.; Hatakenaka, N. *Nature* **1998**, *394*, 659.
(25) Ding, Z.; Quinn, B. M.; Haram, S. K.; Pell, L. E.; Korgel, B. A.; Bard, A. J. *Science* **2002**, *296*, 1293.
(26) Bard, A. J. In *Electrogenerated Chemiluminescence*; Bard, A. J., Ed.; Dekker, New York, 2004; Chapter 1.
(27) Thomson ISI Web of Science, http://scientific.thomson.com/.
(28) Scopus, http://www.scopus.com/scopus/homeurl.
(29) Andersson, A.-M.; Schmehl, R. H. *Mol. Supramol. Photochem.* **2001**, *7*, 153.
(30) Andersson, A.-M.; Schmehl, R. H. In *Electron Transfer in Chemistry*; Balzani, V., Ed.; Wiley-VCH Verlag: Weinheim, Germany, 2001; Vol. 1, p 312.
(31) Anon Indian, J. *Clin. Biochem.* **1998**, *13*, 129.
(32) Armstrong, N. R.; Wightman, R. M.; Gross, E. M. *Annu. Rev. Phys. Chem.* **2001**, *52*, 391.
(33) Balzani, V.; Juris, A. *Coord. Chem. Rev.* **2001**, *211*, 97.
(34) Bard, A. J.; Fan, F.-R. F. *Acc. Chem. Res.* **1996**, *29*, 572.
(35) Bard, A. J.; Park, S. M. *Exciplex, Proc. Meet.* **1975**, 305.
(36) Beier, R. C.; Stanker, L. H. *Recent Res. Dev. Agric. Food Chem.* **2000**, *4*, 59.
(37) Bolletta, F.; Bonafede, S. *Pure Appl. Chem.* **1986**, *58*, 1229.
(38) Fahnrich, K. A.; Pravda, M.; Guilbault, G. G. *Talanta* **2001**, *54*, 531.
(39) Faulkner, L. R.; Glass, R. S. *Chem. Biol. Gener. Excited States* **1982**, 191.
(40) Gerardi, R. D.; Barnett, N. W.; Lewis, A. W. *Anal. Chim. Acta* **1999**, *378*, 1.
(41) Gonzalez Velasco, J. *Electroanalysis* **1991**, *3*, 261.
(42) Gonzalez Velasco, J. *Bull. Electrochem.* **1994**, *10*, 29.
(43) Greenway, G. M. *Trends Anal. Chem* **1990**, *9*, 200.
(44) Kapturkiewicz, A. *Adv. Electrochem. Sci. Eng.* **1997**, *5*, 1.
(45) Kissinger, P. T. *J. Pharm. Biomed. Anal.* **1996**, *14*, 871.
(46) Knight, A. W. *Trends Anal. Chem.* **1999**, *18*, 47.
(47) Knight, A. W.; Greenway, G. M. *Analyst* **1994**, *119*, 879.
(48) Knight, A. W.; Greenway, G. M. *Analyst* **1996**, *121*, 101R
(49) Kukoba, A. V.; Bykh, A. I.; Svir, I. B. *Fresenius' J. Anal. Chem.* **2000**, *368*, 439.

(50) Lee, W. Y. *Mikrochim. Acta* **1997**, *127*, 19.
(51) Miao, W. In *Handbook of Electrochemistry*; Zoski, C. G., Ed.; Elsevier: Amsterdam, The Netherlands, 2007; p 541.
(52) Mitschke, U.; Bauerle, P. *J. Mater. Chem.* **2000**, *10*, 1471.
(53) Nabi, A.; Yaqoob, M.; Anwar, M. *Lab. Rob. Autom.* **1999**, *11*, 91.
(54) Nieman, T. A. *J. Res. Natl. Bur. Stand.* **1988**, *93*, 501.
(55) Nieman, T. A. In *Chemiluminescence and Photochemical Reaction Detection in Chromatography*; Birks, J. W., Ed.; VCH: New York, 1989; p 99.
(56) Park, S.-M.; Tryk, D. A. *Rev. Chem. Intermed.* **1980**, *4*, 43.
(57) Richter, M. M. In *Optical Biosensors: Present and Future*; Ligler, F. S., Taitt, C. A. R., Eds.; Elsevier: New York, 2002; p 173.
(58) Richter, M. M. *Chem. Rev.* **2004**, *104*, 3003.
(59) Xu, X.-H. N.; Zu, Y. In *New Frontiers in Ultrasensitive Bioanalysis*; Xu, X.-H. N., Ed.; Wiley: Hoboken, NJ, 2007; Vol. 172, p 235.
(60) Du, Y.; Wang, E. *J. Sep. Sci.* **2007**, *30*, 875.
(61) Kankare, J. In *Encyclopedia of Analytical Science*; Townshend, A., Ed.; Academic Press: New York, 1995; Vol. 1, p 626.
(62) Yin, X.-B.; Wang, E. *Anal. Chim. Acta* **2005**, *533*, 113.
(63) Gorman, B. A.; Francis, P. S.; Barnett, N. W. *Analyst* **2006**, *131*, 616.
(64) Pyati, R.; Richter, M. M. *Annu. Rep. Prog. Chem. Sect. C: Phys. Chem.* **2007**, *103*, 12.
(65) Meso Scale Discovery, www.mesoscale.com.
(66) Roche Diagnostics Corp., www.roche.com. Note: The initial Igen International and then BioVeris Corp. have now been acquired by Roche Diagnostics Corp.
(67) Kulmala, S.; Suomi, J. *Anal. Chim. Acta* **2003**, *500*, 21.
(68) Agbaria, R. A.; Oldham, P. B.; McCarroll, M.; McGown, L. B.; Warner, I. M. *Anal. Chem.* **2002**, *74*, 3952.
(69) Oldham, P. B.; McCarroll, M. E.; McGown, L. B.; Warner, I. M. *Anal. Chem.* **2000**, *72*, 197R
(70) Powe, A. M.; Fletcher, K. A.; St Luce, N. N.; Lowry, M.; Neal, S.; McCarroll, M. E.; Oldham, P. B.; McGown, L. B.; Warner, I. M. *Anal. Chem* **2004**, *76*, 4614.
(71) Aitken, R. J.; Baker, M. A.; O'Bryan, M. *J. Androl.* **2004**, *25*, 455.
(72) Arnhold, J. In *Chemiluminescence at the Turn of the Millennium*; Albrecht, S., Zimmermann, T., Brandl, H., Eds.; Schweda-Werbedruck: Dresden, Germany, 2001; p 85.
(73) Butkovskaya, N. I.; Setser, D. W. *Int. Rev. Phys. Chem.* **2003**, *22*, 1.
(74) Creton, R.; Jaffee, L. F. *BioTechniques* **2001**, *31*, 1098.
(75) Gaffney, J. S.; Marley, N. A. *Conference on Atmospheric Chemistry: Urban, Regional, and Global Scale Impacts of Air Pollutants*, 4th; Orlando, FL, Jan 13–17, *2002*; p 1.
(76) Garcia-Campana, A. M.; Baeyens, W. R. G.; Cuadros-Rodriguez, L.; Barrero, F. A.; Bosque-Sendra, J. M.; Gamiz-Gracia, L. *Curr. Org. Chem.* **2002**, *6*, 1.
(77) Gubitz, G.; Schmid, M. G.; Silviaeh, H.; Aboul-Enein, H. Y. *Crit. Rev. Anal. Chem.* **2001**, *31*, 167.
(78) Jacobson, K.; Eriksson, P.; Reitberger, T.; Stenberg, B. *Adv. Polym. Sci.* **2004**, *169*, 151.
(79) Kuyper, C.; Milofsky, R. *Trends Anal. Chem* **2001**, *20*, 232.
(80) Li, F.; Zhang, C.; Guo, X.; Feng, W. *Biomed. Chromatogr.* **2003**, *17*, 96.
(81) Liu, Y.-M.; Cheng, J.-K. *J. Chromatogr., A* **2002**, *959*, 1.
(82) Qin, W. *Anal. Lett.* **2002**, *35*, 2207.
(83) Roda, A.; Guardigli, M.; Michelini, E.; Mirasoli, M.; Pasini, P. *Anal. Chem.* **2003**, *75*, 462A
(84) Roda, A.; Guardigli, M.; Pasini, P.; Mirasoli, M. *Anal. Bioanal. Chem.* **2003**, *377*, 826.
(85) Rychla, L.; Rychly, J. In *Polymer Analysis and Degradation*; Jimenez, A., Zaikov, G. E., Eds.; Nova Science Publishers: Huntington, NY, 2000; p 123.
(86) Shah, D. O.; Chang, C. D.; Stewart, J. L. *BIOforum Eur.* **2003**, *7*, 44.
(87) Sherma, J. *J. AOAC Int.* **2004**, *87*, 20A
(88) Stott, R. A. W. In *Protein Protocols Handbook*, 2nd ed.; Humana Press, Inc.: Totowa, NJ, 2002; 1089.
(89) Yamaguchi, M.; Yoshida, H.; Nohta, H. *J. Chromatogr., A* **2002**, *950*, 1.
(90) Harvey, E. N. *Bioluminescence*; Academic Press: New York, 1952.
(91) Ivey, F. *Electroluminescence and Related Effects*; Academic Press: New York, 1963.
(92) Avakyan, G. M.; Avakyan, T. M. *Biol. Zh. Arm.* 1972, 9.
(93) Avakyan, T. M.; Stepanyan, L. G. *Biofizika* **1972**, *17*, 712.
(94) Bistolfi, F. *Panminerva Med.* **2000**, *42*, 69.
(95) Papadopoulos, K.; Lignos, J.; Stamatakisy, M.; Dimotikali, D.; Nikokavouras, J. *J. Photochem. Photobiol. A: Chem.* **1998**, *115*, 137.
(96) Papadopoulos, K.; Triantis, T.; Dimotikali, D.; Nikokavouras, J. *J. Photochem. Photobiol. A: Chem.* **2000**, *131*, 55.
(97) Hakansson, M.; Jiang, Q.; Spehar, A.-M.; Suomi, J.; Kulmala, S. *J. Lumin.* **2006**, *118*, 272.
(98) Kalkar, C. D. *Radiat. Phys. Chem.* **1989**, *34*, 729.
(99) Arakeri, V. H. *Curr. Sci.* **2003**, *85*, 911.
(100) Ashokkumar, M.; Grieser, F. *ChemPhysChem* **2004**, *5*, 439.
(101) Barber, B. P.; Hiller, R. A.; Loefstedt, R.; Putterman, S. J.; Weninger, K. R. *Phys. Rep.* **1997**, *281*, 65.
(102) Brenner, M. P.; Hilgenfeldt, S.; Lohse, D. *Rev. Mod. Phys.* **2002**, *74*, 425.
(103) Cheeke, J. D. N. *Can. J. Phys.* **1997**, *75*, 77.
(104) Cordry, S. M.; Crum, L. A. *Lumin. Solids* **1998**, 343.
(105) Crum, L. A. *Phys. Today* **1994**, *47*, 22.
(106) DiDonna, B. A.; Witten, T. A.; Young, J. B. *Phys. A (Amsterdam, Neth.)* **1998**, *258*, 263.
(107) Greenland, P. T. *Contemp. Phys.* **1999**, *40*, 11.
(108) Hammer, D.; Frommhold, L. *J. Mod. Opt.* **2001**, *48*, 239.
(109) Lepoint, T.; Lepoint-Mullie, F. *Adv. Sonochem.* **1999**, *5*, 1.
(110) Lohse, D.; Hilgenfeldt, S. *Festkoerperprobleme* **1999**, *38*, 215.
(111) Macintyre, F. *Ultrason. Sonochem.* **1997**, *4*, 85.
(112) Margulis, M. A.; Margulis, I. M. *Ultrason. Sonochem.* **2002**, *9*, 1.
(113) Matula, T. J.; Roy, R. A. *Ultrason. Sonochem.* **1997**, *4*, 61.
(114) Mitome, H. *Jpn. J. Appl. Phys., Part 1* **2001**, *40*, 3484.
(115) Ostrovskii, I. V.; Korotchenkov, O. A.; Goto, T.; Grimmeiss, H. G. *Phys. Rep.* **1999**, *311*, 1.
(116) Prevenslik, T. V. *Ultrasonics* **2003**, *41*, 313.
(117) Putterman, S. *Phys. World* **1998**, *11*, 38.
(118) Suslick, K. S. *Proc. IEEE Ultrason. Symp.* **1997**, 523.
(119) Campbell, A. K. *Chemiluminescence. Principles and Applications in Biology and Medicine*; VCH: Weinheim, Germany, 1988.
(120) Wilson, R.; Clavering, C.; Hutchinson, A. *Anal. Chem.* **2003**, *75*, 4244.
(121) Bard, A. J.; Debad, J. D.; Leland, J. K.; Sigal, G. B.; Wilbur, J. L.; Wohlsatdter, J. N. In *Encyclopedia of Analytical Chemistry: Applications, Theory and Instrumentation*; Meyers, R. A., Ed.; Wiley: New York, 2000; Vol. 11, p 9842.
(122) Forry, S. P.; Wightman, R. M. In *Electrogenerated Chemiluminescence*; Bard, A. J., Ed.; Dekker: New York, 2004; Chapter 6, p 273.
(123) Beideman, F. E.; Hercules, D. M. *J. Phys. Chem.* **1979**, *83*, 2203.
(124) Faulkner, L. R.; Tachikawa, H.; Bard, A. J. *J. Am. Chem. Soc.* **1972**, *94*, 691.
(125) Tachikawa, H.; Bard, A. J. *Chem. Phys. Lett.* **1974**, *26*, 246.
(126) Pighin, A.; Conway, B. E. *J. Electrochem. Soc.* **1975**, *122*, 619.
(127) Periasamy, N.; Santhanam, K. S. V. *Proc. Indian Acad. Sci., Sect. A* **1974**, *80*, 194.
(128) Kim, J.; Faulkner, L. R. *J. Am. Chem. Soc.* **1988**, *110*, 112.
(129) Kapturkiewicz, A. *J. Electroanal. Chem.* **1994**, *372*, 101.
(130) Fleet, B.; Kirkbright, G. F.; Pickford, C. J. *J. Electroanal. Chem. Interfacial Electrochem.* **1971**, *30*, 115.
(131) Weller, A.; Zachariasse, K. *Chem. Phys. Lett.* **1971**, *10*, 197.
(132) Maloy, J. T.; Bard, A. J. *J. Am. Chem. Soc.* **1971**, *93*, 5968.
(133) Lai, R. Y.; Fleming, J. J.; Merner, B. L.; Vermeij, R. J.; Bodwell, G. J.; Bard, A. J. *J. Phys. Chem. A* **2004**, *108*, 376.
(134) Lakowicz, J. R. *Principles of Fluorescence Spectroscopy*, 2nd ed.; Kluwer Academic/Plenum Publishers: New York, 1999.
(135) Keszthelyi, C. P.; Bard, A. J.; Dep, C. *Chem. Phys. Lett.* **1974**, *24*, 300.
(136) Ketter, J. B.; Wightman, R. M. *J. Am. Chem. Soc.* **2004**, *126*, 10183.
(137) Libert, M.; Bard, A. J. *J. Electrochem. Soc.* **1976**, *123*, 814.
(138) Park, S. M.; Bard, A. J. *J. Am. Chem. Soc.* **1975**, *97*, 2978.
(139) Tachikawa, H.; Bard, A. J. *Chem. Phys. Lett.* **1974**, *26*, 568.
(140) Choi, J.-P.; Wong, K.-T.; Chen, Y.-M.; Yu, J.-K.; Chou, P.-T.; Bard, A. J. *J. Phys. Chem. B* **2003**, *107*, 14407.
(141) Maness, K. M.; Wightman, R. M. *J. Electroanal. Chem.* **1995**, *396*, 85.
(142) Fan, F. R. F. In *Electrogenerated Chemiluminescence*; Bard, A. J., Ed.; Dekker, New York, 2004; Chapter 2, p 23.
(143) Miao, W.; Choi, J.-P. In *Electrogenerated Chemiluminescence*; Bard, A. J., Ed.; Dekker: New York, 2004; Chapter 5, p213.
(144) Butler, J.; Henglein, A. *Radiat. Phys. Chem.* **1980**, *15*, 603.
(145) Miao, W.; Choi, J.-P.; Bard, A. J. *J. Am. Chem. Soc.* **2002**, *124*, 14478.
(146) Lai, R. Y.; Bard, A. J. *J. Phys. Chem. A* **2003**, *107*, 3335.
(147) Nelsen, S. F.; Landis, R. T., II *J. Am. Chem. Soc.* **1973**, *95*, 5422.
(148) Hercules, D. M. *Acc. Chem. Res.* **1969**, *2*, 301.
(149) Li, B.; Zhang, Z.; Zheng, X.; Xu, C. *Chem. Anal. (Warsaw)* **2000**, *45*, 709.
(150) Hercules, D. M.; Lytle, F. E. *Photochem. Photobiol.* **1971**, *13*, 123.
(151) Martin, J. E.; Hart, E. J.; Adamson, A. W.; Gafney, H.; Halpern, J. *J. Am. Chem. Soc.* **1972**, *94*, 9238.
(152) Memming, R. *J. Electrochem. Soc.* **1969**, *116*, 785.
(153) Bolletta, F.; Ciano, M.; Balzani, V.; Serpone, N. *Inorg. Chim. Acta* **1982**, *62*, 207.
(154) Chandross, E. A.; Sonntag, F. I. *J. Am. Chem. Soc.* **1966**, *88*, 1089.
(155) Akins, D. L.; Birke, R. L. *Chem. Phys. Lett.* **1974**, *29*, 428.
(156) Santa Cruz, T. D.; Akins, D. L.; Birke, R. L. *J. Am. Chem. Soc.* **1976**, *98*, 1677.

(157) Klaning, U. K.; Sehested, K.; Holcman, J. *J. Phys. Chem.* **1985**, *89*, 760.
(158) Koppenol, W. H.; Liebman, J. F. *J. Phys. Chem.* **1984**, *88*, 99.
(159) Schwarz, H. A.; Dodson, R. W. *J. Phys. Chem.* **1984**, *88*, 3643.
(160) Choi, J.-P.; Bard, A. J. *Anal. Chim. Acta* **2005**, *541*, 143.
(161) Cao, W.; Xu, G.; Zhang, Z.; Dong, S. *Chem. Commun.* **2002**, 1540.
(162) Juris, A.; Balzani, V.; Barigelletti, F.; Campagna, S.; Belser, P.; Von Zelewsky, A. *Coord. Chem. Rev.* **1988**, *84*, 85.
(163) Li, F.; Cui, H.; Lin, X.-Q. *Luminescence* **2002**, *17*, 117.
(164) Lu, M.-C.; Whang, C.-W. *Anal. Chim. Acta* **2004**, *522*, 25.
(165) Kanoufi, F.; Bard, A. J. *J. Phys. Chem. B* **1999**, *103*, 10469.
(166) Downey, T. M.; Nieman, T. A. *Anal. Chem.* **1992**, *64*, 261.
(167) Bolletta, F.; Juris, A.; Maestri, M.; Sandrini, D. *Inorg. Chim. Acta* **1980**, *44*, L175.
(168) Debad, J. D.; Glezer, E. N.; Leland, J. K.; Sigal, G. B.; Wohlsadter, J. In *Electrogenerated Chemiluminescence*; Bard, A. J., Ed.; Dekker: New York, 2004; Chapter 8, p 359.
(169) Gross, E. M.; Pastore, P.; Wightman, R. M. *J. Phys. Chem. B* **2001**, *105*, 8732.
(170) He, L.; Cox, K. A.; Danielson, N. D. *Anal. Lett.* **1990**, *23*, 195.
(171) Kanoufi, F.; Zu, Y.; Bard, A. J. *J. Phys. Chem. B* **2001**, *105*, 210.
(172) Zu, Y.; Bard, A. J. *Anal. Chem.* **2000**, *72*, 3223.
(173) Workman, S.; Richter, M. M. *Anal. Chem.* **2000**, *72*, 5556.
(174) Factor, B.; Muegge, B.; Workman, S.; Bolton, E.; Bos, J.; Richter, M. M. *Anal. Chem.* **2001**, *73*, 4621.
(175) Zu, Y.; Bard, A. J. *Anal. Chem.* **2001**, *73*, 3960.
(176) Li, F.; Zu, Y. *Anal. Chem.* **2004**, *76*, 1768.
(177) Parker, S. T.; Slinker, J. D.; Lowry, M. S.; Cox, M. P.; Bernhard, S.; Malliaras, G. G. *Chem. Mater.* **2005**, *17*, 3187.
(178) Gao, Y.; Xiang, Q.; Xu, Y.; Tian, Y.; Wang, E. *Electrophoresis* **2006**, *27*, 4842.
(179) Li, J.; Huang, M.; Liu, X.; Wei, H.; Xu, Y.; Xu, G.; Wang, E. *Analyst* **2007**, *132*, 687.
(180) Xu, Y.; Gao, Y.; Li, T.; Du, Y.; Li, J.; Wang, E. *Adv. Funct. Mater.* **2007**, *17*, 1003.
(181) Quinn, B. M.; Ding, Z.; Moulton, R.; Bard, A. J. *Langmuir* **2002**, *18*, 1734.
(182) Zheng, H.; Zu, Y. *J. Phys. Chem. B* **2005**, *109*, 12049.
(183) Honda, K.; Yoshimura, M.; Rao, T. N.; Fujishima, A. *J. Phys. Chem. B* **2003**, *107*, 1653.
(184) Honda, K.; Yamaguchi, Y.; Yamanaka, Y.; Yoshimatsu, M.; Fukuda, Y.; Fujishima, A. *Electrochim. Acta* **2005**, *51*, 588.
(185) Marselli, B.; Garcia-Gomez, J.; Michaud, P. A.; Rodrigo, M. A.; Comninellis, C. *J. Electrochem. Soc.* **2003**, *150*, D79.
(186) Pastore, P.; Badocco, D.; Zanon, F. *Electrochim. Acta* **2006**, *51*, 5394.
(187) Miao, W.; Bard, A. J. *Anal. Chem.* **2004**, *76*, 7109.
(188) Miao, W.; Bard, A. J. *Anal. Chem.* **2004**, *76*, 5379.
(189) Richter, M. M.; Bard, A. J.; Kim, W.; Schmehl, R. H. *Anal. Chem.* **1998**, *70*, 310.
(190) Fan, F.-R. F.; Cliffel, D.; Bard, A. J. *Anal. Chem.* **1998**, *70*, 2941.
(191) Vinyard, D. J.; Richter, M. M. *Anal. Chem.* **2007**, *79*, 6404.
(192) Bock, C. R.; Connor, J. A.; Gutierrez, A. R.; Meyer, T. J.; Whitten, D. G.; Sullivan, B. P.; Nagle, J. K. *J. Am. Chem. Soc.* **1979**, *101*, 4815.
(193) Liu, X.; Shi, L.; Niu, W.; Li, H.; Xu, G. *Angew. Chem. Int. Ed.* **2007**, *46*, 421.
(194) Vojir, V. *Collect. Czech. Chem. Commun.* **1954**, *19*, 868.
(195) Dorabialska, A.; Kroh, J.; Adolfowna, I. *Zesz. Nauk. Politech. Lodz.* **1955**, *9*, 3.
(196) Kuwana, T.; Epstein, B.; Seo, E. T. *J. Phys. Chem.* **1963**, *67*, 2243.
(197) Wroblewska, A.; Reshetnyak, O. V.; Koval'chuk, E. P.; Pasichnyuk, R. I.; Blazejowski, J. *J. Electroanal. Chem.* **2005**, *580*, 41.
(198) Shi, M.-J.; Cui, H. *Electrochim. Acta* **2006**, *52*, 1390.
(199) Zhang, L.; Zhou, J.; Hao, Y.; He, P.; Fang, Y. *Electrochim. Acta* **2005**, *50*, 3414.
(200) Dong, Y.-P.; Cui, H.; Xu, Y. *Langmuir* **2007**, *23*, 523.
(201) Cui, H.; Dong, Y.-P. *J. Electroanal. Chem.* **2006**, *595*, 37.
(202) Cui, H.; Xu, Y.; Zhang, Z.-F. *Anal. Chem.* **2004**, *76*, 4002.
(203) Cui, H.; Zhang, Z.-F.; Zou, G.-Z.; Lin, X.-Q. *J. Electroanal. Chem.* **2004**, *566*, 305.
(204) Cui, H.; Zou, G.-Z.; Lin, X.-Q. *Anal. Chem.* **2003**, *75*, 324.
(205) Haapakka, K. E.; Kankare, J. J. *Anal. Chim. Acta* **1982**, *138*, 263.
(206) Wang, C.-M.; Cui, H. *Luminescence* **2007**, *22*, 35.
(207) Epstein, B.; Kuwana, T. *Photochem. Photobiol.* **1967**, *6*, 605.
(208) Pastore, P.; Favaro, G.; Gallina, A.; Antiochia, R. *Ann. Chim. (Rome, Italy)* **2002**, *92*, 271.
(209) Sakura, S. *Anal. Chim. Acta* **1992**, *262*, 49.
(210) Wilson, R.; Kremeskoetter, J.; Schiffrin, D. J.; Wilkinson, J. S. *Biosens. Bioelectron.* **1996**, *11*, 805.
(211) Yoshimi, Y.; Haramoto, H.; Miyasaka, T.; Sakai, K. *J. Chem. Eng. Jpn.* **1996**, *29*, 851.
(212) Kulmala, S.; Ala-Kleme, T.; Kulmala, A.; Papkovsky, D.; Loikas, K. *Anal. Chem.* **1998**, *70*, 1112.
(213) Ouyang, C. S.; Wang, C. M. *J. Electrochem. Soc.* **1998**, *145*, 2654.
(214) Verostko, C. E.; Atwater, J. E.; Akse, J. R.; Dehart, J. L.; Wheeler, R. R. Fiber-optic Chemiluminescent Biosensors for Monitoring Aqueous Alcohols and Other Water Quality Parameters. U.S. Patent 5,792,621, Aug. 11, 1998.
(215) Marquette, C. A.; Blum, L. J. *Anal. Chim. Acta* **1999**, *381*, 1.
(216) Ouyang, S. C.; Wang, M. C. *J. Electroanal. Chem.* **1999**, *474*, 82.
(217) Marquette, C. A.; Ravaud, S.; Blum, L. J. *Anal. Lett.* **2000**, *33*, 1779.
(218) Sato, Y.; Yabuki, S.; Mizutani, F. *Chem. Lett.* **2000**, 1330.
(219) Taylor, C. E. I. V.; Creager, S. E. *J. Electroanal. Chem.* **2000**, *485*, 114.
(220) Marquette, C. A.; Leca, B. D.; Blum, L. J. *Luminescence* **2001**, *16*, 159.
(221) Zhu, L.; Li, Y.; Tian, F.; Xu, B.; Zhu, G. *Sens. Actuators, B* **2002**, *B84*, 265.
(222) Marquette, C. A.; Blum, L. J. *Sens. Actuators, B* **2003**, *B90*, 112.
(223) Marquette, C. A.; Thomas, D.; Degiuli, A.; Blum, L. J. *Anal. Bioanal. Chem.* **2003**, *377*, 922.
(224) Wilson, R.; Clavering, C.; Hutchinson, A. *Analyst* **2003**, *128*, 480.
(225) Kamada, M.; Yoshimi, Y. *Proc. Electrochem. Soc.* **2004**, *2004-08*, 275.
(226) Kamada, M.; Yoshimi, Y. *Chem. Sens.* **2004**, *20*, 103.
(227) Kamada, M.; Yoshimi, Y. *Chem. Sens.* **2004**, *20*, 126.
(228) Marquette, C. A.; Blum, L. J. *Biosens. Bioelectron.* **2004**, *20*, 197.
(229) Yoshimi, Y.; Kamada, M.; Ohkawara, Y.; Hattori, K.; Sakai, K. *Electrochemistry (Tokyo, Japan)* **2004**, *72*, 747.
(230) Wang, J.; Chen, G.; Huang, J. *Analyst* **2005**, *130*, 71.
(231) Haan, C.; Behrmann, I. *J. Immunol. Methods* **2007**, *318*, 11.
(232) Pittet, P.; Lu, G.-N.; Galvan, J.-M.; Ferrigno, R.; Blum, L. J.; Leca-Bouvier, B. *Analyst* **2007**, *132*, 409.
(233) Xiao, Y.; Pavlov, V.; Niazov, T.; Dishon, A.; Kotler, M.; Willner, I. *NATO Security Sci., Ser. B: Phys. Biophys.* **2005**, 1.
(234) Vitt, J. E.; Johnson, D. C.; Engstrom, R. C. *J. Electrochem. Soc.* **1991**, *138*, 1637.
(235) Dong, Y.-P.; Cui, H.; Wang, C.-M. *J. Phys. Chem. B* **2006**, *110*, 18408.
(236) Chen, J.; Lin, Z.; Chen, G. *Anal. Bioanal. Chem.* **2007**, *388*, 399.
(237) Yu, H.-X.; Cui, H.; Guo, J.-Z. *Luminescence* **2004**, *19*, 212.
(238) Yu, H.-X.; Cui, H. *J. Electroanal. Chem.* **2005**, *580*, 1.
(239) Wilson, R.; Akhavan-Tafii, H.; DeSilva, R.; Schaap, A. P. *Electroanalysis* **2001**, *13*, 1083.
(240) Leca, B.; Blum, L. J. *Analyst* **2000**, *125*, 789.
(241) Leca, B. D.; Verdier, A. M.; Blum, L. J. *Sens. Actuators, B* **2001**, *B74*, 190.
(242) Cui, H.; Wang, W.; Duan, C.-F.; Dong, Y.-P.; Guo, J.-Z. *Chem. Eur. J.* **2007**, *13*, 6975.
(243) Qian, K.-J.; Zhang, L.; Yang, M.-L.; He, P.-G.; Fang, Y.-Z. *Chin. J. Chem.* **2004**, *22*, 702.
(244) Zhang, L.; Zheng, X. *Anal. Chim. Acta* **2006**, *570*, 207.
(245) Zhang, L.-L.; Zheng, X.-W.; Guo, Z.-H. *Chin. J. Chem.* **2007**, *25*, 351.
(246) Sato, Y.; Kato, D.; Iijima, S.; Mizutani, F.; Niwa, O. *Electrochemistry (Tokyo, Japan)* **2006**, *74*, 202.
(247) Rypka, M.; Lasovsky, J. *J. Electroanal. Chem.* **1996**, *416*, 41.
(248) Fry, A. J. In *Labtoratory Techniques in Electroanalytical Chemistry*, 2nd ed.; Kissinger, P. T., Heineman, W. R., Eds.; Dekker: New York, 1996; Chapter 15.
(249) Creager, S., E. In *Handbook of Electrochemistry*; Zoski, C. G., Ed.; Elsevier: Amsterdam, The Netherlands, 2007; p 57.
(250) Miao, W.; Bard, A. J. *Anal. Chem.* **2003**, *75*, 5825.
(251) Xu, X.-H.; Bard, A. J. *Langmuir* **1994**, *10*, 2409.
(252) Danielson, N. D. In *Electrogenerated Chemiluminescence*; Bard, A. J., Ed.; Dekker: New York, 2004; Chapter 9, p 397.
(253) Chi, Y.; Dong, Y.; Chen, G. *Electrochem. Commun.* **2007**, *9*, 577.
(254) Chi, Y.; Duan, J.; Lin, S.; Chen, G. *Anal. Chem.* **2006**, *78*, 1568.
(255) Chi, Y.; Dong, Y.; Chen, G. *Anal. Chem.* **2007**, *79*, 4521.
(256) Li, F.; Cui, H.; Lin, X.-Q. *Anal. Chim. Acta* **2002**, *471*, 187.
(257) Hosono, H.; Satoh, W.; Fukuda, J.; Suzuki, H. *Sens. Actuators, B* **2007**, *B122*, 542.
(258) Chiang, M.-T.; Whang, C.-W. *J. Chromatogr., A* **2001**, *934*, 59.
(259) Chiang, M.-T.; Lu, M.-C.; Whang, C.-W. *Electrophoresis* **2003**, *24*, 3033.
(260) Wang, X.; Bobbitt, D. R. *Anal. Chim. Acta* **1999**, *383*, 213.
(261) O'Shea, T. J.; Greenhagen, R. D.; Lunte, S. M.; Lunte, C. E.; Smyth, M. R.; Radzik, D. M.; Watanabe, N. *J. Chromatogr.* **1992**, *593*, 305.
(262) Forbes, G. A.; Nieman, T. A.; Sweedler, J. V. *Anal. Chim. Acta* **1997**, *347*, 289.
(263) Dickson, J. A.; Ferris, M. M.; Milofsky, R. E. *J. High. Resolut. Chromatogr.* **1997**, *20*, 643.
(264) Yin, X.-B.; Qiu, H.; Sun, X.; Yan, J.; Liu, J.; Wang, E. *Anal. Chem.* **2004**, *76*, 3846.
(265) Huang, X.-J.; Wang, S.-L.; Fang, Z.-L. *Anal. Chim. Acta* **2002**, *456*, 167.

(266) Cao, W.; Liu, J.; Yang, X.; Wang, E. *Electrophoresis* **2002**, *23*, 3683.
(267) Ding, S.-N.; Xu, J.-J.; Chen, H.-Y. *Talanta* **2006**, *70*, 403.
(268) Du, Y.; Wei, H.; Kang, J.; Yan, J.; Yin, X.-B.; Yang, X.; Wang, E. *Anal. Chem.* **2005**, *77*, 7993.
(269) Qiu, H.; Yan, J.; Sun, X.; Liu, J.; Cao, W.; Yang, X.; Wang, E. *Anal. Chem.* **2003**, *75*, 5435.
(270) Arora, A.; Eijkel, J. C. T.; Morf, W. E.; Manz, A. *Anal. Chem.* **2001**, *73*, 3282.
(271) Zhan, W.; Alvarez, J.; Crooks, R. M. *J. Am. Chem. Soc.* **2002**, *124*, 13265.
(272) Zhan, W.; Alvarez, J.; Crooks, R. M. *Anal. Chem.* **2003**, *75*, 313.
(273) Zhan, W.; Alvarez, J.; Sun, L.; Crooks, R. M. *Anal. Chem.* **2003**, *75*, 1233.
(274) Zhao, X.; You, T.; Qiu, H.; Yan, J.; Yang, X.; Wang, E. *J. Chromatogr., B* **2004**, *810*, 137.
(275) Yin, X.-B.; Du, Y.; Yang, X.; Wang, E. *J. Chromatogr., A* **2005**, *1091*, 158.
(276) Qiu, H.; Yin, X.-B.; Yan, J.; Zhao, X.; Yang, X.; Wang, E. *Electrophoresis* **2005**, *26*, 687.
(277) Ding, S.-N.; Xu, J.-J.; Zhang, W.-J.; Chen, H.-Y. *Talanta* **2006**, *70*, 572.
(278) Ding, S.-N.; Xu, J.-J.; Chen, H.-Y. *Electrophoresis* **2005**, *26*, 1737.
(279) Yotter, R. A.; Wilson, D. M. *IEEE Sensors J.* **2003**, *3*, 288.
(280) Hamamatsu Corp., www.hamamatsu.com.
(281) Kovacs, G. T. A. *Micromachined Transducers Sourcebook*; WCB/McGraw-Hill: Boston, MA, 1998.
(282) Digi-Key Corp., www.digikey.com/.
(283) Roper Scientific Photomatrics, Roper Scientific, Inc., www.roperscientific.com/.
(284) Zhan, W.; Bard, A. J. *Anal. Chem.* **2007**, *79*, 459.
(285) Giles, J. H.; Ridder, T. D.; Williams, R. H.; Jones, D. A.; Denton, M. B. *Anal. Chem.* **1998**, *70*, 663A
(286) Yang, H.; Leland, J. K.; Yost, D.; Massey, R. J. *Biotechnology (N. Y.)* **1994**, *12*, 193.
(287) Remax Electronic Co. Ltd., http://remex.instrument.com.cn.
(288) CH Instruments, Inc., www.chinstruments.com.
(289) Autolab Electrochemical Instruments, www.ecochemie.nl.
(290) Keithley Instruments, Inc., www.keithley.com.
(291) Rosado, D. J., Jr.; Miao, W.; Sun, Q.; Deng, Y. *J. Phys. Chem. B* **2006**, *110*, 15719.
(292) Economou, A.; Nika, M. *J. Autom. Methods Manage. Chem.* **2006**, 1.
(293) Stagni, S.; Palazzi, A.; Zacchini, S.; Ballarin, B.; Bruno, C.; Marcaccio, M.; Paolucci, F.; Monari, M.; Carano, M.; Bard, A. J. *Inorg. Chem.* **2006**, *45*, 695.
(294) Glass, R. S.; Faulkner, L. R. *J. Phys. Chem.* **1981**, *85*, 1160.
(295) Luttmer, J. D.; Bard, A. J. *J. Phys. Chem.* **1981**, *85*, 1155.
(296) Wallace, W. L.; Bard, A. J. *J. Phys. Chem.* **1979**, *83*, 1350.
(297) Zanarini, S.; Bard, A. J.; Marcaccio, M.; Palazzi, A.; Paolucci, F.; Stagni, S. *J. Phys. Chem. B* **2006**, *110*, 22551.
(298) Li, M.; Liu, J.; Zhao, C.; Sun, L. *J. Organomet. Chem.* **2006**, *691*, 4189.
(299) Brooks, S. C.; Vinyard, D. J.; Richter, M. M. *Inorg. Chim. Acta* **2006**, *359*, 4635.
(300) Lee, D. N.; Park, H. J.; Kim, D. H.; Lee, S. W.; Park, S. J.; Kim, B. H.; Lee, W.-Y. *Bull. Korean Chem. Soc.* **2002**, *23*, 13.
(301) Park, S. J.; Kim, D. H.; Kim, D. H.; Park, H. J.; Lee, D. N.; Kim, B. H.; Lee, W.-Y. *Anal. Sci.* **2001**, *17*, a93.
(302) Kim, B. H.; Lee, D. N.; Park, H. J.; Min, J. H.; Jun, Y. M.; Park, S. J.; Lee, W.-Y. *Talanta* **2004**, *62*, 595.
(303) Zhou, M.; Roovers, J. *Macromolecules* **2001**, *34*, 244.
(304) Lee, D. N.; Kim, J. K.; Park, H. S.; Jun, Y. M.; Hwang, R. Y.; Lee, W.-Y.; Kim, B. H. *Synth. Met.* **2005**, *150*, 93.
(305) Lee, D. N.; Park, H. S.; Kim, E. H.; Jun, Y. M.; Lee, J.-Y.; Lee, W.-Y.; Kim, B. H. *Bull. Korean Chem. Soc.* **2006**, *27*, 99.
(306) Zhou, M.; Robertson, G. P.; Roovers, J. *Inorg. Chem.* **2005**, *44*, 8317.
(307) Shin, I.-S.; Kim, J. I.; Kwon, T.-H.; Hong, J.-I.; Lee, J.-K.; Kim, H. *J. Phys. Chem. C* **2007**, *111*, 2280.
(308) Kapturkiewicz, A.; Nowacki, J.; Borowicz, P. *Electrochim. Acta* **2005**, *50*, 3395.
(309) Sigma-Aldrich Co., www.sigmaaldrich.com/.
(310) Wang, P.; Zhu, G. *Luminescence* **2000**, *15*, 261.
(311) Kim, J. I.; Shin, I.-S.; Kim, H.; Lee, J.-K. *J. Am. Chem. Soc.* **2005**, *127*, 1614.
(312) Kapturkiewicz, A.; Angulo, G. *Dalton Trans.* **2003**, 3907.
(313) Kapturkiewicz, A.; Nowacki, J.; Borowicz, P. *Z. Phys. Chem.* **2006**, *220*, 525.
(314) Kapturkiewicz, A.; Chen, T.-M.; Laskar, I. R.; Nowacki, J. *Electrochem. Commun.* **2004**, *6*, 827.
(315) Muegge, B. D.; Richter, M. M. *Luminescence* **2005**, *20*, 76.
(316) Dutta, S. K.; Perkovic, M. W. *Inorg. Chem.* **2002**, *41*, 6938.
(317) Singh, P.; Richter, M. M. *Inorg. Chim. Acta* **2004**, *357*, 1589.
(318) Lai, R. Y.; Bard, A. J. *J. Phys. Chem. B* **2003**, *107*, 5036.
(319) Roehr, H.; Trieflinger, C.; Rurack, K.; Daub, J. *Chem. Eur. J.* **2006**, *12*, 689.
(320) Trieflinger, C.; Roehr, H.; Rurack, K.; Daub, J. *Angew. Chem. Int. Ed.* **2005**, *44*, 6943.
(321) Bruce, D.; Richter, M. M. *Anal. Chem.* **2002**, *74*, 1340.
(322) Elangovan, A.; Chen, T.-Y.; Chen, C.-Y.; Ho, T.-I. *Chem. Commun.* **2003**, 2146.
(323) Elangovan, A.; Yang, S.-W.; Lin, J.-H.; Kao, K.-M.; Ho, T.-I. *Org. Biomol. Chem.* **2004**, *2*, 1597.
(324) Kapturkiewicz, A. J. *Electroanal. Chem. Interfacial Electrochem.* **1991**, *302*, 131.
(325) Chandross, E. A.; Longworth, J. W.; Visco, R. E. *J. Am. Chem. Soc.* **1965**, *87*, 3259.
(326) Elangovan, A.; Lin, J.-H.; Yang, S.-W.; Hsu, H.-Y.; Ho, T.-I. *J. Org. Chem.* **2004**, *69*, 8086.
(327) Elangovan, A.; Lin, J.-H.; Yang, S.-W.; Hsu, H.-Y.; Ho, T.-I. *J. Org. Chem.* **2005**, *70*, 1104.
(328) Elangovan, A.; Kao, K.-M.; Yang, S.-W.; Chen, Y.-L.; Ho, T.-I.; Su, Y. O. *J. Org. Chem.* **2005**, *70*, 4460.
(329) Elangovan, A.; Chiu, H.-H.; Yang, S.-W.; Ho, T.-I. *Org. Biomol. Chem.* **2004**, *2*, 3113.
(330) Ho, T.-I.; Elangovan, A.; Hsu, H.-Y.; Yang, S.-W. *J. Phys. Chem. B* **2005**, *109*, 8626.
(331) Chen, C.-Y.; Ho, J.-H.; Wang, S.-L.; Ho, T.-I. *Photochem. Photobiol. Sci.* **2003**, *2*, 1232.
(332) Sartin, M. M.; Boydston, A. J.; Pagenkopf, B. L.; Bard, A. J. *J. Am. Chem. Soc.* **2006**, *128*, 10163.
(333) Mirkhalaf, F.; Wilson, R. *Electroanalysis* **2005**, *17*, 1761.
(334) Zheng, S.; Shi, J. *Chem. Mater.* **2001**, *13*, 4405.
(335) Li, Y.; Fung, M. K.; Xie, Z.; Lee, S.-T.; Hung, L.-S.; Shi, J. *Adv. Mater. (Weinheim, Germany)* **2002**, *14*, 1317.
(336) Zhang, X. H.; Liu, M. W.; Wong, O. Y.; Lee, C. S.; Kwong, H. L.; Lee, S. T.; Wu, S. K. *Chem. Phys. Lett.* **2003**, *369*, 478.
(337) Cao, W.; Zhang, X.; Bard, A. J. *J. Electroanal. Chem.* **2004**, *566*, 409.
(338) Jiang, X.; Yang, X.; Zhao, C.; Jin, K.; Sun, L. *J. Phys. Chem. C* **2007**, *111*, 9595.
(339) Dawson, W. R.; Windsor, M. W. *J. Phys. Chem.* **1968**, *72*, 3251.
(340) Bard, A. J.; Ding, Z.; Myung, N. *Struct. Bonding (Berlin, Germany)* **2005**, *118*, 1.
(341) Myung, N.; Bae, Y.; Bard, A. J. *Nano Lett.* **2003**, *3*, 1053.
(342) Bae, Y.; Myung, N.; Bard, A. J. *Nano Lett.* **2004**, *4*, 1153.
(343) Ushida, K.; Yoshida, Y.; Kozawa, T.; Tagawa, S.; Kira, A. *J. Phys. Chem. A* **1999**, *103*, 4680.
(344) Myung, N.; Lu, X.; Johnston, K. P.; Bard, A. J. *Nano Lett.* **2004**, *4*, 183.
(345) Haram, S. K.; Quinn, B. M.; Bard, A. J. *J. Am. Chem. Soc.* **2001**, *123*, 8860.
(346) Ren, T.; Xu, J.-Z.; Tu, Y.-F.; Xu, S.; Zhu, J.-J. *Electrochem. Commun.* **2005**, *7*, 5.
(347) Jie, G.-F.; Liu, B.; Miao, J.-J.; Zhu, J.-J. *Talanta* **2007**, *71*, 1476.
(348) Myung, N.; Ding, Z.; Bard, A. J. *Nano Lett.* **2002**, *2*, 1315.
(349) Zhou, J.; Zhu, J.; Ding, Z. *Proc. Electrochem. Soc.* **2005**, *2005-04*, 129.
(350) Ge, C.; Xu, M.; Liu, J.; Lei, J.; Ju, H. *Chem. Commun.* **2008**, 450.
(351) Zhou, B.; Liu, B.; Jiang, L.-P.; Zhu, J.-J. *Ultrason. Sonochem.* **2007**, *14*, 229.
(352) Shen, L.; Cui, X.; Qi, H.; Zhang, C. *J. Phys. Chem. C* **2007**, *111*, 8172.
(353) Bae, Y.; Lee, D. C.; Rhogojina, E. V.; Jurbergs, D. C.; Korgel, B. A.; Bard, A. J. *Nanotechnology* **2006**, *17*, 3791.
(354) Wehrenberg, B. L.; Guyot-Sionnest, P. *J. Am. Chem. Soc.* **2003**, *125*, 7806.
(355) Wang, C.; Shim, M.; Guyot-Sionnest, P. *Appl. Phys. Lett.* **2002**, *80*, 4.
(356) Guyot-Sionnest, P.; Wang, C. *J. Phys. Chem. B* **2003**, *107*, 7355.
(357) Woo, W.-K.; Shimizu, K. T.; Jarosz, M. V.; Neuhauser, R. G.; Leatherdale, C. A.; Rubner, M. A.; Bawendi, M. G. *Adv. Mater. Weinheim, Germany)* **2002**, *14*, 1068.
(358) Coe, S.; Woo, W.-K.; Bawendi, M.; Bulovic, V. *Nature (London, U.K.)* **2002**, *420*, 800.
(359) Hikmet, R. A. M.; Talapin, D. V.; Weller, H. *J. Appl. Phys.* **2003**, *93*, 3509.
(360) Poznyak, S. K.; Talapin, D. V.; Shevchenko, E. V.; Weller, H. *Nano Lett.* **2004**, *4*, 693.
(361) Rubinstein, I.; Bard, A. J. *J. Am. Chem. Soc.* **1980**, *102*, 6641.
(362) Rubinstein, I.; Bard, A. J. *J. Am. Chem. Soc.* **1981**, *103*, 5007.
(363) Zhang, X.; Bard, A. J. *J. Phys. Chem.* **1988**, *92*, 5566.
(364) Miller, C. J.; McCord, P.; Bard, A. J. *Langmuir* **1991**, *7*, 2781.
(365) Obeng, Y. S.; Bard, A. J. *Langmuir* **1991**, *7*, 195.
(366) Tao, Y.; Lin, Z.-J.; Chen, X.-M.; Chen, X.; Wang, X.-R. *Anal. Chim. Acta* **2007**, *594*, 169.
(367) Greenway, G. M.; Greenwood, A.; Watts, P.; Wiles, C. *Chem. Commun.* **2006**, 85.

(368) Armelao, L.; Bertoncello, R.; Gross, S.; Badocco, D.; Pastore, P. *Electroanalysis* **2003**, *15*, 803.
(369) Qiu, B.; Chen, X.; Chen, H.-L.; Chen, G.-N. *Luminescence* **2007**, *22*, 189.
(370) Wang, H.; Xu, G.; Dong, S. *Analyst* **2001**, *126*, 1095.
(371) Wang, H.; Xu, G.; Dong, S. *Electroanalysis* **2002**, *14*, 853.
(372) Zhuang, Y.; Ju, H. *Electroanalysis* **2004**, *16*, 1401.
(373) Zhao, L.; Tao, Y.; Yang, X.; Zhang, L.; Oyama, M.; Chen, X. *Talanta* **2006**, *70*, 104.
(374) Choi, H. N.; Cho, S.-H.; Park, Y.-J.; Lee, D. W.; Lee, W.-Y. *Anal. Chim. Acta* **2005**, *541*, 49.
(375) Yi, C.; Tao, Y.; Wang, B.; Chen, X. *Anal. Chim. Acta* **2005**, *541*, 75.
(376) Zhang, L.; Xu, Z.; Dong, S. *Anal. Chim. Acta* **2006**, *575*, 52.
(377) Lee, J.-K.; Lee, S.-H.; Kim, M.; Kim, H.; Kim, D.-H.; Lee, W.-Y. *Chem. Commun.* **2003**, 1602.
(378) Song, H.; Zhang, Z.; Wang, F. *Electroanalysis* **2006**, *18*, 1838.
(379) Cui, H.; Zhao, X.-Y.; Lin, X.-Q. *Luminescence* **2003**, *18*, 199.
(380) Wei, H.; Du, Y.; Kang, J.; Wang, E. *Electrochem. Commun.* **2007**, *9*, 1474.
(381) Zhang, L.; Guo, Z.; Xu, Z.; Dong, S. *J. Electroanal. Chem.* **2006**, *592*, 63.
(382) Choi, H. N.; Cho, S.-H.; Lee, W.-Y. *Anal. Chem.* **2003**, *75*, 4250.
(383) Zhuang, Y.; Ju, H. *Anal. Lett* **2005**, *38*, 2077.
(384) Shi, L.; Liu, X.; Li, H.; Xu, G. *Anal. Chem.* **2006**, *78*, 7330.
(385) Guo, Z.; Shen, Y.; Zhao, F.; Wang, M.; Dong, S. *Analyst* **2004**, *129*, 657.
(386) Du, Y.; Qi, B.; Yang, X.; Wang, E. *J. Phys. Chem. B* **2006**, *110*, 21662.
(387) Zhang, L.; Xu, Z.; Sun, X.; Dong, S. *Biosens. Bioelectron.* **2007**, *22*, 1097.
(388) Sun, X.; Du, Y.; Zhang, L.; Dong, S.; Wang, E. *Anal. Chem.* **2007**, *79*, 2588.
(389) Sun, X.; Du, Y.; Dong, S.; Wang, E. *Anal. Chem.* **2005**, *77*, 8166.
(390) Guo, Z.; Shen, Y.; Wang, M.; Zhao, F.; Dong, S. *Anal. Chem.* **2004**, *76*, 184.
(391) Dennany, L.; Hogan, C. F.; Keyes, T. E.; Forster, R. J. *Anal. Chem.* **2006**, *78*, 1412.
(392) Guo, S.; Wang, E. *Electrochem. Commun.* **2007**, *9*, 1252.
(393) Wang, H.; Xu, G.; Dong, S. *Talanta* **2001**, *55*, 61.
(394) Lowry, R. B.; Williams, C. E.; Braven, J. *Talanta* **2004**, *63*, 961.
(395) Khramov, A. N.; Collinson, M. M. *Anal. Chem.* **2000**, *72*, 2943.
(396) Zhuang, Y.; Ju, H. *Electroanalysis* **2004**, *16*, 1401.
(397) Kim, D.-J.; Lyu, Y.-K.; Choi, H. N.; Min, I.-H.; Lee, W.-Y. *Chem. Commun.* **2005**, 2966.
(398) Zhuang, Y.; Zhang, D.; Ju, H. *Analyst* **2005**, *130*, 534.
(399) Li, Y.; Wang, C.; Sun, J.; Zhou, Y.; You, T.; Wang, E.; Fung, Y. *Anal. Chim. Acta* **2005**, *550*, 40.
(400) Liu, S.; Liu, Y.; Li, J.; Guo, M.; Pan, W.; Yao, S. *Talanta* **2006**, *69*, 154.
(401) Chang, P.-L.; Lee, K.-H.; Hu, C.-C.; Chang, H.-T. *Electrophoresis* **2007**, *28*, 1092.
(402) Tsukagoshi, K.; Miyamoto, K.; Saiko, E.; Nakajima, R.; Hara, T.; Fujinaga, K. *Anal. Sci.* **1997**, *13*, 639.
(403) Xu, Y.; Gao, Y.; Wei, H.; Du, Y.; Wang, E. *J. Chromatogr., A* **2006**, *1115*, 260.
(404) Liu, Y.; Zhou, W. *Anal. Sci.* **2006**, *22*, 999.
(405) Zhou, M.; Ma, Y.-J.; Ren, X.-N.; Zhou, X.-Y.; Li, L.; Chen, H. *Anal. Chim. Acta* **2007**, *587*, 104.
(406) Huang, J.; Sun, J.; Zhou, X.; You, T. *Anal. Sci.* **2007**, *23*, 183.
(407) Cao, W.; Chen, X.; Yang, X.; Wang, E. *Electrophoresis* **2003**, *24*, 3124.
(408) Cao, W.; Jia, J.; Yang, X.; Dong, S.; Wang, E. *Electrophoresis* **2002**, *23*, 3692.
(409) Fang, L.; Kang, J.; Yin, X.-b.; Yang, X.; Wang, E. *Electrophoresis* **2006**, *27*, 4516.
(410) Fang, L.; Yin, X.-b.; Sun, X.; Wang, E. *Anal. Chim. Acta* **2005**, *537*, 25.
(411) Liu, J.; Cao, W.; Qiu, H.; Sun, X.; Yang, X.; Wang, E. *Clin. Chem.* **2002**, *48*, 1049.
(412) Li, J.; Zhao, F.; Ju, H. *J. Chromatogr., B* **2006**, *835*, 84.
(413) Sreedhar, M.; Lin, Y.-W.; Tseng, W.-L.; Chang, H.-T. *Electrophoresis* **2005**, *26*, 2984.
(414) Li, J.; Ju, H. *Electrophoresis* **2006**, *27*, 3467.
(415) Gao, Y.; Tian, Y.; Wang, E. *Anal. Chim. Acta* **2005**, *545*, 137.
(416) Yin, J.; Guo, W.; Du, Y.; Wang, E. *Electrophoresis* **2006**, *27*, 4836.
(417) Liu, J.; Yang, X.; Wang, E. *Electrophoresis* **2003**, *24*, 3131.
(418) Cao, W.; Yang, X.; Wang, E. *Electroanalysis* **2004**, *16*, 169.
(419) Liang, H.; Xue, J.; Li, T.; Wu, Y. *Luminescence* **2005**, *20*, 287.
(420) Wu, Y.; Li, T.; Liang, H.; Xue, J. *Luminescence* **2005**, *20*, 352.
(421) Liu, J.; Cao, W.; Yang, X.; Wang, E. *Talanta* **2003**, *59*, 453.
(422) Yuan, J.; Yin, J.; Wang, E. *J. Chromatogr., A* **2007**, *1154*, 368.
(423) Huang, Y.; Pan, W.; Guo, M.; Yao, S. *J. Chromatogr., A* **2007**, *1154*, 373.
(424) Li, J.; Yan, Q.; Gao, Y.; Ju, H. *Anal. Chem.* **2006**, *78*, 2694.
(425) Park, Y.-J.; Lee, D. W.; Lee, W.-Y. *Anal. Chim. Acta* **2002**, *471*, 51.
(426) Yi, C.; Li, P.; Tao, Y.; Chen, X. *Microchimica Acta* **2004**, *147*, 237.
(427) Chen, X.; Yi, C.; Li, M.; Lu, X.; Li, Z.; Li, P.; Wang, X. *Anal. Chim. Acta* **2002**, *466*, 79.
(428) Hori, T.; Hashimoto, H.; Konishi, M. *Biomed. Chromatogr.* **2006**, *20*, 917.
(429) Morita, H.; Konishi, M. *Anal. Chem.* **2002**, *74*, 1584.
(430) Morita, H.; Konishi, M. *Anal. Chem.* **2003**, *75*, 940.
(431) Forry, S. P.; Wightman, R. M. *Anal. Chem.* **2002**, *74*, 528.
(432) Uchikura, K.; Kirisawa, M.; Sugii, A. *Anal. Sci.* **1993**, *9*, 121.
(433) McCall, J.; Alexander, C.; Richter, M. M. *Anal. Chem.* **1999**, *71*, 2523.
(434) McCall, J.; Richter, M. M. *Analyst* **2000**, *125*, 545.
(435) Cao, W.; Ferrance, J. P.; Demas, J.; Landers, J. P. *J. Am. Chem. Soc.* **2006**, *128*, 7572.
(436) Spehar, A.-M.; Koster, S.; Kulmala, S.; Verpoorte, E.; de Rooij, N.; Koudelka-Hep, M. *Luminescence* **2004**, *19*, 287.
(437) Kang, J.; Liu, J.; Yin, X.-B.; Qiu, H.; Yan, J.; Yang, X.; Wang, E. *Anal. Lett.* **2005**, *38*, 1179.
(438) Zheng, H.; Zu, Y. *J. Phys. Chem. B* **2005**, *109*, 16047.
(439) Cui, H.; Li, F.; Shi, M.-J.; Pang, Y.-Q.; Lin, X.-Q. *Electroanalysis* **2005**, *17*, 589.
(440) Pang, Y.-Q.; Cui, H.; Zheng, H.-S.; Wan, G.-H.; Liu, L.-J.; Yu, X.-F. *Luminescence* **2005**, *20*, 8.
(441) Li, F.; Pang, Y.-Q.; Lin, X.-Q.; Cui, H. *Talanta* **2003**, *59*, 627.
(442) Waseem, A.; Yaqoob, M.; Nabi, A.; Greenway, G. M. *Anal. Lett.* **2007**, *40*, 1071.
(443) Wu, X.; Huang, F.; Duan, J.; Chen, G. *Talanta* **2005**, *65*, 1279.
(444) Kang, J.; Yin, X.-B.; Yang, X.; Wang, E. *Electrophoresis* **2005**, *26*, 1732.
(445) Chi, Y.; Xie, J.; Chen, G. *Talanta* **2006**, *68*, 1544.
(446) Chen, X.; Tao, Y.; Zhao, L.; Xie, Z.; Chen, G. *Luminescence* **2005**, *20*, 109.
(447) Lindino, C. A.; Bulhoes, L. O. S. *Talanta* **2007**, *72*, 1746.
(448) Tomita, I. N.; Bulhoes, L. O. S. *Anal. Chim. Acta* **2001**, *442*, 201.
(449) Zhao, X.; You, T.; Liu, J.; Sun, X.; Yan, J.; Yang, X.; Wang, E. *Electrophoresis* **2004**, *25*, 3422.
(450) Liu, Y.; Pan, W.; Liu, Q.; Yao, S. *Electrophoresis* **2005**, *26*, 4468.
(451) Yuan, J.; Wei, H.; Jin, W.; Yang, X.; Wang, E. *Electrophoresis* **2006**, *27*, 4047.
(452) Yuan, J.; Li, T.; Yin, X.-B.; Guo, L.; Jiang, X.; Jin, W.; Yang, X.; Wang, E. *Anal. Chem.* **2006**, *78*, 2934.
(453) Haenel, C.; Satzger, M.; Ducata, D. D.; Ostendorp, R.; Brocks, B. *Anal. Biochem.* **2005**, *339*, 182.
(454) Piao, J.; Mitoma, Y.; Uda, T.; Hifumi, E.; Shimizu, K.; Egashira, N. *Electroanalysis* **2004**, *16*, 1262.
(455) Zheng, X.; Guo, Z.; Zhang, Z. *Anal. Chim. Acta* **2001**, *441*, 81.
(456) Zheng, X.; Zhang, Z.; Guo, Z.; Wang, Q. *Analyst* **2002**, *127*, 1375.
(457) Ma, H.-Y.; Zheng, X.-W.; Zhang, Z.-J. *Chin. J. Chem.* **2004**, *22*, 279.
(458) Sun, Y. G.; Cui, H.; Li, Y. H.; Lin, X. Q. *Talanta* **2000**, *53*, 661.
(459) Li, J. J.; Du, J. X.; Lu, J. R. *Talanta* **2002**, *57*, 53.
(460) Zhu, L.; Li, Y.; Zhu, G. *Sens. Actuators, B* **2004**, *B98*, 115.
(461) Tsafack, V. C.; Marquette, C. A.; Leca, B.; Blum, L. J. *Analyst* **2000**, *125*, 151.
(462) Ma, H.; Zheng, X.; Zhang, Z. *Luminescence* **2005**, *20*, 303.
(463) Kenten, J. H.; Smith, R. BioVeris Corp. , U.S. 6890712B1, 2005.
(464) Lo, W.-Y.; Baeumner, A. J. *Anal. Chem.* **2007**, *79*, 1386.
(465) Lo, W.-Y.; Baeumner, A. J. *Anal. Chem.* **2007**, *79*, 1548.
(466) Kibbey, M. C.; MacAllan, D.; Karaszkiewicz, J. W. *JALA* **2000**, *5*, 45.
(467) Wilchek, M.; Bayer, E. A. *Anal. Biochem.* **1988**, *171*, 1.
(468) Beier, M.; Hoheisel, J. D. *Nucleic Acids Res* **1999**, *27*, 1970.
(469) Phinney, J. R.; Conroy, J. F.; Hosticka, B.; Power, M. E.; Ferrance, J. P.; Landers, J. P.; Norris, P. M. *J. Non-Cryst. Solids* **2004**, *350*, 39.
(470) Glazer, M.; Frank, C.; Lussi, J.; Fidanza, J.; McGall, G. *Mater. Res. Soc. Symp. Proc.* **2001**, *628*, CC10 4 1.
(471) Aguilar, Z. P.; Vandaveer, W. R. I. V.; Fritsch, I. *Anal. Chem.* **2002**, *74*, 3321.
(472) Patel, N.; Davies, M. C.; Hartshorne, M.; Heaton, R. J.; Roberts, C. J.; Tendler, S. J. B.; Williams, P. M. *Langmuir* **1997**, *13*, 6485.
(473) Yin, X.-B.; Qi, B.; Sun, X.; Yang, X.; Wang, E. *Anal. Chem.* **2005**, *77*, 3525.
(474) Fawcett, N. C.; Craven, R. D.; Zhang, P.; Evans, J. A. *Langmuir* **2004**, *20*, 6651.
(475) Fawcett, N. C.; Evans, J. A.; Craven, R. D.; Zhang, P.; Harvey, K.; Towery, R. B. *Polym. Mater. Sci. Eng.* **1997**, *76*, 461.

(476) Chang, Z.; Zhou, J.; Zhao, K.; Zhu, N.; He, P.; Fang, Y. *Electrochim. Acta* **2006**, *52*, 575.
(477) Lopez-Gallego, F.; Montes, T.; Fuentes, M.; Alonso, N.; Grazu, V.; Betancor, L.; Guisan, J. M.; Fernandez-Lafuente, R. *J. Biotechnol.* **2005**, *116*, 1.
(478) Guisan, J. M.; Bastida, A.; Blanco, R. M.; Fernandez-Lafuente, R.; Garcia-Junceda, E. *Methods Biotechnol.* **1997**, *1*, 277.
(479) Xu, X.-H.; Bard, A. J. *J. Am. Chem. Soc.* **1995**, *117*, 2627.
(480) Xu, X.-H.; Yang, H. C.; Mallouk, T. E.; Bard, A. J. *J. Am. Chem. Soc.* **1994**, *116*, 8386.
(481) *Immunofluorescence: Antigen Detection Techniques in Diagnostic Microbiology*; Caul, E. O., Ed.; Public Health Laboratory Service: London, U.K., 1992.
(482) Famulok, M.; Hartig, J. S.; Mayer, G. *Chem. Rev.* **2007**, *107*, 3715.
(483) Li, Y.; Qi, H.; Peng, Y.; Yang, J.; Zhang, C. *Electrochem. Commun.* **2007**, *9*, 2571.
(484) Xu, X. H.; Jeffers, R. B.; Gao, J.; Logan, B. *Analyst* **2001**, *126*, 1285.
(485) Li, Y.; Qi, H.; Fang, F.; Zhang, C. *Talanta* **2007**, *72*, 1704.
(486) Lee, J.-G.; Yun, K.; Lim, G.-S.; Lee, S. E.; Kim, S.; Park, J.-K. *Bioelectrochemistry* **2007**, *70*, 228.
(487) Wang, H.; Zhang, C.; Li, Y.; Qi, H. *Anal. Chim. Acta* **2006**, *575*, 205.
(488) Bertolino, C.; MacSweeney, M.; Tobin, J.; O'Neill, B.; Sheehan, M. M.; Coluccia, S.; Berney, H. *Biosens. Bioelectron.* **2005**, *21*, 565.
(489) Firrao, G. *Int. J. Environ. Anal. Chem.* **2005**, *85*, 609.
(490) Hsueh, Y.-T.; Collins, S. D.; Smith, R. L. *Sens. Actuators, B* **1998**, *B49*, 1.
(491) Spehar-Deleze, A.-M.; Schmidt, L.; Neier, R.; Kulmala, S.; de Rooij, N.; Koudelka-Hep, M. *Biosens. Bioelectron.* **2006**, *22*, 722.
(492) Kenten, J. H.; Casadei, J.; Link, J.; Lupold, S.; Willey, J.; Powell, M.; Rees, A.; Massey, R. *Clin. Chem.* **1991**, *37*, 1626.
(493) Siddiqi, A. M.; Jennings, V. M.; Kidd, M. R.; Actor, J. K.; Hunter, R. L. *J. Clin. Lab. Anal.* **1996**, *10*, 423.
(494) Bruno, J. G.; Kiel, J. L. *Biosens. Bioelectron.* **1999**, *14*, 457.
(495) Boom, R.; Sol, C.; Weel, J.; Gerrits, Y.; de Boer, M.; Wertheim-van Dillen, P. *J. Clin. Microbiol.* **1999**, *37*, 1489.
(496) de Jong, M. D.; Weel, J. F.; Schuurman, T.; Wertheim-van Dillen, P. M.; Boom, R. *J. Clin. Microbiol.* **2000**, *38*, 2568.
(497) Zhu, D.; Xing, D.; Shen, X.; Liu, J.; Chen, Q. *Biosens. Bioelectron.* **2004**, *20*, 448.
(498) Zhu, D.; Xing, D.; Shen, X.; Liu, J. *Biochem. Biophys. Res. Commun.* **2004**, *324*, 964.
(499) Tang, Y.-B.; Xing, D.; Zhu, D.-B.; Liu, J.-F. *Anal. Chim. Acta* **2007**, *582*, 275.
(500) Liu, J.; Xing, D.; Shen, X.; Zhu, D. *Anal. Chim. Acta* **2005**, *537*, 119.
(501) Zhang, L.; Schwartz, G.; O'Donnell, M.; Harrison, R. K. *Anal. Biochem.* **2001**, *293*, 31.
(502) Yang, M.; Liu, C.; Qian, K.; He, P.; Fang, Y. *Analyst* **2002**, *127*, 1267.
(503) Calvo-Munoz, M. L.; Dupont-Filliard, A.; Billon, M.; Guillerez, S.; Bidan, G.; Marquette, C.; Blum, L. *Bioelectrochemistry* **2005**, *66*, 139.
(504) Spehar-Deleze, A.-M.; Suomi, J.; Jiang, Q.; De Rooij, N.; Koudelka-Hep, M.; Kulmala, S. *Electrochim. Acta* **2006**, *51*, 5438.
(505) Dennany, L.; Forster, R. J.; White, B.; Smyth, M.; Rusling, J. F. *J. Am. Chem. Soc.* **2004**, *126*, 8835.
(506) Hvastkovs, E. G.; So, M.; Krishnan, S.; Bajrami, B.; Tarun, M.; Jansson, I.; Schenkman, J. B.; Rusling, J. F. *Anal. Chem* **2007**, *79*, 1897.
(507) Cote, C. K.; Rossi, C. A.; Kang, A. S.; Morrow, P. R.; Lee, J. S.; Welkos, S. L. *Microb. Pathog.* **2005**, *38*, 209.
(508) Guglielmo-Viret, V.; Attree, O.; Blanco-Gros, V.; Thullier, P. *J. Immunol. Methods* **2005**, *301*, 164.
(509) Keener, W. K.; Rivera, V. R.; Young, C. C.; Poli, M. A. *Anal. Biochem.* **2006**, *357*, 200.
(510) Merrill, G. A.; Rivera, V. R.; Neal, D. D.; Young, C.; Poli, M. A. *Anal. Biochem.* **2006**, *357*, 181.
(511) Rivera, V. R.; Gamez, F. J.; Keener, W. K.; White, J. A.; Poli, M. A. *Anal. Biochem.* **2006**, *353*, 248.
(512) Poli, M. A.; Rivera, V. R.; Neal, D. D.; Baden, D. G.; Messer, S. A.; Plakas, S. M.; Dickey, R. W.; El Said, K.; Flewelling, L.; Green, D.; White, J. *J. AOAC Int.* **2007**, *90*, 173.
(513) Schmidt-Gayk, H.; Spanuth, E.; Koetting, J.; Bartl, R.; Felsenberg, D.; Pfeilschifter, J.; Raue, F.; Roth, H. J. *Clin. Chem. Lab. Med.* **2004**, *42*, 90.
(514) Dominici, R.; Infusino, I.; Valente, C.; Moraschinelli, I.; Franzini, C. *Clin. Chem. Lab. Med.* **2004**, *42*, 945.
(515) Alber, B.; Hein, R.; Garbe, C.; Caroli, U.; Luppa, P. B. *Clin. Chem. Lab. Med.* **2005**, *43*, 557.
(516) Hammerer-Lercher, A.; Mair, J.; Tews, G.; Puschendorf, B.; Sommer, R. *Clin. Chem.* **2005**, *51*, 913.
(517) Prontera, C.; Emdin, M.; Zucchelli, G. C.; Ripoli, A.; Passino, C.; Clerico, A. *Clin. Chem. Lab. Med.* **2004**, *42*, 37.
(518) Reynders, M.; Anckaert, E.; Schiettecatte, J.; Smitz, J. *Clin. Chem. Lab. Med.* **2005**, *43*, 86.
(519) Santini, S. A.; Carrozza, C.; Vulpio, C.; Capoluongo, E.; Luciani, G.; Lulli, P.; Giardina, B.; Zuppi, C. *Clin. Chem.* **2004**, *50*, 1247.
(520) Verschraegen, I.; Anckaert, E.; Schiettecatte, J.; Mees, M.; Garrido, A.; Hermsen, D.; Lentjes, E. G. W. M.; Liebert, A.; Roth, H.-J.; Stamminger, G.; Smitz, J. *Clin. Chim. Acta* **2007**, *380*, 75.
(521) Lev-Sagie, A.; Bar-Oz, B.; Salpeter, L.; Hochner-Celnikier, D.; Arad, I.; Nir, A. *Clin. Chem* **2005**, *51*, 1909.
(522) Moxness, M.; Tatarewicz, S.; Weeraratne, D.; Murakami, N.; Wullner, D.; Mytych, D.; Jawa, V.; Koren, E.; Swanson, S. J. *Clin. Chem* **2005**, *51*, 1983.
(523) Shelton, D. R.; Higgins, J. A.; Van Kessel, J. A. S.; Pachepsky, Y. A.; Belt, K.; Karns, J. S. *J. Microbiol. Methods* **2004**, *58*, 223.
(524) Proenca, H.; Ferreira, C.; Miranda, M.; Castanheira-Dinis, A.; Monteiro-Grillo, M. *Eur. J. Ophthalmol.* **2007**, *17*, 404.
(525) Ala-Kleme, T.; Maekinen, P.; Ylinen, T.; Vaere, L.; Kulmala, S.; Ihalainen, P.; Peltonen, J. *Anal. Chem.* **2006**, *78*, 82.
(526) Zhang, C.; Qi, H.; Zhang, M. *Luminescence* **2007**, *22*, 53.

CR068083A